THE PROCEEDINGS OF
THE PHYSICAL SOCIETY

Section B

VOL. 64, PART 1 | 1 January 1951 | No. 373 B

Some Further Investigations of Ionospheric Cross-Modulation

BY I. J. SHAW
Late of the Cavendish Laboratory, Cambridge

Communicated by W. L. Bragg; MS. received 5th June 1950

ABSTRACT. The work in this paper forms the continuation and development of the experiments described in a paper by Ratcliffe and Shaw published in 1948. Measurements of the phase and amplitude of the modulation transferred to an unmodulated wave by a modulated disturbing wave in the ionosphere are used to provide information about that part of the ionosphere in which the cross-modulation occurs.

By measuring almost simultaneously the height of reflection of the wanted wave and the characteristics of the transferred modulation, a value of $1{\cdot}4 \times 10^6$ per second for the collision frequency of electrons with molecules at a height of 92 kilometres has been deduced. This measurement has been made possible by the use of a very sensitive automatic apparatus which is briefly described.

Special attention has been paid to the ' gyro-resonance effect ' in cross-modulation first pointed out in a theoretical paper by Bailey in 1937. The experiments appear to show that the predicted enhancement of the cross-modulation when the disturbing station radiates on the local gyro-magnetic frequency does not exist.

A modification of the original theory is given which is of great use in the calculation of the cross-modulation to be expected for a given pair of transmitters. This modified theory is used in the discussion of the gyro-resonance effect and of the observed decrease of the cross-modulation at dawn. The agreement between the calculated and observed magnitudes of cross-modulation is stressed in view of the fact that the calculations involve a knowledge of the absorption of the wanted wave incident obliquely upon the ionosphere.

§ 1. INTRODUCTION

IN a previous paper, which will be referred to here as I, Ratcliffe and Shaw (1948) described experiments made to investigate the phenomenon of ionospheric cross-modulation * and indicated how it was possible to deduce some important facts about the ionosphere from the investigation. This possibility has been discussed also by Huxley, Foster and Newton (1948), and Huxley and Ratcliffe (1949).

It is the purpose of this paper to outline a modification of the apparatus † described in I, and to discuss some of the results of importance in the study of

* The phenomenon has previously been called ' wave-interaction ' or ' Luxembourg effect '. Huxley and Ratcliffe (1949) have suggested the more precise description ' ionospheric cross-modulation '.

† A full description of the experimental technique will be given elsewhere.

the ionosphere which have been obtained with it. The present paper forms a sequel to I but, where appropriate, the nomenclature has been altered to conform with that suggested by Huxley and Ratcliffe.

In I, it was shown how it is possible, by measuring the phase of the transferred modulation at a series of modulation frequencies, to determine the collision frequency in the ionosphere at a height which could be deduced from the experimental data. The deduction of the height required a knowledge of the height of reflection of the wanted wave, and as this could not be measured it was assumed to be 100 kilometres. Any error in this assumed height would give rise to a corresponding error in the estimated height for the observed value of the collision frequency. In § 3 of the present paper a series of measurements of cross-modulation is described in which the height of reflection of the wanted wave was measured simultaneously. This leads to what is considered to be a reliable value of the collision frequency at a known height.

In the experiments of I, the phase and amplitude of the transferred modulation were determined by a comparatively slow method of visual observation so that about 20 minutes were required to make a full ' sweep ' of modulation frequency from 60 c/s. to 2,000 c/s. During this time the ionospheric conditions were often found to have changed so that considerable inaccuracy was introduced. In § 2 an automatic measuring equipment which considerably speeds up the rate of observation is briefly described. With this apparatus it is possible to obtain in four minutes a photographic record of the phase and amplitude of the transferred modulation over the required range of modulation frequencies. Errors due to alterations in the ionosphere during the period of an experiment are thereby considerably reduced. The automatic equipment is also more sensitive than visual observation so that much smaller depths of modulation can be measured.

In I, the original theory of Bailey and Martyn which has so far proved adequate to explain the observations was re-stated in a form more closely related to Appleton's magneto-ionic theory and this formulation, with some improvements in nomenclature, was extended by Huxley and Ratcliffe. If it is required to use the theory given in these papers to calculate the cross-modulation expected with a given pair of transmitting stations, it is necessary first to assume a distribution of electron density with height. It is shown in § 5, that with certain simplifying assumptions it is possible to deduce a general expression which relates the amplitude of cross-modulation to the total power absorbed from the disturbing wave, whatever the distribution of the electrons may be. This expression is used in a discussion of the following points:

(i) It has sometimes been suggested that markedly increased cross-modulation should be observed when the disturbing wave has a frequency equal to the ' gyro-frequency ' of the magneto-ionic theory. Experiments described in § 8 have not shown this increased cross-modulation and the theory of § 5 does not lead us to expect it.

(ii) The observed decrease of cross-modulation at dawn is discussed in terms of the theory.

(iii) The theory in its simple form is found adequate for the calculation of the absolute magnitude of the cross-modulation observed with different pairs of transmitting stations. The implications of this result for the theory of the absorption of radio waves at oblique incidence are discussed in § 6.

§ 2. EXPERIMENTAL TECHNIQUE

The general form of the experiments has been similar to that described in I and is illustrated diagrammatically in Figure 1. A ' wanted wave ' is transmitted from a station W and received, via the ionosphere, at a receiver R. A ' disturbing station ' D radiates a modulated wave which is received at R by the direct path DR over the ground. At some region B in the ionosphere modulation is transferred from the disturbing wave to the wanted wave. The experiment consists in comparing, at R, the phase of the modulation received via the direct path DR with that of the transferred modulation received on the wanted wave, over the range of modulation frequencies 60 c/s. to 2,000 c/s. Measurements are also made of the magnitude of the transferred modulation.

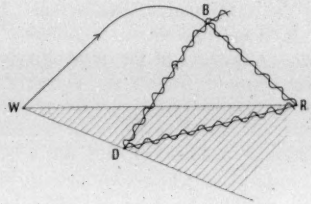

Figure 1. Schematic diagram of experimental arrangement of transmitters and receiver.

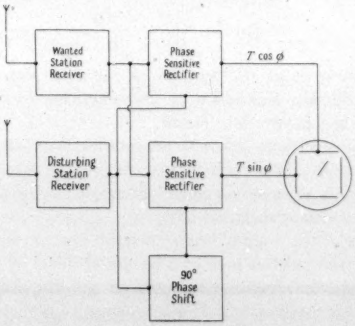

Figure 2. Simplified schematic diagram of automatic recording apparatus.

With the valuable help of Mr. S. W. Falloon equipment has been developed with which the amplitude of the transferred modulation and its phase relative to that of the direct wave from the disturbing station can be rapidly recorded photographically. As this apparatus will be described in detail elsewhere, it is sufficient here to describe it in outline only. For this purpose reference should be made to the block schematic diagram of Figure 2.

The basic element of the apparatus is the phase-sensitive rectifier circuit. The cross-modulation signal $T\cos(\omega t+\phi)$ and the reference signal $M\cos\omega t$ are mixed in the rectifier, giving an output, when M is large compared with T, proportional to $T\cos\phi$. From a second phase-sensitive rectifier, driven with the same cross-modulation signal and with the reference signal shifted 90° in phase,

an output proportional to $T\sin\phi$ is obtained. The two output voltages proportional to $T\cos\phi$ and $T\sin\phi$ are applied to the X and Y plates of a cathode-ray tube. The spot then moves from its rest position to a point defined by T and ϕ, and this movement is recorded photographically as a vector. Figure 3 shows the type of record obtained.

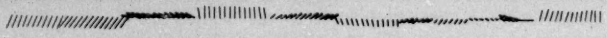

Figure 3. A typical record of the phase and amplitude of the transferred modulation at frequencies 60, 120, 300, 500, 700, 1,000, 1,250, 1,500 and 2,000 c/s.

With this apparatus it is possible to obtain about twelve readings of the phase and amplitude of the transferred modulation in 30 seconds with an accuracy far above that obtained by the visual method used before. A complete variation of modulation frequency in steps from 60 c/s. to 2,000 c/s. can be made in four minutes. It is possible, on account of the great discrimination of the phase-sensitive rectifier against noise, to measure transferred modulation of the order of 0·1% in the presence of noise and adjacent channel interference.

§ 3. THE COLLISION FREQUENCY AT A KNOWN HEIGHT

In I it was shown that the phase difference ϕ between the modulation received via the path DR and that received via the path DBR (Figure 1) is related to the modulation frequency by the equation

$$\phi = \tan^{-1}\frac{2\pi f}{Gv} + \frac{2\pi f d}{\mathbf{c}},$$

where d is the difference of the lengths of the two paths, f the modulation frequency, ν the collision frequency of the electrons in the region of cross-modulation, and G the energy loss factor.

From observations of ϕ at different modulation frequencies it is possible to determine both ν and d. If the trajectory of the wanted wave can be determined, it is then possible from geometrical considerations to determine the point on the trajectory at which cross-modulation occurs.

The actual path of the wanted wave through the ionosphere is not known, but the equivalent triangulated path can be determined by observing the delay between pulses from the transmitter received via the ionosphere and those received directly along the ground. It is important to notice that the assumption is made here, and also in the phase-frequency equation quoted above, that the velocity of propagation of the waves in the ionosphere is equal to the velocity in free space, and that the wanted wave follows a linear path from the transmitter to the receiver with a sharp change of direction at the virtual level of reflection. The consequences of these assumptions will be examined in the Appendix.

The transmitters used in these experiments were normal B.B.C. stations situated at Stagshaw and Ottringham (see map of Figure 7). Stagshaw radiated the wanted signal of 1,050 kc/s. and Ottringham the disturbing wave on a frequency of 167 kc/s.*

The distance from Cambridge where the receiver was situated, and the power of the Stagshaw station were such that a ground wave which was, in general, small compared with the wave reflected from region E at night, reached the receiver.

* I am indebted to the B.B.C. for allowing these transmitters to be used for the experiments.

It was therefore possible to determine the equivalent path of the wanted wave. At the same time, the intensity of the ground wave was not sufficiently high to upset the phase measurements (see Appendix of paper I).

Experiments were so arranged that a short pulse transmission from the wanted station preceded and followed each determination of ν and d from the modulation run. In this way the equivalent height of reflection of the wanted wave was determined at intervals of about four minutes throughout the night.

Figures 4 (*a*) and 4 (*b*) show the values of $G\nu/2\pi$ and the heights of the region of cross-modulation throughout the nights of 28th April 1949 and 5th June 1949. A striking difference in the curves is immediately obvious, a difference which will be discussed later. On three occasions on which measurements of collision

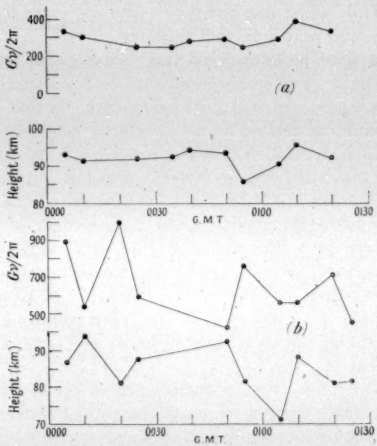

Figure 4. Values of $G\nu/2\pi$ and heights of regions of cross-modulation on (*a*) a quiet night, and (*b*) a disturbed night.

frequencies and the associated heights of the region of cross-modulation have been made throughout the night, the following average results were obtained :

28th April 1949. $G\nu/2\pi = 307$, $\nu = 1{\cdot}48 \times 10^6$, height = 91·7 km.
5th June 1949. $G\nu/2\pi = 552$, $\nu = 2{\cdot}66 \times 10^6$, height = 86·1 km.
21st June 1949. $G\nu/2\pi = 612$, $\nu = 2{\cdot}96 \times 10^6$, height = 86·5 km.

Of these results, the first is undoubtedly the most accurate since the measurements on this occasion showed that conditions remained constant, the mean deviation in the value of the collision frequency being $\pm 15\%$. As far as the height measurement is concerned, although the equivalent height can be measured from the observations to an accuracy of within $\pm 1\%$ it does not necessarily represent the actual height of the region of cross-modulation. Considerations elaborated in the Appendix indicate, however, that although the real height may be a little lower than the equivalent height, the difference is not greater than 2·5 kilometres.

The last two results are practically identical, and if we take their average and combine with the first result, the scale height of the atmosphere at this level may be deduced. This calculation gives $H = 8{\cdot}5$ km. a result in good agreement with those obtained by other methods. On account of the rather small difference in the heights at which the two measurements were made no great accuracy is claimed for this determination of scale height.

§ 4. VARIATIONS IN THE MEASURED VALUE OF ν

On the majority of occasions on which measurements were made throughout the night, graphs of $G\nu/2\pi$ and heights of the region of cross-modulation had the form shown in Figure 4(*b*). Only very seldom were conditions as stable as those shown in Figure 4(*a*), when measurements over an extended period of time were constant or showed only a smooth variation.

It might at first sight be considered that variations in the value of $G\nu/2\pi$ mean merely that the level of cross-modulation had changed, due, perhaps, to some irregularity or inhomogeneity in the ionosphere. If this were the case, the values of $G\nu/2\pi$ should be related to the measured heights by the usual scale height formula. No such relation is found and indeed, on many occasions, an increase of $G\nu/2\pi$ is associated with an increase of height and vice versa.

A change in the value of $G\nu/2\pi$ and in the height of the region of cross-modulation could be brought about by the displacement of *one* point of the phase-frequency curve by a large amount from its normal position. Such a change of phase could easily be produced by selective fading although it is unlikely that this effect would persist for 30 seconds (i.e. the time of measurement on each modulation frequency). In any case, it was found that on the majority of occasions the phase-frequency curve was of the normal type, with all the points lying nicely on the curve.

To help in relating this type of disturbance to other disturbances in the ionosphere a ' disturbance figure ' for measurements of collision frequency has been defined. The disturbance figure k_ν is obtained by multiplying the maximum spread of values of $G\nu/2\pi$ by the number of times the curve relating $G\nu/2\pi$ and time changes direction, and dividing by the total number of points in the interval considered. This somewhat arbitrary process leads to values of the disturbance figure which fit in well with intuitive ideas of the disturbance on different occasions.

Attempts have been made to correlate k_ν with: (1) the magnetic K indices, (2) the disturbance of propagation conditions of long waves (data were kindly supplied by Dr. K. Weekes of the Cavendish Laboratory), (3) the incidence of sporadic E ionization, (4) meteoric activity.

As far as (1), (2) and (3) are concerned, there appears to be no correlation. With meteoric activity, it is not easy to draw any definite conclusions on account of the rather small amount of meteoric data available for the nights on which experiments were carried out. It may, however, be significant that on the very few occasions on which conditions were not disturbed, no meteoric showers were forecast, whereas on all other occasions showers of varying intensities were expected to occur.

In the absence of further information, it is not safe to draw definite conclusions. It is hoped that more definite results, one way or the other, will be obtained when the analysis of certain records of meteoric activity has been completed.

§ 5. THEORETICAL CALCULATION OF THE ABSOLUTE MAGNITUDE OF CROSS-MODULATION

The theory of ionospheric cross-modulation proposed originally by Bailey and Martyn (1934) and adapted recently (Ratcliffe and Shaw 1948, Huxley *et al.* 1948, Huxley and Ratcliffe 1949) to conform with the nomenclature of Appleton's magneto-ionic theory, gives an expression for the modulation impressed by a disturbing wave of known field strength upon a wanted wave passing simultaneously through a medium of uniform electron density and collision frequency. In attempting to apply this theory to the ionosphere we must first make assumptions about the variation of electron density and collision frequency with height. We must remember also that the field strength of the disturbing wave is itself reduced in its passage through the ionosphere in a way which depends upon the assumptions made. We shall then be in a position to calculate the modulation transferred at each level of the ionosphere. If the calculation is done in this way it becomes apparent that the reduction in the field strength of the disturbing wave in any narrow layer in the ionosphere is closely related to the amount of modulation transferred in that layer and that, in a straightforward case the amount of transferred modulation can be related to the reduction in amplitude of the disturbing wave without a detailed knowledge of the distribution of electron density. This important fact was pointed out to me by Mr. J. A. Ratcliffe and I am indebted to him for indicating the following simple way of making the calculation.

Let T_0 be the coefficient of modulation transferred from a disturbing wave to a wanted wave at a modulation frequency approaching zero. Suppose $\mathscr{P}$ is the power flux per unit area of the disturbing wave at the region of cross-modulation. The energy left per second in an elementary slab of unit area and thickness δx is $-(\partial\mathscr{P}/\partial x)\delta x$ and this energy is taken up by the electrons in the slab in the process of absorption. If the electron density is N and if P is the power expended on each electron in the slab by the disturbing wave, then

$$PN\delta x = -\frac{\partial\mathscr{P}}{\partial x}\delta x, \text{ i.e. } P = -\frac{1}{N}\frac{\partial\mathscr{P}}{\partial x}.$$

When the disturbing wave has been acting long enough to establish equilibrium conditions a stage is reached at which, on the average, the energy gained by an electron per second from the disturbing wave is equal to the energy lost to molecules in collisions. We then have $P = \nu G\Delta Q$ where ν is the collision frequency of electrons with molecules. G is the energy loss factor which defines the average proportion of its excess energy lost by an electron in a collision. ΔQ is the difference between the energies of the electrons and the surrounding gas molecules.

The electron energy Q is given by

$$Q = \tfrac{1}{2}mv^2 = \tfrac{1}{2}ml^2\nu^2,$$

where m is the mass of the electron, v is its velocity, l the mean free path and ν the collision frequency. Then $\Delta Q = ml^2\nu\Delta\nu$ and the change $\Delta\nu$ in the collision frequency of the electrons is given by

$$\Delta\nu = \frac{\Delta Q}{ml^2\nu} = \frac{P}{\nu Gml^2\nu} = \frac{P}{3G\boldsymbol{k}\theta}$$

since

$$Q = \tfrac{1}{2}\,ml^2\nu^2 = \tfrac{3}{2}\,\boldsymbol{k}\theta,$$

where $\boldsymbol{k}$ is Boltzmann's constant and θ is the temperature in degrees Kelvin.

From a consideration of the exponential law describing the absorption of a radio wave in the ionosphere, it can be seen that the element dT_0 of cross-modulation impressed upon a vertically travelling wanted wave by virtue of the change in collision frequency is given by $dT_0 = \Delta\kappa_W \delta x$ where κ_W is the coefficient of absorption of the wanted wave.

If it is assumed that $p_W^2 \gg \nu^2$*, then κ_W may be written in the form $\kappa_W = \alpha(p_W)N\nu$ where $\alpha(p_W)$ is a function of the angular frequency of the wanted wave and the natural gyro-frequency, and depends upon the conditions of propagation.

Then over the region δx

$$dT_0 = \alpha(p_W)N\Delta\nu\delta x = \alpha(p_W)\frac{NP}{3G\boldsymbol{k}\theta}\delta x$$

$$= -\alpha(p_W)\frac{1}{3G\boldsymbol{k}\theta}\frac{\partial\mathscr{P}}{\partial x}\delta x.$$

It should be noticed that, in this equation, neither of the quantities N and ν appear explicitly, and that the amount dT_0 of modulation transferred is related directly to the change $(\partial\mathscr{P}/\partial x)\delta x$ of the power flux of the disturbing wave as it passes through the element of ionosphere concerned. It is therefore possible to integrate and to obtain an expression for the total amount of transferred modulation in the passage through a layer of finite thickness in terms of the total decrease of power flux of the disturbing wave, and without any further assumptions about the variations of N and ν through the layer. We then obtain

$$T_0 = \int dT_0 = -\frac{\alpha(p_W)}{3G\boldsymbol{k}\theta}\int_{h_1}^{h_2}\frac{\partial\mathscr{P}}{\partial x}\delta x$$

$$= \frac{\alpha(p_W)}{3G\boldsymbol{k}\theta}(\mathscr{P}_1 - \mathscr{P}_2). \qquad \ldots\ldots(1)$$

This result holds for a wave travelling upwards through the ionosphere. If a downcoming reflected wave is added, it can be shown that our result still holds if $\mathscr{P}_1$ represents the power flux in the wave as it begins its upward journey, and $\mathscr{P}_2$ that as it returns to the earth.

Equation (1) can be used to calculate the modulation transferred when both waves travel vertically and traverse the same region. But we know that the heights of reflection of different frequencies are different, and we must consider in more detail which parts of the region the waves traverse together. Let us call the wanted wave W and the disturbing wave D, and let their vertical paths be represented diagrammatically in Figure 5. We shall assume that D has the lower frequency and is reflected from the lower level. We further assume that for each wave the absorption is important only above the level where $\nu = (p_W + p_L)$ or $\nu = (p_D + p_L)$† (the shaded regions in the figure). It is clear in this case that the whole of the power absorbed from D will be effective in producing cross-modulation, and equation (1) applies. Absorption of W in regions where D is not absorbed (e.g. above the level of reflection of D) will not produce cross-modulation, and is equivalent merely to a decrease in the power of the wanted station.

* The assumption $p_W^2 \gg \nu^2$ is appropriate to the ordinary magneto-ionic component in quasi-transverse propagation. In the quasi-longitudinal case, the corresponding assumption is $(p_W + p_L)^2 \gg \nu^2$.

† This point is discussed by Farmer and Ratcliffe (1935).

If the frequency of D is greater than that of W, D is reflected from the higher level and the lettering in Figure 5 is reversed. The term $(\mathscr{P}_1 - \mathscr{P}_2)$ in equation (1) does not now refer to the total power lost from D in its passage through the ionosphere. If equation (1) is to be used in this case, we are forced again to make assumptions about the electron distribution to decide what proportion of the total power lost by D is effective in producing cross-modulation. Alternatively, by comparing the observed and calculated values of cross-modulation in cases such as these we may obtain an estimate of the ionization density gradient in the region. Considerations of this nature lead to the deduction of ionization gradients discussed in §9.

If D and W are incident obliquely upon the ionosphere the situation is more complicated. The oblique incidence case is represented diagrammatically in Figure 6.

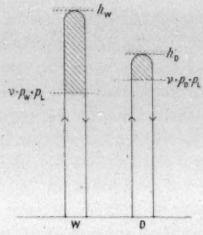

Figure 5. The relative positions of regions of appreciable absorption of wanted and disturbing waves for normal incidence.

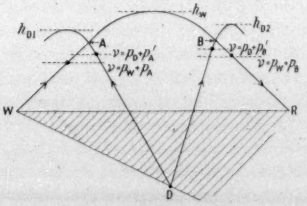

Figure 6. The relative positions of regions of appreciable absorption of wanted and disturbing waves for oblique incidence.

The value of p_L to be used for each wave depends upon the angle between the direction of propagation of the wave and the earth's magnetic field. For the wanted wave, we shall call the appropriate value of p_L for the upgoing portion of the trajectory p_A, and for the downcoming portion p_B. For the disturbing wave we shall call the appropriate value of p_L, p_A' for the wave producing cross-modulation in region A and p_B' for that producing cross-modulation in region B.

Consider first region A. If the frequencies and directions of propagation of the waves are such that $h_W > h_{D1}$, and $(p_W + p_A) > (p_D + p_A')$ we have the case where the region of absorption of W completely encloses the region of absorption of D. We shall assume, as a reasonable approximation, that the trajectory of W is

straight over the region of cross-modulation, so that equation $dT_0 = \Delta\kappa_W \delta x$ is replaced by $dT_0 = \Delta\kappa_W \delta x \sec i_W$ and equation (1) becomes

$$T_0 = \frac{\alpha(p_W)_A}{3Gk\theta} \sec i_W (\mathscr{P}_1 - \mathscr{P}_2)_A.$$

Similarly for region B we have

$$T_0 = \frac{\alpha(p_W)_B}{3Gk\theta} \sec i_W (\mathscr{P}_1 - \mathscr{P}_2)_B.$$

In practice it is generally found that since the disturbing station is somewhat to one side of the plane of propagation of the wanted wave, that the ' angles of fire ' of the disturbing station to the regions A and B are not greatly different. Hence $(\mathscr{P}_1 - \mathscr{P}_2)_A$ will be nearly equal to $(\mathscr{P}_1 - \mathscr{P}_2)_B$ and the final equation may be written

$$T_0 = \frac{\alpha(p_W)_A + \alpha(p_W)_B}{3Gk\theta} (\mathscr{P}_1 - \mathscr{P}_2) \sec i_W. \qquad \ldots\ldots(2)$$

It might be argued that in the case of oblique incidence the disturbing wave after reflection does not pass again through the region of cross-modulation as is the case with normal incidence. Hence for oblique incidence, the term $(\mathscr{P}_1 - \mathscr{P}_2)$ should not refer to the total loss of power of the disturbing wave but only to that absorbed on the upward trajectory. This is, in fact, true, but we have reason to believe that the maximum loss of power per unit distance occurs before the disturbing wave reaches its level of reflection (see § 9) and that the power remaining for absorption on the downward path is a relatively small fraction of the incident power. It must be remembered also that although the particular trajectory which we have considered will not pass again through the region of cross-modulation, a wave which leaves the disturbing transmitter at a slightly greater angle of elevation will, after reflection, pass through the region of cross-modulation. It appears therefore, that as a good working approximation, we may take $(\mathscr{P}_1 - \mathscr{P}_2)$ in the oblique incidence equation to refer to the total power loss on the double journey through the absorbing region.

There may, of course, be conditions for which $h_D > h_W$ or for which the lower edge of the absorption region for the disturbing station is below the corresponding level for the wanted station. A knowledge of the angles of incidence of the two waves on the ionosphere and of the angles between the directions of propagation of the various waves and the earth's magnetic field is sufficient to determine, for give values of p_W and p_D, whether the conditions illustrated in Figure 6 apply. In the majority of cases which have been investigated experimentally the conditions illustrated do apply.

The function $\alpha(p_W)$ is not a complicated one and has, in fact, been discussed by Booker (1935) although not explicitly. Booker has shown that under appropriate conditions, the propagation of a radio wave in the ionosphere may adequately be described by the use of two approximations to the general magneto-ionic formula. These are the quasi-longitudinal (Q.L.) and quasi-transverse (Q.T.) approximations, and conditions are given for which each approximation holds. Applying Booker's criterion, it is found that in England for the frequencies in which we are interested (i.e. up to about 1 Mc/s.) the propagation may generally

be described by the Q.L. approximation except for cases where the direction of propagation is almost exactly perpendicular to the earth's magnetic field, and provided that the frequency is not too near the critical frequency. For example, for a 200 kc/s. wave, the Q.L. approximation holds until the angle between the direction of propagation and the earth's magnetic field is 89°; for 1·4 Mc/s., the Q.L. approximation holds up to 75°. Booker shows also that for wave frequencies less than the local gyro-magnetic frequency (approximately 1·3 Mc/s.) the ordinary component only is reflected, and we need consider, therefore, only the ordinary component of the downcoming wanted wave in our work.

Applying Booker's approximations, the function $\alpha(p_W)$ becomes

(1) Q.L. $$\alpha(p_W)=\frac{2\pi e^2}{\epsilon_0 mc}\frac{1}{(p_W+p_L)^2+\nu^2}.$$

(2) Q.T. $$\alpha(p_W)=\frac{2\pi e^2}{\epsilon_0 mc}\frac{1}{p_W{}^2+\nu^2}.$$

If, in addition, the effective radio frequency is large compared with the collision frequency (as is nearly always the case) further simplification may be effected :

(1) Q.L. $$\alpha(p_W)=\frac{2\pi e^2}{\epsilon_0 mc}\frac{1}{(p_W+p_L)^2}.$$

(2) Q.T. $$\alpha(p_W)=\frac{2\pi e^2}{\epsilon_0 mc}\frac{1}{p_W{}^2}.$$

§ 6. COMPARISON OF CALCULATED AND OBSERVED MAGNITUDES

In view of the simplicity of equation (1) and its extension, equation (2), for oblique incidence, it is no difficult matter to make a comparison of the observed and calculated values of cross-modulation for different pairs of stations. This comparison is tabulated. The following assumptions have been made in the calculation :

(i) The disturbing wave is completely absorbed in the region of cross-modulation. If the reflection coefficient is about $\frac{1}{3}$, about 90% of the incident energy is absorbed so that this assumption will not lead to any great error.

(ii) The wave radiated from the disturbing transmitter is assumed to have a cosine angular distribution of intensity in the vertical plane. This is probably very nearly correct in the case of the long wave stations but may not be correct for the medium wave disturbing stations.

(iii) The region of absorption of the disturbing wave (as discussed in § 5 above) is contained entirely within the region of absorption of the wanted wave. This is generally, but not invariably, the case in our experiments.

(iv) The temperature of the ionosphere is taken as 300° K.

(v) The energy loss factor G is taken as $1{\cdot}3\times10^{-3}$ according to a recent determination by Huxley and Zaazou (1949).

In making the calculation it is first decided whether the propagation of the wanted wave through the region of cross-modulation can be described by use of the Q.L. or Q.T. approximations. If the former is the case, the required values of p_L for the upgoing and downcoming parts of the trajectory are calculated from the gyro-magnetic frequency and the angles between the earth's

magnetic field and the appropriate parts of the trajectory. The two values of $\alpha(p_w)$ are then found.

Disturbing Station	Frequency (kc/s.)	Power (kw.)	Wanted Station	Frequency (kc/s.)	Magnitude of T_0 (%) Calc.	Obs.
Ottringham	167	120	Westerglen	767	3·7	6
			Lisnagarvey	1050	1·6	1
			Droitwich	1050	1·4	3
			Ottringham	1122	0·7	0·5
			Stagshaw	1050	1·8	2
Droitwich	200	180	Lisnagarvey	1050	4·3	4
			Droitwich	1050	1·2	1·5
			Washford	804	2·6	2
			Decca	70	2·2	<0·1
Rubgy	68	80	Lisnagarvey	1050	1·7	<0·1
Moorside Edge	668	100	Lisnagarvey	1050	3·6	2
Ottringham *	167	120	Droitwich	200	13	10–20

* The observations on this pair of stations were made in Copenhagen by Professors Rybner and Nielsen, and I am indebted to them for permission to quote this result.

The map of Figure 7 shows the approximate positions of the stations used; each station is marked with the initial letter of its name, and the Decca Navigation Station mentioned is situated at Warwick. The receiving station was at Cambridge in all cases. The Post Office transmitter at Rugby is constructed for single sideband telephony. It was used as a disturbing station in two different

Figure 7. Map giving positions of transmitters used in the experiments.

ways: in the first method, an audio-frequency tone injected into the speech circuit was keyed on and off, thus producing an intermittent sideband simulating keyed C.W.: in the second method a 1,000 c/s. audio tone was itself modulated at 50 c/s., so that the sideband emitted was effectively a single carrier modulated at 50 c/s. All the measurements, with the exception of those using Decca and Rugby transmitters were made with the automatic apparatus.

The agreement between the calculated and observed values is seen to be quite good except in the two cases where very low frequency stations are concerned.

In the case of Droitwich 200 kc/s. disturbing Decca 70 kc/s. the disagreement may be due to the fact that the level of reflection of the 200 kc/s. wave is above that of the wanted wave (i.e. assumption (iii) above does not hold). For Rugby 68 kc/s. disturbing Lisnagarvey, 1,050 kc/s. it is difficult to see why the calculated and observed values do not agree.

The agreement in the majority of cases is of importance in view of the fact that the absorption of the wanted wave at oblique incidence is involved. The phenomenon of cross-modulation offers a powerful method of investigating the absorption of radio waves incident obliquely upon the ionosphere, uncomplicated by considerations of the loss of energy by scattering and similar processes. It appears from these results that the true absorption of a wave incident obliquely upon the ionosphere at night can be calculated by the straightforward application of the magneto-ionic formula when due attention is paid to the increase in the length of the path of the wave in the region of absorption, and to the change in the value of p_L brought about by the obliquity of the trajectory.

§7. VARIATION OF CROSS-MODULATION AT DAWN

Since the absorption of radio waves in the ionosphere begins to increase at dawn it might be expected that the depth of modulation should also increase. Previous experiments by Ratcliffe and Shaw (1948) using Lisnagarvey 1,050 kc/s. as wanted station and Droitwich 200 kc/s. as disturbing station showed, however, that the depth of transferred modulation decreased at sunrise. This result is difficult to understand, and in order to gain more information on the subject experiments have been carried out on different pairs of stations on frequencies separated as widely as possible. Combinations of stations for which results have been obtained are:

(1) Droitwich 200 kc/s. disturbing Lisnagarvey 1,050 kc/s.
(2) Ottringham 167 kc/s. disturbing Westerglen 767 kc/s.
(3) Ottringham 1,340 kc/s. disturbing Westerglen 767 kc/s.
(4) Moorside Edge 668 kc/s. disturbing Lisnagarvey 1,050 kc/s.

All the results show a decrease in cross-modulation as sunrise approaches. The decrease begins about 80 minutes before sunrise at ground level, a time which corresponds to sunrise at a level of about 100 km. at this latitude in summer when the experiments were made. By the time of ground sunrise there is generally only an extremely small amount of transferred modulation remaining. It should be noticed that Huxley (1950) has recently published experimental evidence which appears to show, on the contrary, an increase in the depth of cross-modulation at dawn. In the light of our own experimental results we shall assume that there is a decrease of cross-modulation at dawn and shall consider possible theoretical reasons for it.

In order that cross-modulation should occur, it is necessary that both the wanted and disturbing waves should be absorbed in the same region of the ionosphere. It might be considered then, that the decrease at dawn is due to the fact that the regions of absorption of the two waves no longer overlap.

We have seen that the absorption of a radio wave of angular frequency p is most important between the level where $(p+p_L)=\nu$ and the level of reflection. In the cases of Droitwich 200 kc/s. disturbing Lisnagarvey 1,050 kc/s. and

Ottringham 167 kc/s. disturbing Westerglen 767 kc/s., the regions of absorption of the disturbing waves are contained entirely within the regions of absorption of the wanted waves and no alteration of the ionization density, or of its gradient, at dawn can alter the disposition of the absorbing regions. It follows, therefore, that at dawn, as the absorption of the disturbing wave increases, the term $(\mathscr{P}_1-\mathscr{P}_2)$ in equation (1) increases, and the cross-modulation should increase also. The decrease at dawn cannot, therefore, be explained in these cases on the hypothesis that the regions of absorption of the two waves drift apart as dawn approaches.

Were there appreciable absorption of the disturbing station below the region where $(p_D+p_L)=\nu$, the effect would be to reduce considerably the effective power of the disturbing station penetrating to levels higher than this, and hence to reduce the cross-modulation. But absorption below the region where $(p_D+p_L)=\nu$ is independent of frequency (the coefficient of absorption proportional to N/ν) and if such a region is responsible for the increase of absorption of the disturbing wave, then it must be equally effective for the wanted wave, and therefore there must be an increase in the cross-modulation.

By no mechanism of change of reflection height or absorbing levels does it seem possible to explain the dawn decrease of cross-modulation in all cases.

It will be remembered that in the derivation of equation (1) the assumption was made that $(p_W+p_L)^2 \gg \nu^2$. If this restriction is removed and if it is assumed that ν is approximately constant over the region of cross-modulation the final equation becomes

$$T_0=\frac{2\pi e^2}{\epsilon_0 mc}\,\frac{1}{3Gk\theta}\,\frac{(p_W+p_L)^2-\nu^2}{\{(p_W+p_L)^2+\nu^2\}^2}(\mathscr{P}_1-\mathscr{P}_2). \qquad \ldots\ldots(3)$$

From this equation it is seen that any variation of the collision frequency caused by the absorption of the disturbing wave at the level where $\nu=(p_W+p_L)$ cannot cause cross-modulation.

The region in the ionosphere where cross-modulation is most important is that where the absorption per unit distance of power from the disturbing wave is a maximum. The loss of power per unit distance at a given level depends upon (1) the coefficient of absorption at that level, and (2) the amount of power left in the wave when it reaches the level concerned. As dawn approaches, there is a general increase in the ionization density at all levels of the ionosphere and a change from a steep gradient of ionization in the lower levels of region E to one which is rather less abrupt. Both of these effects will cause the level of maximum absorption per unit distance to become lower (i) because the coefficient of absorption at a given level is increased, and (ii) because the overall attenuation is increased so that the amount of power remaining in the wave when it reaches a given level is decreased.

If the change in the ionization density and gradient is sufficiently great to bring the level of maximum power loss of the disturbing wave down near to the level at which $\nu=(p_W+p_L)$, then, as shown by equation (3), the cross-modulation will decrease to a very small value.

If this is the true explanation of the dawn decrease of cross-modulation, the values of $G\nu/2\pi$ should increase as the amplitude of the cross-modulation decreases. There are indications that this increase does take place, though it has not been established definitely in our experiments. The reasons for this are (i) a large

value of $Gv/2\pi$ gives a phase-frequency curve that is nearly a straight line and the consequent analysis is difficult and inaccurate, and (ii) the associated sudden decrease in amplitude renders it all the more difficult to make the measurements accurately.

§8. CROSS-MODULATION ON THE GYRO-FREQUENCY

Bailey (1937, 1938) predicted that if the disturbing wave had a frequency equal to the local gyro-magnetic frequency there should be strongly enhanced cross-modulation brought about by the great increase in ionospheric absorption. Cutolo (1947) has obtained some experimental evidence in support of this idea, for he claims to have observed depths of transferred modulation of the order of 3% with disturbing stations of 5 or even 1 kilowatt power. This result would correspond to depth of modulation of more than 100% with powers of 100–200 kilowatts such as we use.

Experiments have been carried out to look for an increased cross-modulation when the disturbing station radiated on the gyro-frequency. Westerglen 767 kc/s. was used as the wanted station, and Ottringham, 120 kw., on 1,122, 1,312, and 1,474 kc/s. as the disturbing station. Over about 24 hours' observation on different nights, no significant difference was found in the depth of transferred modulation. It was considered that the frequencies might have been too widely separated and that a sharp resonance effect could possibly have been overlooked.

For this reason a more complicated experiment was planned and carried out with the cooperation of the B.B.C.* The frequency of the disturbing station at Ottringham was varied from 1,325 kc/s. to 1,355 kc/s. in steps of 5 kc/s. The radiated power was of the order of 100 kw. On each radio frequency, tone modulation at 60 c/s. was radiated for two minutes and a measurement of the depth of modulation made at two-second intervals. Thus each measurement was the mean of about 60 readings. The whole run from 15 kc/s. on one side of the calculated gyro-frequency to 15 kc/s. on the other side was repeated twice each night, and the whole experiment was repeated on four nights.

When the depth of modulation for any particular run from 1,325 to 1,355 kc/s. was plotted as a function of frequency, it was found that there were quite large variations in the depth of modulation from frequency to frequency. But points of high cross-modulation did not repeat from one experiment to the next, and these variations must therefore be attributed to changes in the ionosphere. When the means of all observations were plotted as a function of the frequency of the disturbing station there was found to be practically no variation of the depth of cross-modulation with frequency. The general level of cross-modulation in these experiments was about 3%.

Engineers of the B.B.C., using an entirely different technique of measurement and situated at a different receiving point, also carried out measurements during these tests. Their observations agree completely with those obtained at Cambridge in showing no sign of a maximum at the gyro-frequency.*

We now consider the matter from the theoretical standpoint. In the equation

$$T_0 = \frac{\alpha(p_w)}{3Gk\theta}(\mathscr{P}_1 - \mathscr{P}_2)$$

* I am indebted to Mr. H. L. Kirke, Head of the Research Department of the B.B.C., for arranging for these observations to be made and for permission to quote the results.

it is the term $(\mathscr{P}_1 - \mathscr{P}_2)$ which determines the behaviour of T_0 as the frquency of the disturbing station is altered. For a disturbing wave of low frequency, say 200 kc/s., the reflection coefficient of region E at night is of the order of 0·2. This means that about 96% of the total incident power remains in the ionosphere.

Now consider a disturbing wave of frequency equal to the local gyro-magnetic frequency. The coefficient of absorption per unit path in the ionosphere may be many hundreds of times greater than that of the low-frequency wave, but it is the term $(\mathscr{P}_1 - \mathscr{P}_2)$ which is important, and this can never be greater than $\mathscr{P}_1$. The cross-modulation with the disturbing station on the gyro-frequency can thus be only about 4% greater than that for the low-frequency disturbing station.

We conclude, therefore, that there is not likely to be any great increase in the cross-modulation when the disturbing station radiates on the local gyro-frequency. This theoretical conclusion is in agreement with our experimental results.

In his discussion of the phenomenon of gyro-resonant cross-modulation, Bailey made detailed calculations of a special hypothetical case where the disturbing wave was on the gyro-frequency and the wanted wave on a frequency of about 50 kc/s. and showed that the transferred modulation would be unusually great (20% for 100 kw. power radiated by the disturbing station). It is of interest to examine Bailey's result in detail, and to relate it to our conclusions.

Examination shows that the large value of the cross-modulation is brought about, in the main, by the large absorption of the wanted wave under the chosen conditions, and that the increase of the collision frequency of the electrons with the change of frequency of the disturbing station is relatively unimportant. Translating Bailey's nomenclature to ours, the change in $(\mathscr{P}_1 - \mathscr{P}_2)$ is unimportant, but the large value of the cross-modulation is brought about by a greatly increased value of $\alpha(p_W)$.

§ 9. SOME FURTHER POINTS

(i) *Gradients of Ionization Density*

From a consideration of the difference between the calculated and observed value of cross-modulation in the cases where the two regions of absorption do not completely overlap it is possible to make an estimate of the gradient of the ionization in the lower part of region E at night. For instance, in the case of Droitwich 200 kc/s. disturbing a transmission from the Decca Navigation station on 70 kc/s., the low value of cross-modulation can be explained on the assumption of an ionization density which increases by a factor of 1·7 per kilometre height.

Ottringham 167 kc/s. disturbing Westerglen 767 kc/s. gives 6% cross-modulation, whereas Ottringham 1,112 kc/s. disturbing the same station gives only 2%. The geometrical arrangement and the frequencies of the second pair of stations are such that the level of reflection of the 767 kc/s. wave is below that of the 1,122 kc/s. disturbing wave. Again this gives sufficient data for the calculation of an ionization gradient and the factor of increase is here found to be 1·6 per kilometre.

The calculations are approximate and the good agreement between the two cases must be regarded as fortuitous, but the order magnitude may be assumed to be correct. For purpose of comparison, it may be pointed out that this gradient is considerably steeper than the maximum gradient of a Chapman region with a scale height of 10 kilometres. This figure supports the impressions gained from other experiments that, at night, the lower part of region E is sharply bounded.

(ii) *Position of Region of Cross-Modulation*

Reference once again to equation (1) leads to the conclusion that the level at which cross-modulation occurs is controlled by the absorption of energy from the disturbing wave alone. It is to be expected that the level of maximum cross-modulation will be that level at which the power extracted from the disturbing wave per unit distance is a maximum. At any level the power absorbed from the wave will depend upon the coefficient of absorption and upon the power entering the level. If the gradient of ionization density in region E at night is as great as we have calculated, then the coefficient of absorption must increase rapidly with height. It might reasonably be expected, therefore, that the region of maximum power loss from the disturbing wave will be somewhere near, though not necessarily at, its level of reflection. It is further to be expected that, provided the geometrical conditions are the same, the heights of the regions of cross-modulation for different wanted stations acted upon by the same disturbing station will be identical.

The first point was checked in experiments in which Ottringham 167 kc/s. disturbed a wave from Stagshaw 1,050 kc/s. In these experiments all the necessary heights are known, and using our calculated value of the ionization gradient, it can be shown that the level of cross-modulation is about 2 kilometres below the level of reflection of the wanted wave. This is in reasonable agreement with the ideas outlined above.

The second point was verified by experiments carried out with two wanted transmitters at Westerglen, radiating on 767 kc/s. and 1,149 kc/s.; the disturbing station was Ottringham in both cases. The average values of $G\nu/2\pi$ measured on the two wanted stations were 671 and 668, showing that the level at which cross-modulation takes place is independent of the frequency of the wanted station.

(iii) *Cross-Modulation with High-power Disturbing Station*

According to the full theory of cross-modulation (Ratcliffe and Shaw 1948) the depth of the cross-modulation should be directly proportional to the power of the disturbing station, and to its depth of modulation, provided that the increase of the energy of the electrons due to absorption is not comparable with their mean thermal energy. In other words, proportionality to power and depth of modulation of the disturbing station holds so long as $P/G\nu \ll Q_0$.

Experiments in which a wave from Westerglen 767 kc/s. was disturbed by Ottringham 167 kc/s. radiating 173 kw., 346 kw. and 520 kw., showed that even at the highest power used, the depth of the transferred modulation was still proportional to the power of the disturbing station. From this we may deduce that the increase in electron temperature due to absorption is certainly not greater than 10% of the mean thermal value, even when 520 kw. of power are radiated from the disturbing station.

Other experiments, in which the depth of modulation of the disturbing station was varied gave, as expected, a completely linear relation between the transferred modulation and the depth of modulation of the disturbing station.

(iv) *The Energy Loss Factor*

Ratcliffe and Shaw in I used the value $G = 2{\cdot}6 \times 10^{-3}$. In this paper the value used, $1{\cdot}3 \times 10^{-3}$, is the result of a more recent determination of the quantity by Huxley and Zaazou (1949). Some of the experiments which have been carried

out are capable of being used to give some idea of the magnitude of G in the ionosphere. This is important for the following reason: Laboratory experiments indicate that G is a function of Z/p, where Z is the accelerating field and p the pressure of the gas. Although the actual value of Z/p which obtains in the ionosphere for the disturbing powers used in these experiments is approximately equal to that used in the laboratory determination, the actual values of Z and p separately are far larger in the laboratory determination than in the ionosphere. It is important to know whether the assumption that G is a function of Z/p holds over the rather large range of values of Z and p involved.

If cross-modulation takes place below the level where $\nu=(p_W+p_L)$, equation (3) shows that there will be a change of phase of 180° compared with the more normal conditions. If we take the greatest value of $G\nu/2\pi$ measured, for which the normal phase relationship applies, we know then that the value of ν deduced from this maximum value of $G\nu/2\pi$ must be less than (p_W+p_L). If we assume this upper limit for the value of ν we can deduce a lower limit for the value of G. For the case of Droitwich disturbing Lisnagarvey we find $G>0{\cdot}9\times10^{-3}$ and for Ottringham disturbing Westerglen, $G>1{\cdot}2\times10^{-3}$.

The experiments with the high power disturbing station can also give a lower limit to G if the temperature of the ionosphere is assumed. Taking the temperature to be 300° K. we find $G>0{\cdot}6\times10^{-3}$.

None of our experiments gives an upper limit to G, but the good agreement between the calculated and observed magnitudes of the cross-modulation using $G=1{\cdot}3\times10^{-3}$ is reassuring.

The above results show that it appears safe to assume that the value of G determined for air in the laboratory holds also for the ionosphere.

ACKNOWLEDGMENTS

The radio transmissions without which the experiments described in this paper could not have been carried out were provided by the British Broadcasting Corporation and the Post Office. I gratefully acknowledge the willing co-operation I have received from these organizations. In particular, I should like to thank Mr. H. L. Kirke, Head of the Research Department of the B.B.C., and the Chief Engineer of the Post Office and their staffs. Mr. R. A. Rowden of the B.B.C. has been particularly helpful in arranging transmissions and in suggesting the use of various B.B.C. transmitters.

Mr. J. A. Ratcliffe of the Cavendish Laboratory has at all times shown a keen interest in the work, and I cannot fully express my gratitude for his invaluable help during the course of the experiments, and for criticism and advice during the preparation of this paper.

I have received great help from my colleagues in the Radio Section of the Cavendish Laboratory. I thank in particular Mr. S. W. Falloon and Sir Claude Hagart-Alexander for assistance with apparatus and observations, Mr. H. A. Whale for the use of equipment for the measurement of the equivalent heights of reflection, and Dr. K. Weekes for help with the observations of cross-modulation on the Decca station.

Observations on the transmissions were also made by Professor L. G. H. Huxley and his colleagues at Birmingham, by Professors Rybner and Nielsen in Copenhagen and by engineers of the B.B.C. I have been most fortunate in being able to discuss with them the results they obtained.

I am indebted to the Government of New Zealand for a Rehabilitation Grant which has enabled me to study at the Cavendish Laboratory for the past three years.

The work described in this paper forms part of a programme of radio research supported by the Department of Scientific and Industrial Research at the Cavendish Laboratory.

APPENDIX

Since the experiments described in this paper appear to provide the opportunity for measuring the collision frequency at a known height, it is important to discuss in more detail the accuracy to which that height is known. For this purpose consider Figure 8 in which B represents the region of cross-modulation and in which the actual and triangulated trajectories of the wanted and disturbing waves are shown. To simplify the problem we shall neglect the earth's magnetic field.

As is well known, it can be shown (Breit and Tuve 1926, Appleton 1928) that for any distribution of electron density, the time for a group (pulse) to traverse a certain horizontal component of the actual path is equal to the time required to cover the same horizontal distance by travelling along the triangulated path with the free-space velocity. As a special case, the total time from the transmitter to the receiver is the same for the actual path traversed with the group velocity and the triangulated path traversed with the free-space velocity.*

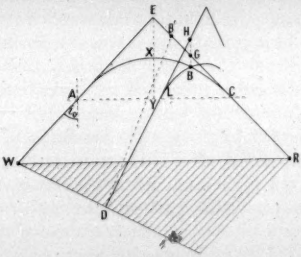

Figure 8. Diagram to illustrate the difference in the heights of the true and deduced regions of cross-modulation.

Now in the cross-modulation experiment mentioned in § 3 we determine the time $t = t'(\mathrm{DLB})\,(f_D) + t'(\mathrm{BCR})\,(f_W)$ where $t'(\mathrm{DLB})\,(f_D)$ and $t'(\mathrm{BCR})\,(f_W)$ represent the times for groups, of frequencies f_D and f_W, to traverse the paths DLB and BCR respectively. But by the theorem just quoted

$$t'(\mathrm{DLB})\,(f_D) = \frac{\mathrm{DH}}{c} \quad \text{and} \quad t'(\mathrm{BCR})\,(f_W) = \frac{\mathrm{GR}}{c}$$

so that the time t corresponds to the passage of the wave over the distance (DH + GR) with the free space velocity.

From the experiment, the triangulated path WER is known and on the simplest theory the apparent region of cross-modulation is located at B′ by a geometrical construction which makes

$$\mathrm{DB'} + \mathrm{B'R} = ct = \mathrm{DH} + \mathrm{GR}.$$

* Breit and Tuve and Appleton prove the theorem only for the total path but the extension mentioned above is implicit in their work.

In the case illustrated the actual region B of cross-modulation is below the calculated region B′.

Before we can decide how far B is below B′ we need some knowledge of the actual trajectory of the wave, which depends upon the distribution of electron density. It will be sufficient for our purpose to assume that the electron gradient is a linear function of the height above the lower edge AYC of the ionosphere. Appleton has shown that with this assumption, the curved parts of the trajectories are parabolae and that

$$\mathrm{EX}=\mathrm{XY}=y_1=\frac{\cos^2 i_0}{\alpha},$$

where i_0 is the angle of incidence, and α is a constant which determines the rate of increase of electron density through the formula $\mu^2=1-\alpha y$, y being the height above the reference level AYC.

The calculation of the difference y_2 of the heights B and B′ is made difficult by the fact that B is not necessarily vertically below B′. In order to get some idea of the uncertainty we may notice that if the cross-modulation takes place near the level AYC, the apparent and true heights will be practically coincident, whereas if cross-modulation takes place at the top of the trajectory of the wanted wave, the maximum uncertainty which can exist will be equal to the maximum difference in the heights of the true and triangulated paths. We shall therefore take this difference (y_1) as giving an approximate maximum value of the uncertainty.

We attempt to estimate y_1 as follows. For waves incident vertically upon the ionosphere the equivalent height of reflection is at a distance $2/\alpha$ above AYC, and for waves incident at an angle i_0, it is at a distance $(2\cos^2 i_0)/\alpha$ above AYC. The difference in equivalent heights measured at vertical and oblique incidence is therefore $(\sin^2 i_0)/\alpha$. Now in the experiments which were carried out with Stagshaw, the equivalent height of reflection for the particular angle of incidence, 60°, was found to be 96 kilometres. The equivalent height at vertical incidence was not actually measured at the time of the experiments, but we may assume, probably without serious error, that it was about 110 kilometres. Hence we have $14=(2\sin^2 60)/\alpha$ whence $\alpha=\frac{1}{10}$ approximately and using this value of α we then obtain $y_1=\cos^2 i/\alpha=10\times\frac{1}{4}=2{\cdot}5$ kilometres.

The uncertainty in the height measurement is seen to be not greater than 2·5 kilometres.

REFERENCES

Appleton, E. V., 1928, *Proc. Phys. Soc.*, **41,** 50.
Bailey, V. A., 1937, *Phil. Mag.*, **23,** 929; 1938, *Ibid.*, **26,** 425.
Bailey, V. A., and Martyn, D. F., 1934, *Phil. Mag.*, **18,** 369.
Booker, H. G., 1935, *Proc. Roy. Soc.* A, **150,** 267.
Breit, G., and Tuve, M., 1926, *Phys. Rev.*, **28,** 554.
Cutolo, M., 1947, *Nature, Lond.*, **160,** 834.
Farmer, F. T., and Ratcliffe, J. A., 1935, *Proc. Roy. Soc.* A, **151,** 370.
Huxley, L. G. H., 1950, *Proc. Roy. Soc.* A, **200,** 486.
Huxley, L. G. H., Foster, H. G., and Newton, C. C., 1948, *Proc. Phys. Soc.*, **61,** 134.
Huxley, L. G. H., and Ratcliffe, J. A., 1949, *J. Instn. Elect. Engrs.*, Pt. III, **96,** 433.
Huxley, L. G. H., and Zaazou, A. A., 1949, *Proc. Roy. Soc.* A, **196,** 402.
Ratcliffe, J. A., and Shaw, I. J., 1948, *Proc. Roy. Soc.* A, **193,** 311.

Some Meteorological Aspects of Radio Duct Formation

By E. KNIGHTING
Meteorological Office, London

Communicated by H. W. L. Absalom; MS. received 16th June 1950, and in amended form 3rd July 1950

ABSTRACT. Three problems of meteorological interest concerning the formation of radio ducts are treated. The first concerns the rate of growth of ducts, with special reference to ducts over the sea; it is shown that ducts form quickly at first and then more slowly as the maximum duct width is approached. The second problem concerns the formation of ducts under conditions of nocturnal cooling; it is shown that there is a limit to the height which the duct may attain. The third problem concerns the width of a radio duct necessary to enclose the track width of a mode associated with a propagated signal of wavelength λ assuming a power law of modified refractive index with height; it is shown that the necessary width is proportional to $\lambda^{2/3}$, and the factor of proportionality, which depends upon the index in the assumed power law, is calculated.

The three problems have a common meteorological basis, for each is concerned with turbulent motion near the earth's surface. The law of turbulent diffusion assumed here is that the coefficient of eddy diffusion is proportional to a power of the height, following the theory developed by O. G. Sutton and others.

§ 1. INTRODUCTION

The following symbols are used: x, z, t, horizontal, vertical and time co-ordinates; u, v, horizontal and vertical velocities; K, eddy diffusivity in the atmosphere, assumed given by $K=az^{1-m}$, a and m being parameters; V, a meteorological variable, either θ the potential temperature in the atmosphere, or q the water vapour content of the atmosphere; α, the critical value of the gradient of V necessary for duct formation, equal to $5{\cdot}4^\circ$ F/100 ft. or $10^{-3}\,^\circ$C/cm. for $V=\theta$, and $-0{\cdot}54$ gm. water vapour/kg. air/100 ft. for $V=q$; ρ, density of the air; c_p, specific heat of air at constant pressure; T, temperature in the earth; K_1, conductivity in the upper layers of the earth; ρ_1, density in the upper layers of the earth; c_1, specific heat in the upper layers of the earth; R, rate of loss of heat by radiation at the earth's surface; λ, wavelength of a propagated signal; μ, ratio of modified refractive index of the atmosphere to that at the surface.

A radio duct is formed in the atmosphere when the variation with height of the modified refractive index obeys certain conditions; in particular there is a surface based duct if the modified refractive index decreases from the surface upwards to a minimum and then increases again, and the top of the duct is at the same height as the minimum of modified refractive index. The variation with height of modified refractive index may be expressed in terms of gradients of temperature and humidity in the atmosphere; if there is a layer above the earth's surface in which the gradient of potential temperature is positive and exceeds $5{\cdot}4^\circ$ F/110 ft. or $10^{-3}\,^\circ$C/cm., then this layer will form a radio duct, and the top of the duct is the height at which the gradient falls below this critical value. This criterion assumes that the humidity remains constant in the vertical, and the duct is termed a 'dry' duct. Similarly if the gradient of specific humidity is negative and is less than $-0{\cdot}54$ gm. water vapour/kg. air/100 ft. a 'wet' duct is formed, it being assumed that the potential temperature remains constant with height.

The temperature and humidity gradients near the earth's surface are controlled by turbulent exchange of heat and water vapour. The three problems treated below are aspects of the same fundamental meteorological problem, the effect of a boundary upon the air mass above it, although there is dissimilarity in the methods of attack. The theory of turbulence developed by Sutton (1949) and others in connection with the diffusion of smoke near the earth's surface is used and this implies taking the coefficient of eddy diffusivity to be a power law of the height above the surface, i.e.

$$K = az^{1-m},$$

where a and m are assumed constant in any one meteorological situation.

The three problems arise in practical forecasting for radio purposes and the object is to give numerical estimates of important quantities arising from the problems.

§ 2. THE RATE OF GROWTH OF RADIO DUCTS OVER THE SEA

When relatively warm dry air flows over the sea, or any cool moist surface, there is turbulent exchange of heat and moisture and a radio duct is formed. No estimate seems to have been made of the time interval for the duct to reach a given height, although the problem is of importance to the meteorologist forecasting for radio purposes.

The problem considered here is associated with the modification of an air mass in juxtaposition with a surface of different physical properties. The conditions assumed are: (*a*) At the lower boundary, $z = 0$, V remains constant; the sea surface is a boundary satisfying this condition approximately both for $V = \theta$ and for $V = q$. (*b*) Above the turbulent layer the boundary condition is the same; V remains constant. This condition is satisfied in the case of a well mixed homogeneous air mass passing over, and being modified in the lower layers by, a surface of different physical properties.

(i) *The Differential Equation*

Assuming that turbulence is horizontally isotropic and that the diffusivity follows a power law, then the governing differential equation is

$$\frac{\partial}{\partial z}\left(az^{1-m}\frac{\partial V}{\partial z}\right) = \frac{\partial V}{\partial t} + u\frac{\partial V}{\partial x} + w\frac{\partial V}{\partial z},$$

where x is measured in the direction of horizontal velocity u. Except in special cases this equation is difficult to deal with; it is noted, however, that if $w = 0$, the term $u(\partial V/\partial x)$ is such as to *increase* the rate of transfer of V, compared with that when $u = 0$, by continuously replacing the air at any point by less modified air. Thus in the case considered the solution of

$$\frac{\partial}{\partial z}\left(az^{1-m}\frac{\partial V}{\partial z}\right) = \frac{\partial V}{\partial t}, \qquad \ldots\ldots(1)$$

will give an *upper* limit to the time required to form a duct of given height. The actual time required may well be much less than that calculated from the above equation, but it cannot be greater.

If the values of V at the boundaries are:

$$V = V_0 \quad \text{at} \quad z = 0, \qquad V = V_1 \quad \text{as} \quad z \to \infty,$$

then the appropriate solution of (1) is

$$\frac{V-V_0}{V_1-V_0} = \frac{1}{\Gamma\{m/(m+1)\}}\int_0^{\psi} e^{-u}u^{\{m/(m+1)\}-1}\,du$$

and

$$\frac{\partial V}{\partial z} = \frac{V_1-V_0}{\Gamma\{m/(m+1)\}}e^{-\psi}\psi^{m/(m+1)}\frac{m+1}{z}, \qquad \ldots\ldots(2)$$

where

$$\psi = \frac{z^{m+1}}{(m+1)^2 at}$$

(ii) *The Maximum Duct Height*

If α is the critical value of the gradient of V at the top of the duct then

$$\alpha = \frac{V_1-V_0}{\Gamma\{m/(m+1)\}}e^{-\psi}\psi^{m/(m+1)}\frac{m+1}{z} \qquad \ldots\ldots(3)$$

is simply an equation in the duct height z and the time t. Noting that $e^{-\psi}\psi^{m/(m+1)}$ has a maximum value at $\psi = m/(m+1)$, then there is an upper limit to the height of the duct z given by

$$z_{\max} = \frac{V_1-V_0}{\Gamma\{m/(m+1)\}\alpha}(m+1)\psi^{m/(m+1)}e^{-\psi}, \quad \psi = \frac{m}{m+1}. \qquad \ldots\ldots(4)$$

This is a somewhat different maximum height from that obtained by considering the steady state, but the two maxima only differ numerically by about 10% in extreme cases. Figure 1 shows the maximum duct width for various values of m.

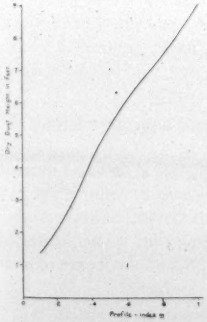

Figure 1. Maximum duct height for values of m. For 1° F. difference between upper and lower boundaries. For difference T° F. multiply d by T. For wet duct multiply d by 10 for each 1 gm. water vap/kg. air difference between upper and lower boundaries.

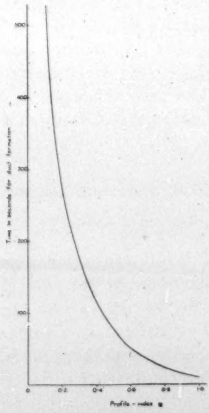

Figure 2. Time in seconds for formation of maximum duct for values of m, assuming $az^{1-m} = 3\times10^8$ at $z = 100$ metres referring to 1° F. difference between boundaries. For T °F. difference, multiply time by T^{1+m}. For a wet duct, difference x gm. water vap/kg. air between boundaries, multiply time by $(10x)^{m+1}$.

The time taken to reach the maximum is given by the equations

$$\psi = \frac{m}{m+1} = \frac{z_{\max}^{m+1}}{(m+1)^2 at}. \qquad \ldots\ldots(5)$$

Some determination of the values of a and m is necessary in order to give some idea of the magnitude of the upper limit to the time taken to reach the maximum duct width. Sir G. I. Taylor found values of K of the order 3×10^3 in C.G.S. units for moderate winds over the sea (Brunt 1939, Chap. XII). With this value of K, Figure 2 shows the dependence on m of the time taken to reach the maximum duct width.

(iii) *Ducts less than Maximum*

From Figure 1 it can be determined whether a duct of given height will or will not be formed. For duct heights less than the maximum the time t taken to reach any specified height z_0 is determined from

$$e^{-\nu_1}\psi^{m/(m+1)} = \frac{\alpha z_0 \Gamma\{m/(m+1)\}}{(m+1)(V_1 - V_0)}, \qquad \psi = \frac{z_0^{m+1}}{(m+1)^2 at}.$$

As an illustration take $m = \frac{1}{2}$ and let the temperature difference between the upper and lower boundaries be 9° F. Then from Figure 1 the maximum duct width is about 50 ft. and from Figure 2 it will be formed in less than about $\frac{1}{2}$ hour. If the humidity difference between the boundaries is 2 gm. water vapour per kg. air, the maximum duct height is about 80 ft. and the upper limit to the time taken for the duct to grow to this height is about $1\frac{1}{2}$ hours. For a 9° F. difference between the boundaries the upper limit for the time for the duct to rise to a height of 25 ft. is calculated as follows.

Setting $V_1 - V_0 = 5°$ C. ($= 9°$ F.), $\alpha = 10^{-3}$ °C/cm., $z_0 \simeq 750$ cm. ($= 25$ ft.), $m = \frac{1}{2}$,

we find $$e^{-\nu_1}\psi^{1/3} = \frac{750 \times 10^{-3} \times \Gamma(\frac{1}{3})}{5 \times 3/2} = 0{\cdot}267,$$

whence $\psi = 1{\cdot}4$ and

$$t = \frac{z_0^{m+1}}{(m+1)^2 a\psi} = \frac{750^{3/2}}{(3/2)^2 \times 30 \times 1{\cdot}4} \simeq 220 \text{ sec.}$$

The half maximum duct width is thus reached very quickly.

(iv) *Conclusion*

It may be concluded in general that the duct forms rapidly at first and approaches its maximum height more slowly. In the case of a warm dry airstream passing over the sea, where the air speed is approximated from synoptic observations, the duct probably forms sufficiently quickly for the time lag to be neglected in comparison with the errors in speed estimation, since the duct must extend laterally for a great distance to be effective in a radio sense.

§ 3. THE FORMATION OF RADIO DUCTS UNDER CONDITIONS OF NOCTURNAL COOLING

At night heat is radiated from the earth's surface and the heat loss is greatest when the sky is clear; the rate at which heat is lost is sensibly constant (Brunt 1939) and is derived both from the top layers of the earth and from the lower layers of the atmosphere. An inversion of temperature forms in the atmosphere and if radiation continues for a sufficient length of time there is a layer in the atmosphere

in which the gradient of potential temperature exceeds the critical value for duct formation and a radio duct is formed. It is assumed that the humidity remains constant in the vertical; a remark about this assumption will be made later.

Conduction of heat in the earth's surface is assumed to follow the classical law. In the atmosphere the diffusion coefficient is again assumed to follow the power law.

(i) *Mathematical Equations*

The differential equations governing the system are:

$$\frac{\partial}{\partial z}\left(az^{1-m}\frac{\partial\theta}{\partial z}\right)=\frac{\partial\theta}{\partial t}, \quad z\geqslant 0, \quad t\geqslant 0, \qquad \ldots\ldots(6)$$

$$K_1\frac{\partial^2 T}{\partial z^2}=\frac{\partial T}{\partial t}, \quad z\leqslant 0, \quad t\geqslant 0, \qquad \ldots\ldots(7)$$

where z is measured from the earth's surface.

The boundary conditions are:

$$\theta=T \quad \text{at} \quad z=0, \quad t\geqslant 0 \qquad \ldots\ldots(8)$$

$$-K_1\rho_1 c_1\frac{\partial T}{\partial z}=-az^{1-m}\rho c_p\frac{\partial\theta}{\partial z}+R \quad \text{at} \quad z=0, \quad t\geqslant 0, \qquad \ldots\ldots(9)$$

where θ is the change in potential temperature of the atmosphere from the value at $t=0$, T is the change in temperature in the earth's upper layers from the value at $t=0$, and the other symbols are as defined above. These equations have been given by Jaeger (1945).

It should be pointed out that at some time shortly after dusk the temperature in the first hundred metres of the air becomes almost constant with changing height, and so a natural time zero is provided (Johnson and Heywood 1938). Since the gradients in the atmosphere with which we are concerned in this problem are large this time zero can be taken as a time at which the potential temperature is almost independent of height.

(ii) *The Solution of the Equations*

The solution of equations (6) to (9) is effected by the operational method, in which the transform $\overline{F}(z,p)$ of $F(z,t)$ is defined by:

$$\overline{F}(z,p)=p\int_0^\infty \exp(-pt)F(z,t)\,dt.$$

We find (Knighting 1950)

$$\overline{\theta}=A\xi^{1/m(m+1)}K_{m/(m+1)}(\xi), \qquad \xi=\frac{2z^{(m+1)/2}}{m+1}\left(\frac{p}{a}\right)^{1/2} \qquad \ldots\ldots(10)$$

$$\frac{\partial\overline{\theta}}{\partial z}=-A\xi^{1/(m+1)}K_{1/(m+1)}(\xi)\left(\frac{m+1}{2}\right)^{(1-m)/(m+1)}\left(\frac{p}{a}\right)^{m/(m+1)}z^{m-1}, \qquad \ldots\ldots(11)$$

where

$$A=\frac{-2^{1/(m+1)}R}{\Gamma\{m/(m+1)\}\rho_1 c_1 K_1^{1/2}p^{1/2}+a\rho c_p(m+1)^{(1-m)/(m+1)}\left(\frac{p}{a}\right)^{m/(m+1)}\Gamma\{1/(m+1)\}}$$

where K_n is the modified Bessel function.

(iii) *Application of the Solution to the Formation of Radio Ducts*

For a particular value α of $\partial\theta/\partial z$ equation (11) is simply an equation between z and p, or alternatively between z and t, and we have

$$\alpha z^{1-m} = \frac{2^{\frac{m}{m+1}} R(m+1)^{\frac{1-m}{m+1}} \left(\frac{p}{a}\right)^{\frac{m}{m+1}} \xi^{\frac{1}{m+1}} K_{1/(m+1)}(\xi)}{\Gamma\{m/(m+1)\}\rho_1 c_1 K_1^{1/2} p^{1/2} + a\rho c_p (m+1)^{\frac{1-m}{(m+1)}} \left(\frac{p}{a}\right)^{\frac{m}{m+1}} \Gamma\left(\frac{1}{m+1}\right)}. \quad \ldots\ldots(12)$$

For the purpose of calculating duct heights α is 10^{-3} °c/cm. To interpret (12) split the right-hand side into two factors, the first of these being

$$\xi^{1/(m+1)} K_{1/(m+1)}(\xi),$$

and apply Duhamel's theorem. The transform of this factor is always positive and less than $2^{\{1/(m+1)\}-1}\Gamma\{1/(m+1)\}$. Since m is known to be less than unity, an *upper limit* to the value of z given by equation (12) is found by putting

$$\xi^{1/(m+1)} K_{1/(m+1)}(\xi) \sim 2^{1/(m+1)}\Gamma\{1/(m+1)\}.$$

Making this approximation and carrying out some simplifications the upper limit of the value of z, say z_0, is given by:

$$\alpha z_0^{1-m} = \frac{R(m+1)^{\frac{1-m}{m+1}} p^{\frac{m}{m+1}} \Gamma\{1/(m+1)\}}{a^{\frac{m}{m+1}} \Gamma\{m/(m+1)\}\rho_1 c_1 K_1^{1/2}\{p^{1/2} + \beta p^{\frac{m}{m+1}}\}} \quad \ldots\ldots(13)$$

where

$$\beta = \frac{a\rho c_p (m+1)^{2/(m+1)}\Gamma\{1+1/(m+1)\}}{a^{m/(m+1)}\rho_1 c_1 K_1^{1/2}\Gamma\{m/(m+1)\}}. \quad \ldots\ldots(14)$$

$m = 1/7$.

Appropriate values of the constants near the earth's surface are, in c.g.s. units, $R = 2{\cdot}1 \times 10^{-3}$, $\rho_1 = 1{\cdot}6$, $c_1 = 0{\cdot}2$, $K_1 = 4{\cdot}7 \times 10^{-3}$, $c_p = 0{\cdot}24$, $\rho = 1{\cdot}27 \times 10^{-3}$. The value given for R is applicable to Southern England and the surface values for fine dry loam. Values of m and a vary with the meteorological conditions. Taking $m = 1/7$, and $a = 1{\cdot}12$ so that the diffusivity at 100 metres is 3×10^3, equation (13) becomes

$$z_0^{6/7} = \frac{2{\cdot}1 \times (8/7)^{3/4}\Gamma(7/8)}{16p^{3/8}(1 + 2{\cdot}5 \times 10^{-3} p^{-3/8})}.$$

Expanding in negative powers of p and interpreting term by term, the series in t is

$$\frac{t^{3/8}}{\Gamma(1+3/8)} - 2{\cdot}5 \times 10^{-3} \frac{t^{6/8}}{\Gamma(1+6/8)}, \quad \text{etc.}$$

This series is rapidly convergent for $t = 3{,}600$ sec. and with this value of t only the first term need be retained; it is found that $z_0 \sim 11$ m. or 35ft. Hence the maximum height the duct can attain after radiative cooling has been operative for one hour is about 35 ft.

$m = 1/3$.

The method of the preceding section is useful when β is sufficiently small and the resulting series is rapidly convergent. Cowling and White (1941) analysed some experiments carried out by Johnson and Heywood (1938) and gave

values for the diffusivity at various times through the night. In the mean the values may be represented by the law $az^{1-m}=25z^{1-1/3}$. Using these values for a and m equation (13) reduces to

$$z_0^{2/3}=\frac{15}{p^{1/4}+1/18}=\frac{15}{p^{1/4}+\beta}. \qquad \ldots\ldots(15)$$

To interpret this equation a contour integration is carried out and it is found that

$$z_0^{2/3}=15\left\{\frac{1}{\beta}-\frac{2\sqrt{2}}{\pi}\int_0^{\infty}\frac{\exp(-u^4t)}{u^2+\sqrt{2}u\beta+\beta^2}\,du\right\}. \qquad \ldots\ldots(16)$$

Taking a value of $t=3{,}600$ sec. and performing the integration it is found that $z_0\sim 10$ m. or 30 ft. Hence again we find that the maximum height the duct can attain after radiative cooling has been operative for one hour is about 30 ft.

(iv) *The Maximum Possible Duct Height*

An important point to note is that the term in $1/\beta$ in equation (16) is independent of the approximation made for $\xi^{1/(m+1)}K_{1/(m+1)}(\xi)$, for it arises from integration around a small circle at the origin where the approximation is exact. Hence the maximum possible duct height is given in the case treated in sub-section (iii) by $z^{2/3}=15/\beta$ or $z\sim 40$ m. or 120 ft. From the definition of β the maximum possible duct height is given by $z^{1-m}=R/\alpha a\rho c_p$. The maximum is large for small values of a as might be expected since small values of a indicate that diffusion is acting slowly. A time calculation shows that for small values of a the maximum is approached after a very long time and the physical conditions would have changed, making equations (6) to (9) inapplicable.

(v) *Calculation of the Duct Height from the Ground Temperatures*

We can also use the fall in temperature at the ground to calculate the height of the duct. Consider again the case treated in sub-section (iii). From equation (10) the fall in temperature at the surface is given by

$$\begin{aligned}\bar{\theta}_{z=0}&=\frac{-R}{\rho_1c_1K_1^{1/2}\{p^{1/2}+\beta p^{1/4}\}}\\&=\frac{-R}{\beta\rho_1c_1K_1^{1/2}}\left\{\frac{1}{p^{1/4}}-\frac{1}{p^{1/4}+\beta}\right\}. \qquad \ldots\ldots(17)\end{aligned}$$

The height of the duct is given, from equation (11), by

$$\alpha z^{2/3}=\frac{R(\frac{4}{3})^{1/2}a^{-1/4}}{\rho_1c_1K_1^{1/2}\Gamma(\frac{1}{4})(p^{1/4}+\beta)}. \qquad \ldots\ldots(18)$$

Substituting from (18) into (17) and interpreting the equation so formed

$$\Delta T=\frac{Rt^{1/4}}{\beta\rho_1c_1K_1^{1/2}\Gamma(\frac{5}{4})}-\frac{\alpha z^{2/3}a^{1/4}\Gamma(\frac{1}{4})}{\beta(\frac{4}{3})^{1/2}\Gamma(\frac{3}{4})}, \qquad \ldots\ldots(19)$$

where ΔT denotes the fall in temperature at the ground in the time interval $(0, t)$. With the values of the constants used above equation (19) reduces to

$$z^{2/3}=16t^{1/4}-9{\cdot}5\Delta T. \qquad \ldots\ldots(20)$$

This formula refers to summer conditions in Southern England, since the parameters used correspond to those observed in summer. At the end of a June night $t\sim 7\times 3{,}600$ sec., $\Delta T\sim 10°$ c. which gives $z\sim 30$ ft. Equation (20) does not hold everywhere, the constants varying both with place and time of year, but it should be possible to obtain a similar formula for many parts of the world.

It is important to note that the duct height attained after radiative cooling has been operative for seven hours is about the same as the maximum duct height attainable after one hour. We may infer that ducts grow rapidly at first and then more slowly approach their final height.

(vi) *The Effect of Water Vapour*

The calculations of the dry duct heights have been made on the assumption that the vertical gradient of water vapour remains constant. Measurements of temperature and water vapour have been made at Rye at various heights in the atmosphere. The analysed results, which have not yet been published, show that during the night there is generally a positive gradient of water vapour. The effect of this inversion of water vapour is to inhibit duct formation and hence the duct heights given in this paper will generally be overestimated. A quantitative attack on the problem has not yet been made.

§4. THE DUCT WIDTHS ASSOCIATED WITH A POWER LAW PROFILE OF MODIFIED REFRACTIVE INDEX

Assuming that the diffusion coefficient in the atmosphere follows the power law an approximation to the variation of modified refractive index with height has been given (Booker and Walkinshaw 1946) as

$$\mu^2 = 1 - 2C\left(z - D^{1-m}\frac{z^m}{m}\right), \qquad \ldots\ldots (21)$$

where μ is the ratio of the modified refractive index at height z to that at the surface, m is the index in the power law, and C, D are constants. Since μ is very approximately unity

$$\frac{d\mu}{dz} \to -C \quad \text{as} \quad z \to \infty.$$

It is known (Booker and Walkinshaw 1946) that $d\mu/dz \to 4K_e/5$ as $z \to \infty$, where K_e is the curvature of the earth, and hence $C = -4K_e/5$. From equation (21) μ has a minimum at $z = D$ and hence a surface-based duct exists to the height D. The minimum value of μ is given by

$$\mu^2_{\min} = 1 - 2CD(1 - 1/m) \qquad \ldots\ldots (22)$$

Although the value of μ given by equation (21) depends essentially upon a single parameter, a modified refractive index profile of this form can often be fitted to experimental data.

(i) *The Eigenvalue Problem*

Following the electromagnetic theory of mode propagation as presented by Booker and Walkinshaw the eigenvalue problem to be solved is

$$\int_0^{w_n} q\,dz = \tfrac{1}{2}(n - \tfrac{1}{4})\lambda, \qquad \ldots\ldots (23)$$

where n is a positive integer, w_n is the track width of the nth mode, λ the propagated wavelength, and q is defined by

$$q^2 = \mu^2 - \cos^2\gamma, \qquad \ldots\ldots (24)$$

γ being the angle of propagation with the horizon at the transmitter. w_n is further related to the variables being a solution of the equation

$$q = 0. \qquad \ldots\ldots (25)$$

Equation (23) is regarded by the authors as an eigenvalue equation in γ and leads to solutions of the problems that they formulate. Equation (23) can be regarded as an eigenvalue equation in w_n, and so treated leads to a simple result concerning the duct width necessary to enclose the track widths of the first n modes.

(ii) *The Duct Width enclosing n Track Widths*

From equation (23) if w_n is identified with D then the problem of determining the duct width enclosing the first n track widths is formulated. For the trapping of electromagnetic energy in a duct in the atmosphere the angle of propagation is small, being certainly less than one degree. From equations (21) and (24)

$$q^2=\gamma^2-2C\left(z-D^{1-m}\frac{z^m}{m}\right). \qquad \ldots\ldots(26)$$

Now from equation (25) $q=0$ at $z=D$, and hence

$$q^2=2C\left(D-\frac{D}{m}-z+D^{1-m}\frac{z^m}{m}\right). \qquad \ldots\ldots(27)$$

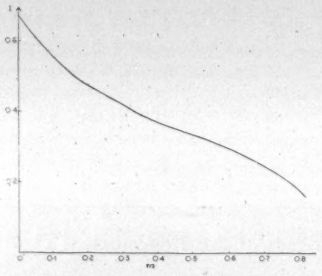

Figure 3. Graph of $I=\int_0^1\left\{\frac{1}{m}-1+t-\frac{t^m}{m}\right\}^{1/2}dt$.

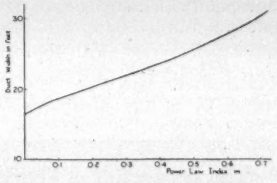

Figure 4. Duct width for wavelength $\lambda=1$ cm. for values of m between 0 and 0·7. For wavelength λ cm. multiply D by $\lambda^{2/3}$.

The eigenvalue equation, equation (23), is now

$$\int_0^D\left[2C\left(D-\frac{D}{m}-z+D^{1-m}\frac{z^m}{m}\right)\right]^{1/2}dz=\tfrac{1}{2}(n-\tfrac{1}{4})\lambda. \qquad \ldots\ldots(28)$$

Setting $z=Dt$ in this equation

$$(-2C)^{1/2}D^{3/2}\int_0^1\left(\frac{1}{m}-1+t-\frac{t^m}{m}\right)^{1/2}dt=\tfrac{1}{2}(n-\tfrac{1}{4})\lambda. \qquad \ldots\ldots(29)$$

The integral in equation (29) is purely a function of m, and writing

$$I=I(m)=\int_0^1\left(\frac{1}{m}-1+t-\frac{t^m}{m}\right)^{1/2}dt, \qquad \ldots\ldots(30)$$

then

$$D=\left\{\frac{\frac{1}{2}(n-\frac{1}{4})}{I}\right\}^{2/3}(-2C)^{1/3}\lambda^{2/3}. \qquad \ldots\ldots(31)$$

The values of $I(m)$ have been plotted against m in Figure 3. Equation (31) gives in general the duct width required to enclose the first n track widths. In practice

the first mode is often the most important, and setting $n=1$ in equation (31) and inserting the value of $C(=-4K_e/5)$

$$D=12{\cdot}5\left\{\frac{\lambda}{I}\right\}^{2/3} \text{ ft.} \qquad \ldots\ldots(32)$$

where λ is measured in centimetres. Figure 4 gives D in terms of m for $\lambda=1$ cm. It is easily seen that for $m=\frac{1}{3}$ the duct width necessary to enclose the track width of the first mode, and hence to suppress leakage, is about 50 ft. for a wavelength of 3 cm. and about 120 ft. for a wavelength of 10 cm. Equation (32) thus provides an estimate of the duct width necessary to enclose the first track width of a propagated signal of wavelength λ, with the assumed relation between modified refractive index and height.

ACKNOWLEDGMENT

The author is indebted to the Director, Meteorological Office, for permission to publish this paper.

REFERENCES

Booker, H. G., 1948, *Quart. J. R. Met. Soc.*, **74**, 277.
Booker, H. G., and Walkinshaw, W., 1946, *Meteorological Factors in Radio-Wave Propagation* (London : Physical Society), p. 80.
Brunt, D., 1939, *Physical and Dynamical Meteorology* (Cambridge : University Press).
Cowling, T. G., and White, A., 1941, *Quart. J. R. Met. Soc.*, **67**, 276.
Jaeger, J. C., 1945, *Quart. J. R. Met. Soc.*, **71**, 388.
Johnson, N. K., and Heywood, G. S. P., 1938, *Geophysical Memoirs*, No. 77 (London : Meteorological Office).
Knighting, E., 1950, *Quart. J. R. Met. Soc.*, **76**, 173.
Sutton, O. G., 1949, *Atmospheric Turbulence* (London : Methuen).

The Properties of Spark Counters of the Rosenblum Type

By R. D. Connor
Department of Natural Philosophy, Edinburgh University

Communicated by N. Feather; MS. received 4th July 1950

ABSTRACT. The design and operation of Rosenblum-type spark counters having plane, concave and convex cathodes is described, and discussed with reference to the counting characteristics, useful life and background counting rate. The absolute efficiency of the counter in air has been determined for α-particles, knock-on protons, and β-particles, giving values of about 90%, 5% and 0·0002%, respectively. A marked dependence of efficiency on specific ionization and air pressure is evident. The counter is directional in all its forms. The effect of employing gases other than air is also investigated and a qualitative description of the counting characteristics is given. Alpha-particle ranges may be determined using either a single counter or two counters used in anticoincidence as is described in the text.

§1. INTRODUCTION

The original paper describing an arrangement whereby ionizing particles or quanta, passing through the sensitive region of an electrode assembly, are registered by sparks passing across the electrode gap, is that due to Greinacher (1934 a). The name ' Spark Counter ' was proposed, and subsequent papers by the same author described in general terms the properties of various

types of electrodes and various geometrical arrangements (Greinacher 1934 b, 1935 a, b, c, 1938 a, b). Later more detailed investigations were reported by other workers (Stuber 1939, Jeanguenin 1944, Frey 1946, Rytz 1949). In all these counters the electrode separation was small and one electrode, usually the anode, had a small radius of curvature. The counters described by Greinacher and Stuber were sensitive to gamma rays and ultra-violet photons as well as to alpha- and beta-particles, but they had many important disadvantages:

(i) No 'plateau' region in the counting characteristics appeared for any of the radiations mentioned, unless very particular electrode systems were used (Frey 1946).

(ii) The sensitive volume increased with applied voltage, and was different for the different ionizing radiations. Similarly, the threshold voltage was different for radiations of different ionizing power.

(iii) Operation was extremely sensitive to the surface conditions of the metal electrodes.

(iv) A high 'background' counting rate was usually observed and the resolving time was long (about 0·03 sec.).

It was shown by Chang and Rosenblum (1945) that the principal disadvantages were removed if a flat metal plate acted as the cathode and the anode was a fine wire stretched in front of the plate at a distance of about 1·5 mm. The counter operated in air at atmospheric pressure. A quench circuit was used to enable the counter to recover after the passage of a spark. Applied voltages were of the order of 3 kv. and the counter was sensitive to alpha-particles only. Rosenblum found the background to be small (about one count in three minutes for a wire 4 cm. long). When the properties of this type of spark counter were still unpublished, an examination of the counter was undertaken by the present author with a view to its development, and a brief summary of part of this work has appeared elsewhere (Connor 1949). It is the purpose of this communication to present a fuller account of these researches. Since the appearance of the preliminary account, a report of similar but independent work on some of these topics has been published by Payne (1949).

§ 2. APPARATUS

In the course of the present work, it has been shown that the original wire-plate counter of Rosenblum is a particular case of a more general type of counter in which the anode is a fine wire, and the cathode may be convex, planar or concave with respect to the anode. Throughout most of the work the anode–cathode separation was about 1 mm., and under these conditions the counting threshold voltage was of the order of 3 kv. The counters were operated in air at atmospheric pressure in all but a few experiments which are mentioned separately below. In order to facilitate changes in the counter geometry, two electrode carriages were constructed, one of which is shown in Figure 1. The essential features are two ebonite blocks on which the anode and cathode can be mounted. The lower block is fixed to the vertical brass plate and carries the cathode clamped in position, while the upper block, which carries the anode, can be made to move vertically into any desired position with respect to the lower block by the action of an accurate screw. Side play is avoided by the careful milling of the slot in which the upper block moves. The screw is provided with a divided head and acts against the controlling action of two springs so that backlash is avoided. The

anode, a fine wire of diameter 0·05 mm., is stretched horizontally across the ends of two glass pillars or other insulators, which protrude from the lower surface of the upper ebonite block, the wire being pulled taut and secured at each side of the block by friction between two nuts on a screw sunk into the side of the block. Tungsten is chosen as the anode material on account of the tension to which the anode wire is subjected. The cathode, formed either of wires of larger diameter than the anode, plates or hollow cylinders (representing convex, planar or concave geometries with respect to the anode), was secured by clamping to the other ebonite block. In the first two cases, the anode and cathode were aligned by screwing the electrodes together and adjusting them until the tungsten anode wire lay evenly along the cathode in a symmetrical fashion. By means of the screw,

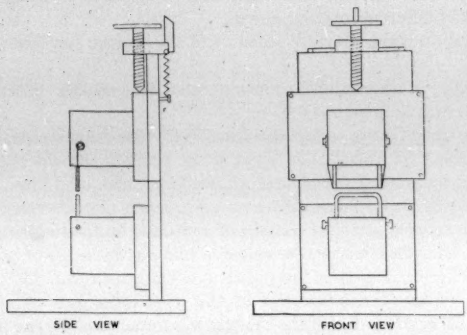

Figure 1.

the gap could then be set at any desired value, the parallelism between the electrodes being maintained by the carriage. In the case of the hollow cylinder arrangement, the anode wire passed centrally down the cylinder and a slit or window was provided to permit entry of α-particles from a direction normal to the axis of symmetry. It is clearly of importance to have the electrode separation uniform along the entire length of the anode wire, for the counter will tend to spark preferentially at points of minimum spacing. In order to avoid end and edge effects, a vertical slit was placed between the source of α-particles and the electrodes, thus restricting the particles to the central region of the counter wire. In the majority of these investigations, the source of α-particles was the active deposit of thorium collected, by recoil from a dry emanating source of radio-thorium, on the surface of a small 8 B.A. screw head which had been filed flat and polished.

The cathode was connected directly to the negative output of a stabilized power supply, having an output voltage variable up to 4,000 volts, and the anode was connected to earth via a resistance capacity potentiometer. This served two purposes: firstly, it acted as a quench circuit to extinguish the discharge, and secondly, it provided a known fraction of the voltage surge for application to a scaler. The potentiometer circuit was connected to the anode with the shortest possible length of lead. This precaution was necessary, since, if the connection was more than a few inches long, a damped oscillation appeared on the pulse after

the leading edge and in certain arrangements lasted for several microseconds and was of such amplitude as to produce ' double counts ' in a sensitive scaler. Visual examination on a calibrated cathode-ray oscillograph of pulses, obtained under good conditions, revealed an exceedingly sharp leading edge, the rise time being estimated as less than 10^{-7} sec. The recovery time was of course largely controlled by the time constant of the quench circuit. A time constant of 50 microseconds was found to be suitable and the smallest value consistent with stable operation was shown to be 20 microseconds for the counters here described.

Measurement of the total pulse height indicated that on discharge all but a few per cent of the total anode–cathode potential difference is developed across the quench circuit. Clearly, no amplifier is needed when pulses of such magnitude are available and, as Figure 2 shows, the quench circuit used supplied about 1/51 of the total surge directly to the scaler.

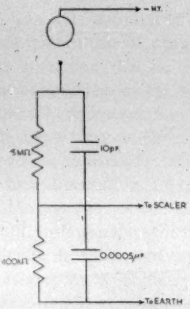

Figure 2.

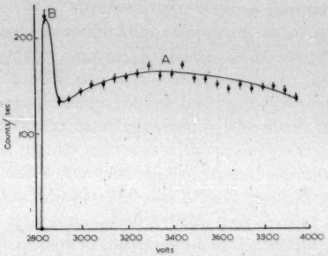

Figure 3.

§3. THE COUNTING CHARACTERISTICS

From the geometrical details given above, it will be seen that for counters having wire and plate cathodes, α-particles can approach the counter gap from two principal directions, both normal to the anode, the one parallel (' End-on ' direction) and the other perpendicular (' Broadside ' direction) to the plane containing the axes of the electrodes. For counters with hollow cylindrical cathodes, in which the anode passes centrally down the axis of the cylinder, only one principal direction can be specified, corresponding to the ' End-on ' direction of the other arrangements, in which the α-particles pass through a slit in the cathode into the sensitive volume in the direction of the normal to the axis of symmetry. Figure 3 shows the Broadside characteristic obtained with an anode consisting of a tungsten wire 0·05 mm. in diameter and a cathode of copper wire 0·9 mm. in diameter, the electrode spacing being 0·75 mm. Figure 4 shows an End-on characteristic for the same counter. In these figures the counting rate has been corrected for source decay and normalized to a constant source–counter geometry. The radioactive source was placed 7·9 cm. from the anode wire in each case, the atmospheric pressure being 76·7 cm. Hg. In these experiments only the ThC′ α-particles could reach the counter. At this stage it is appropriate to mention that at no time was it found possible to record, with counters of the

types here used, any appreciable effect due to the β- or γ-rays from sources up to 10 mc. in activity. Furthermore, α-particles having ranges too short to reach the counter gap produce no effect, although they are producing intense ionization only a few millimetres away from the gap. The Broadside curve is of a type not found with any other counter. After a rapid rise from the counting threshold, the curve passes through a sharp maximum marked B in Figure 3, subsequently falling to a minimum value. The counting rate therafter increases to a flat maximum (point A on Figure 3) as the applied voltage is further increased. About A, the curve exhibits a 'usable' region of some 300 to 400 volts in which the dependence of counting rate on voltage is small. In general, it is found that for a given anode the voltage at which the flat maximum occurs is greater, the larger the cathode diameter and the larger the electrode spacing. Also the flat maximum

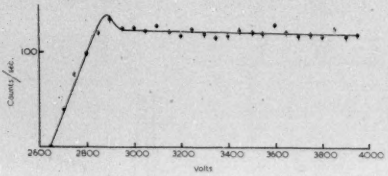

Figure 4.

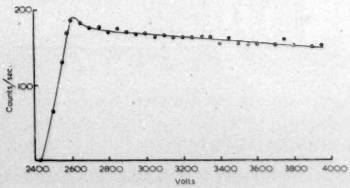

Figure 5.

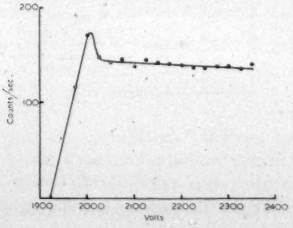

Figure 6.

counting rate increases with spacing. It should be mentioned that the abscissae of all counting curves shown in this paper represent the voltage as read on the output meter of the power supply. For reasons which will appear later, this voltage is not that appearing across the electrode gap.

The End-on characteristic is quite different from the other. After a more gradual rise, the counting-rate curve passes through a small peak and thereafter enters a long plateau region which can extend for 1,000 volts or more. Figure 5 shows the End-on curve for a Rosenblum wire-plate arrangement of spacing 1 mm. and Figure 6 the corresponding curve for a hollow cathode counter, the cathode being of brass and of internal diameter 2·07 mm. The same anode arrangement was used throughout. With wire cathodes, the plateau is not strictly flat but falls by 1 or 2% over the entire plateau region. In this way, Figure 4 is seen to resemble the curves for the other two geometries but with features less marked. Wire cathode counters have been investigated for cathode diameters ranging from 4·7 to 0·4 mm. using several different materials and with spacings ranging

from 0·5 to 1·25 mm. The graphs of Figures 3 to 6 inclusive refer to counters which have been suitably conditioned. This procedure consists in cleaning the cathode with metal polish, then washing with chloroform and alcohol, and finally, allowing the counter to operate for some 5,000 to 10,000 counts, which precaution, according to Stuber and others, removes the small irregularities from the electrodes. Should this precaution be omitted, the counting rate is found to be a few per cent too low. Counters with tungsten anodes of 0·1 mm. diameter exhibit characteristics similar to those using 0·5 mm. diameter wires, but higher voltages are required. No stable characteristic could be obtained when the polarity of the counter was reversed, that is, with a fine wire cathode and an anode having any of the geometrical forms mentioned above.

§4. THE CHARACTERISTICS OF THE COUNTER IN THE QUIESCENT STATE

If a microammeter is incorporated in series with the quench circuit, some information can be obtained as to the current passing between the electrodes in the quiescent, that is, non-sparking state. It is observed that, when a counter having any one of the three types of cathode described above operates in air at atmospheric pressure in the absence of a source, a corona discharge occurs round the anode wire as the voltage applied is raised above that corresponding to the counting threshold. With anode wires approximately 2 cm. in length, the corona is first observed in a darkened room when the current registered by the meter is of the order of 5×10^{-7} amps. This current rapidly increases with applied voltage until, with a spacing of the order of 1 mm. and 4,000 volts applied from the power supply, the quiescent current reaches a value between 100 and 200 $\mu\Omega$ depending on the cathode geometry. To the eye the glow is not at all diffuse, appearing as a fine line of light somewhat thicker and more intense in the direction of the cathode, and extremely faint if not actually invisible on the side of the anode away from the cathode. This visible corona extends about 0·01 mm. into the gap from the surface of the anode in the direction of the shortest path between anode and cathode, and the luminous boundary appears to the eye to be sharply defined. The glow possesses a sharp ' offset ' or extinguishing voltage and a higher but somewhat variable ' onset ' voltage, this being a common effect noticed by other observers in a positive point to plane corona. The ' offset ' voltage has been shown to coincide with the voltage of the peak B of the Broadside, and also with that of the small peak of the End-on characteristic. It may be noted here that, because of the existence of the quiescent (corona) current, the voltage actually appearing across the electrode gap during any counting experiment is less than that read on the meter of the power supply as already briefly mentioned.

It should also be mentioned that for counters having wire cathodes of copper, nickel silver and aluminium, of the same diameter and the same electrode spacing, the counting rate at the flat maximum of the characteristic was the same to within the experimental error, irradiation being under standard Broadside conditions throughout.

When the quiescent discharge was examined on a cathode-ray oscillograph, ' corona pulses ' were observed corresponding to those photographed by Trichel (1939). The corona pulses were of particularly large amplitude at the voltage corresponding to the peak B of the Broadside characteristic. The corona fluctuations at this and adjacent voltages were sufficiently large as to be audible.

§5. THE EFFECT OF SPECIFIC IONIZATION

The probability of recording the passage of an α-particle through the potentially sensitive region of the counter (or, alternatively, the extent of the truly sensitive region) has been shown to be a function of the specific ionization of the α-particle as was to be expected from the almost complete insensitivity of the counter to β-radiation. In Figure 7 the normalized counting rate–range curves are given for the Broadside and End-on positions, and for 15° c., 760 mm. Hg. The term ' Range ' is here taken as being the distance of the source from the anode wire, thus it has not precisely the same significance in the two cases, but it is interesting to note that both curves lie within Henderson's (1921) ionization curve. In each case the voltage corresponding to the flat maximum of the Broadside counting curve was used.

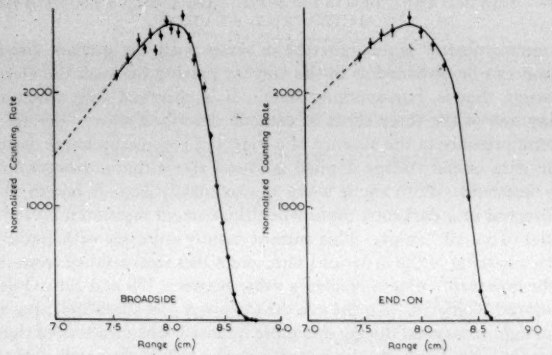

Figure 7.

In view of this effect of specific ionization, it is to be expected that the counting characteristic will show some variation if the residual range of the incident α-particles is altered. Using the Broadside position, it was found that for residual ranges greater than about 6 mm. (in standard air), using cylindrical wire cathodes, the sharp peak of the counting curve no longer occurred at the corona offset voltage, the counting threshold being some 20 volts or more above the latter. Under such conditions the rise in the counting rate from the threshold is particularly steep, and the fall, in passing through the sharp peak, is correspondingly rapid. The normalized height of this peak decreases as the residual range is increased, and the flat maximum shifts to regions of higher voltage. The shift of the threshold is small, but the shift of the flat maximum can be as much as 300 volts for a change in residual range from 0·5 to 2·5 cm.

§6. THE USEFUL LIFE OF THE COUNTER

Five Broadside counting characteristics were taken with one counter in which more than four million sparks passed between the taking of the first and last curves, and no significant change in the characteristics was found. The length of time for which a counter of this type can be used is determined principally by the extent to which dust, fibres, etc. collect on the electrodes. If the counter is operated in a bell jar using filtered air, it does not require cleaning so frequently

as does the same counter used in open air, but if anode and cathode are cleaned each time prior to use, the same electrodes can be used over and over again, until finally it is observed that the counter is discharging locally. Usually local discharge arises from an irregularity in the electrodes, some pitting or erosion, and both electrodes should be replaced when this occurs.

§7. BACKGROUND

The smallness of the background counting rate is one of the attractive features of counters of the Rosenblum type. Under 'clean' conditions, viz. freedom from α-emitting radioactive contamination and dust, the background has been determined on occasion as less than two counts per hour. With the counter uncovered, the background is generally less than ten counts per hour, but naturally it varies with the dust content of the air. In a room with a wooden floor, vigorous brushing of the floor has been known to result in a temporary rise in rate to the startling figure of five counts per minute when the counter was uncovered!

§8. COUNTING IN AIR UNDER REDUCED PRESSURE

Counting characteristics for both Broadside and End-on positions have been obtained for air pressures lower than 1 atmosphere. The general shape of the curve remains unaltered, but the counting threshold moves to lower and lower voltages as the pressure is reduced. The entire curve also contracts so that the voltage range between threshold and continuous discharge becomes smaller. Broadside counting curves were obtained for a counter having a spacing of 0·75 mm. with a cathode 0·9 mm. in diameter and a series of values was obtained for the normalized flat maximum counting rate as a function of pressure. The position of the source was adjusted so that the greatest normalized counting rate was obtained in each case. The graph exhibiting these values is equivalent to an efficiency–pressure graph and is shown in Figure 8. The rate of variation of efficiency with pressure is seen to be small in the region of 76 cm. Hg but not

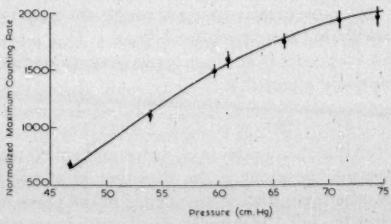

Figure 8.

negligible, but at half an atmosphere pressure, the rate of variation is relatively large. It is therefore both convenient and expedient to operate the counter in air at atmospheric pressure.

This result has obvious correlations with that concerning the effect of residual range and provides further confirmation for the view that the probability of spark formation depends on the amount of ionization produced by the individual α-particles in a specified region of the counter.

§9. THE ABSOLUTE EFFICIENCY OF THE COUNTER

Since the efficiency of the counter was found to vary with the air pressure and the residual range of the α-particle, it became important to measure the absolute efficiency of the counter under standard conditions, viz. in air at atmospheric pressure and with the source–counter distance such as to give the maximum normalized counting rate. This was done for the Broadside position, using a collimating slit to define the length of counter employed. The number of α-particles per second passing this slit and subsequently passing between the counter electrodes was determined in a separate experiment with a thin windowed proportional counter of known aperture. The ratio of actual counting rate to the number of α-particles passing through the spark counter gap per second is taken as a measure of the absolute efficiency (Table 1).

Table 1. Spark Counter

Cathode diameter (mm.)	Spacing (mm.)	Measured Efficiency
0·93	0·71	0·98±0·04
0·93	0·71	1·04±0·04
0·93	0·78	0·98±0·06
0·70	0·80	0·90±0·04
0·70	0·61	0·96±0·04
0·70	0·65	0·84±0·03
0·70	0·74	0·90±0·05
0·70	0·87	0·83±0·06

Unit efficiency can only be obtained if the whole width of the gap is completely effective, but the presence of the corona discharge around the anode wire indicates the occurrence of space charge and a consequent reduction in the field in the immediate vicinity of the anode. Workers on positive corona in molecular nitrogen (Rubens and Henderson 1940) have shown that the voltage drop through the visible discharge to the anode surface is small, being close to the first ionization potential of that gas. Thus the actual field in the electrode gap is entirely different from that calculated on the assumption of no space-charge distortion, and we might well believe that α-particles passing through the gap in the immediate vicinity of the anode will not cause spark breakdown.

On the other hand, it appears from these investigations that an efficiency of the order of 90% is commonly attained.

§10. DIRECTIONAL EFFECTS

It has been observed that the counter in all its forms displays marked directional effects. In the Broadside position, if the direction of the incident α-particle beam is altered to be other than that of the normal to the plane of symmetry, the counting rate is observed to fall. Maximum sensitivity occurs when the direction of incidence is normal to the plane of symmetry. The counter has a very small sensitivity for α-particles whose direction is that of the axes of the electrodes. In a similar way in the End-on position, the counting rate falls as the α-particle beam is rotated in the plane containing the axes of the two electrodes, to make increasing angles with the normal to the axes which lies in this plane.

These effects may be described as follows. In the Broadside case, when an α-particle passes through the counter gap normal to the plane of symmetry, the electrons produced in the sensitive region can all be expected to converge on the

anode. The lateral diffusion of the electrons in the direction along the anode wire will be small, thus a dense local concentration of electrons will arrive at the anode and the probability of initiating the spark mechanism will be large. When an α-particle traverses the gap obliquely, the electrons are no longer concentrated by the field to arrive at one locality on the anode surface. The avalanche is diffuse and may arrive at the anode over a considerable length of the electrode. The more oblique the incidence, the more dispersed along the anode will be the avalanche, and under such circumstances the probability of sparking will fall correspondingly. A similar qualitative description obviously applies in the End-on case.

§ 11. QUALITATIVE DESCRIPTION OF THE COUNTING CHARACTERISTICS

In the pre-visible corona-onset region of voltage, electron avalanches will give rise to photons, and these in turn may liberate electrons from the cathode. These electrons will produce further avalanches and the likelihood of a second avalanche following the first will increase with the voltage. In this way, with large and frequent avalanches occurring according to the theory postulated by Meek (Meek 1940, Loeb and Meek 1940), streamer formation near the anode can be expected to occur. In a highly diverging field such as is employed in these counters, the streamers are unlikely to bridge the gap and so cause spark breakdown, but a corona will be set up when the critical voltage is reached. At voltages somewhat below this critical voltage, it is likely that the dense highly localized ionization of an α-particle will produce an avalanche large enough to cause a spark. The counting threshold is defined as the voltage at which this process commences. At this stage the field in the gap will be comparatively free from space-charge distortion, and if the field is maintained, the very intense burst of photons produced by the spark will have a large probability of liberating sufficient electrons from the gas molecules and the cathode to produce further avalanches of sparking magnitude. That this ' after effect ' can persist for relatively long intervals is shown by the necessity of using very long (0·05 sec.) quench times with parallel plate spark counters (Keuffel 1949, Pidd and Madansky 1949). The rapid rise to the high counting rate (peak B) of the Broadside counting characteristic is attributed to such effects.

Conditions alter greatly once the anode corona occurs. At the voltage corresponding to corona onset, the quiescent space charge in the gap becomes enormously greater than that existing in the pre-corona region of voltage. Consequently that part of the columnar ionization of the α-particle which is formed in the gap now finds itself surrounded by relatively large space charges. Meek's criterion for streamer formation is that the radial field of any localized space charge must be of the same order as the applied field at the location of the space charge. If we consider the dense, highly localized ionization of an α-particle in the light of this criterion, we see that the ionization of the α-particle is likely to cause such distortion of the quiescent corona space charge as to have a likelihood of leading to spark breakdown. The quiescent space charge will swamp any small ionizing event in the electrode gap. Thus we see from the counting characteristic that once the corona onset is reached, the counting rate falls rapidly, indicating that the spurious electron-producing events following the passage of a spark are no longer of sufficient magnitude as to lead to spark breakdown. It is

thought unlikely that any spurious electron avalanche will be able to cause sparking once the trough of the counting characteristic has been passed. These views are in accord with the observed dependence of counting rate on specific ionization and gas pressure.

With increasing applied voltage, the *a priori* probability that a given electron avalanche will reach sparking magnitude increases, but at the same time the corona space charges in the gap will increase, thereby tending to reduce the sparking probability. Finally, the stage is reached with increasing voltage that the *a priori* probability of an avalanche leading to a spark can increase only slightly, but corona-space charges will continue to increase in effectiveness, and so it is not surprising to find the counting rate falling somewhat after reaching a maximum.

Similar reasoning can be applied to the End-on case, with the difference that here the ionization of the α-particle provides a conducting path between anode and cathode, and we would expect the voltage dependence to be slight as is indeed the case.

Counters having hollow cathodes yield important information on these points. The general shape of characteristic for a hollow cathode counter of about 2 mm. inside diameter is seen to be similar to that of the curve of Figure 4, but when the diameter is increased beyond 3 mm., the glow discharge (corona) has its onset potential about 250 volts below the spark threshold for α-particles. In two cases examined the diameters were 3·25 and 3·4 mm. and the respective corona onset potentials and spark thresholds were 2,280 and 2,500 volts, and 2,500 and 2,850 volts, respectively. On amplifying the quench-circuit output about one hundredfold, the electron avalanches produced by α-particles at voltages below spark threshold could be made to activate a scaler. Under these conditions the graph of counting rate against voltage gave a curve similar to that of Figure 4, the peak occurring at corona onset. Taken under normal working conditions the spark-counting characteristic showed a slow rise from threshold to a short plateau terminated by the onset of continuous discharge. It is significant that the plateau of the 'non-sparking' curve was found to link up with that of the 'sparking' curve.

When the non-sparking pulses were examined on a cathode-ray oscillograph, a wide range of pulse size was apparent, the maximum pulse size increasing with voltage until the spark threshold was reached. Above this voltage the number of non-sparking pulses decreased (the spark rate increasing), until on the plateau of the spark curve, no non-spark pulses were seen.

§ 12. THE SYMMETRICAL COUNTER

The properties of counters having anode and cathode of exactly similar form have been examined for the case in which the electrodes are parallel wires. Such counters are in general not very satisfactory, in that the counting characteristics showed no plateau for quench-circuit time constants ranging from 2 to 400 μsec. It was not thought worth while to increase the time constant further, so work in this field was discontinued after some of the properties of these counters had been investigated. It was shown that the voltage interval between the α-counting threshold and the onset of continuous discharge was small, and that this interval increased with the electrode spacing. It depended on the diameter of the electrodes, being a maximum for electrodes of diameter about 0·45 mm. in

laboratory air. Electrodes of diameters in the range 0·05–1·0 mm. were used in this investigation.

Some dependence on the electrode material was also noticed. Electrodes of copper, brass, iron and platinum were used, the latter material giving the largest voltage interval for α-counting. Considerable dependence on surface conditions was observed, so for all these reasons such counters were not thought to be of any great service. Under no conditions was an anode corona observed.

§ 13. THE USE OF GASES OTHER THAN AIR

The behaviour of the ordinary (asymmetric) type of counter has been examined using several gases and gaseous mixtures. Only the main features of the results will be summarized here.

No counting plateau was obtained with either argon or helium at atmospheric pressure. With argon–air mixtures a plateau appears for a small admixture of air, and lengthens as the proportion of air is increased, until the typical air characteristic is obtained when the mixture is rich in air. In an argon–air mixture containing 1·5% air the dependence of counting efficiency on specific ionization is less than in air; in this mixture a fair approximation to a true number–distance curve may be obtained. Water vapour was found to cause a deterioration in the argon–air counting characteristic, and a drying agent was therefore usually incorporated in the chamber. The addition of air to helium

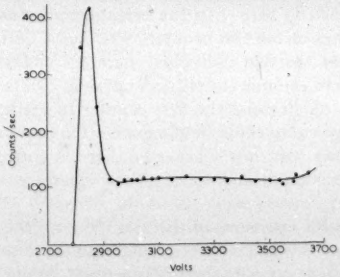

Figure 9.

produced no improvement in the characteristic. Oxygen is a reasonably suitable counter gas: a rather large plateau slope of about 0·2% per volt was recorded with this gas. Nitrogen is unsuitable; in nitrogen a beaded corona forms on the anode, not a sheath corona as is observed in air, thus the sensitivity is variable along the wire. Nitrogen–argon mixtures are unsuitable for similar reasons, but nitrogen–oxygen mixtures are generally satisfactory. For small percentages of oxygen (~8%), the Broadside curve, after the large peak (Figure 9), shows a very flat plateau region. The counter is somewhat unstable in the region of the large peak, but this instability disappears after the corona is established. Carbon dioxide at atmospheric pressure was found to be unsuitable as a counter gas; no plateau was obtained and no corona was observed. Carbon dioxide–oxygen mixtures were no better, but with carbon dioxide–nitrogen mixtures a poor plateau of 0·24% per volt was plotted.

§ 14. THE COUNTING OF PARTICLES OTHER THAN α-PARTICLES

As has been previously mentioned, the counter in air does not register β- or γ-rays to any appreciable extent. A direct measurement of the efficiency of the counter in the End-on position for β-particles was made using a strong source of thorium active deposit, and the efficiency was found to be of the order of 2×10^{-6}. Nevertheless, a counting characteristic for β-particles was obtained with a plate cathode using the End-on position, the curve having a plateau and shape similar to that obtained for α-particles.

Gamma-rays produce no observable effect, but the counter was found to count ' knock-on ' protons in air, the End-on position being used again, with a plate cathode.

The protons were produced by bombarding Styrafoil with the α-particles from polonium, and by comparison with the counting rate in a thin windowed Geiger counter, the efficiency of the spark counter for these protons was shown to be about 5%.

Payne (1949) has shown that β-particles and knock-on protons are counted in carbon dioxide at atmospheric pressure. This has been verified, but an extensive examination has failed to show even the short plateau mentioned in that paper.

§ 15. THE DIFFERENTIAL COUNTER

In this arrangement, two wire cathode counters are placed one behind the other so that α-particles approaching from the Broadside position can pass through the gap of each in turn. In the arrangement studied, the separation between the axial planes of the two counters was about 2 mm. Separate power supplies were used for the two individual counters and their quench-circuit output pulses were fed to a simple anticoincidence unit. In this way, by recording only those α-particles which cause the first counter to spark alone, it was hoped that a differential range curve could be obtained. On approaching an α-particle source to such a counter pair, it was expected that the anticoincidence counting rate would reach a maximum and subsequently decrease as the range of the particles was traversed.

Clearly, for successful operation of the arrangement, the individual counters must exhibit stable and reproducible counting, and there must be no coupling between them. The rear counter should only spark when α-particles actually pass through its gap. It was to eliminate coupling that the separate power supplies were used, and the smallest quench capacity consistent with stable operation was employed. The general result of the latter precaution was that all sparks were extremely faint; under these conditions the protons produced in one counter gap did not produce spark breakdown in the other. Thus it was possible to have the front counter sparking rapidly due to a strong source of α-particles whose range was too short to reach the rear counter, and the rear counter would not discharge. Figure 10 gives details of the quench circuits employed as well as of the anticoincidence circuit, which is essentially a modification of the cathode-coupled amplifier due to Schmitt (Schmitt 1938 a, b, 1941). From a study of this circuit, it will be apparent that, when the front counter sparks alone, the output to the scaler consists of negative pulses while coincidences and pulses from the rear counter alone give positive pulses to the scaler. With the scaler set to register only negative pulses, anticoincidences of the type required will thus be recorded. A differential range curve obtained with this arrangement is given in Figure 11.

A flat maximum was found to exist in the counting characteristics of both front and rear counters; and the voltages appropriate to these maxima were used throughout the operation of the differential arrangement. From graphs like that shown in Figure 11, an 'extreme' and an 'extrapolated' range can be defined (see §5). For ThC′ α-particles, the 'extrapolated' range so obtained was $8{\cdot}49 \pm 0{\cdot}02$ cm. (at 15° c. and 760 mm. Hg pressure). This is somewhat shorter than the extrapolated range of $8{\cdot}56 \pm 0{\cdot}03$ cm. obtained with a single counter in the Broadside position—and the latter figure is a few tenths of a millimetre less than the standard value. This result indicates that in the double counter a larger ionizing event is needed than in the single counter to produce the same probability of sparking, and this again is probably due to the fact that in the double counter

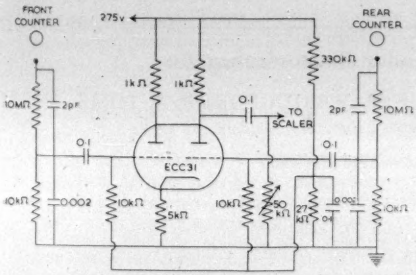

Figure 10.

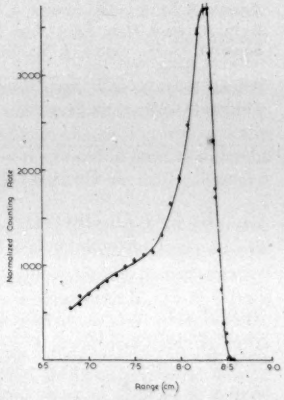

Figure 11.

the field is considerably distorted due to the close proximity of the two systems. In practice therefore, any double counter arrangement must be calibrated with some standard α-particle range, and even with a single counter this is necessary as the range value obtained varies slightly with the geometry of the system and the quiescent corona current used.

With each arrangement, however, range differences as between α-particle groups agree with standard values. Using ThC′ and ThC α-particles, for example, the following range differences at 15° c. and 760 mm. Hg were obtained: single counter: extreme $3{\cdot}90 \pm 0{\cdot}015$ cm., extrapolated $3{\cdot}84 \pm 0{\cdot}015$ cm.; differential counter: extreme $3{\cdot}86 \pm 0{\cdot}02$ cm., extrapolated $3{\cdot}83 \pm 0{\cdot}02$ cm. These values are to be compared with $3{\cdot}88 \pm 0{\cdot}01$ cm. and $3{\cdot}838 \pm 0{\cdot}002$ cm., respectively, deduced from Henderson's ionization curve (Henderson 1921).

ACKNOWLEDGMENTS

The author would like to express his thanks to Professor N. Feather, for suggesting this work, for his many helpful suggestions and guidance, and for his assistance in the preparation of the text.

The author's thanks are also due to the Department of Scientific and Industrial Research for a grant which permitted this work to be undertaken.

REFERENCES

CHANG, W. Y., and ROSENBLUM, S., 1945, *Phys. Rev.*, **67**, 222.
CONNOR, R. D., 1949, *Nature, Lond.*, **163**, 540.
FREY, P., 1946, *Helv. Phys. Acta*, **19**, 41.
GREINACHER, H., 1934 a, *Helv. Phys. Acta*, **7**, 360 ; 1934 b, *Ibid.*, **7**, 514 ; 1935 a, *Ibid.*, **8**, 89 ; 1935 b, *Ibid.*, **8**, 265 ; 1935 c, *Z. tech. Phys.*, **16**, 165 ; 1938 a, *Ibid.*, **19**, 132 ; 1938 b, *Ibid.*, **19**, 592.
HENDERSON, G. H., 1921, *Phil. Mag.*, **42**, 538.
JEANGUENIN, P., 1944, *Helv. Phys. Acta*, **17**, 319.
KEUFFEL, J. W., 1949, *Rev. Sci. Instrum.*, **20**, 202.
LOEB, L. B., and MEEK, J. M., 1940, *J. Appl. Phys.*, **11**, 438.
MEEK, J. M., 1940, *Phys. Rev.*, **57**, 722.
PAYNE, R. M., 1949, *J. Sci. Instrum.*, **26**, 321.
PIDD, R. W., and MADANSKY, L., 1949, *Phys. Rev.*, **75**, 1175.
RUBENS, S. M., and HENDERSON, J. E., 1940, *Phys. Rev.*, **58**, 446.
RYTZ, A., 1949, *Helv. Phys. Acta*, **22**, 1.
SCHMITT, O. H., 1938 a, *J. Sci. Instrum.*, **15**, 136; 1938 b, *Ibid.*, **15**, 234 ; 1941, *Rev. Sci. Instrum.*, **12**, 548.
STUBER, R., 1939, *Helv. Phys. Acta*, **12**, 109.
TRICHEL, G. W., 1939, *Phys. Rev.*, **55**, 382.

A Coaxial-Cylinder Elastoviscometer

BY J. G. OLDROYD, D. J. STRAWBRIDGE AND B. A. TOMS
Courtaulds Limited, Research Laboratory, Maidenhead, Berks.

MS. received 15*th May* 1950

ABSTRACT. An instrument is described which was designed to measure the elastic and viscous properties of liquids, primarily of solutions of linear high polymers whose elastic properties had already been observed qualitatively. The liquid is contained in a narrow annulus between two long vertical cylinders. The outer cylinder can be driven in steady rotation at a known speed, or in harmonic angular oscillations of known amplitude and frequency. In steady rotation, the torque on the stationary inner cylinder is measured at different speeds, and interpreted to give a viscosity coefficient as a function of shear stress. In oscillatory motion, the amplitude of oscillation of the inner cylinder, when constrained by a torsion wire, is measured and plotted against the frequency. The shape of the resulting graph can be interpreted so as to distinguish and measure different types of elastic behaviour. The annular gap, the restoring constant of the torsion wire and the amplitude of oscillation of the outer cylinder can be varied in discrete steps. The angular velocity of the outer cylinder can be varied continuously from 0·3 to 3,000 rev/min. in steady rotation, and the frequency can be varied continuously from 0·25 to 25 c/s. in steady oscillation. The performance of the instrument in both steady-state and oscillatory experiments is assessed by comparing observed and predicted results for Newtonian liquids of known viscosity. An example is given of the behaviour of a typical polymer solution in both kinds of experiment, together with a suggested quantitative interpretation of the results.

§ 1. INTRODUCTION

THE observed rheological behaviour of certain solutions of linear high polymers in simple solvents cannot be completely explained in terms of a single variable viscosity coefficient depending on the rate of strain. For example, the recoil of air bubbles in a mixture of *poly*(methyl methacrylate) and *cyclo*hexanone*, contained in a bottle which has been suddenly turned through an angle and then brought to rest, is interpreted as direct evidence of liquid elasticity.

* Made, for example, by dissolving 3 gm. ' Perspex ' in 100 ml. solvent.

The instrument described in the present paper was designed for the purpose of measuring both the elastic and viscous properties of such elastico-viscous liquids. The properties in a simple shearing motion can be measured directly by this instrument; the properties of the liquid in more complicated types of motion can then be deduced by a process of generalization (Oldroyd 1950), in which further experiments of a different type may well be required to resolve ambiguities.

In order to observe the liquid in (as nearly as possible) a simple shearing motion, a *coaxial-cylinder elastoviscometer* was envisaged, with an annular gap small in relation to the diameter and with cylinders sufficiently long to make end-corrections relatively small. These requirements called for a high degree of precision in the construction and alignment of the cylinders. The simplest type of experiment in such an instrument, involving a steady relative rotation of the cylinders at various speeds, can readily be interpreted to give the viscosity of the material as a function of the shear stress. Stability of the flow at high speeds demands that the *outer* cylinder should rotate (Taylor 1922) at known speeds; the torsional couple on the stationary inner cylinder is then to be measured. For the purpose of detecting and measuring any wall effects which may be shown by polymer solutions (Toms 1949), it must be possible to change the width of the annular gap, and to compare observations on the same liquid in gaps of different widths. In every experiment the temperature must be known and maintained constant.

Some simple kind of non-steady motion must also be achievable, in order that elastic properties can be measured conveniently. A uniform harmonic angular oscillation provides a type of motion which is especially amenable to mathematical analysis. If it is possible to make observations on the same liquid at various frequencies, different types of elastic behaviour can be distinguished and measured. When the outer cylinder oscillates in a known way, it is not very easy to arrange that the inner cylinder remains perfectly stationary while the forces on it are recorded. It seemed preferable, therefore, at the expense of some facility in the mathematical analysis of results, to observe the small amplitude of oscillation of the inner cylinder, when constrained by a torsion wire of known elastic constant. The phase difference in the motion of the inner and outer cylinders could also be measured, if required.

As a result of the above considerations, it was decided to construct an instrument of the following type. A vertical outer cylinder, surrounded by a water jacket for temperature control, can either be rotated steadily at any speed within a wide range or put into forced harmonic angular oscillations at a wide range of known frequencies, with one of several possible known amplitudes. Any one of three inner cylinders, with slightly different diameters, can be accurately aligned coaxially with the bore of the outer cylinder. It is possible to measure the torsional couple on the inner cylinder in a steady state by means of a torsion wire, and to observe optically the amplitude of oscillation of the inner cylinder in a state of uniform oscillation. The apparatus described in the present paper differs in several important features from that of Goldberg and Sandvik (1947).

§ 2. DESCRIPTION

The parts of the elastoviscometer are separately and rigidly fixed on a concrete bed. Three major components may be distinguished : the coaxial-cylinder assembly, the driving mechanism, and the measuring devices.

(i) *The Coaxial-Cylinder Assembly*

The general appearance of this unit and the framework in which it is mounted is represented in Figure 1; important details of the construction are shown in Figures 2 and 3. For convenience, we shall refer to the inner and outer cylinders as the 'bob' and the 'pot' respectively.

The coaxial-cylinder assembly is held in horizontal bridges, or cross-pieces, extending between two vertical pillars 120 cm. in length made from steel rod of 2·5 cm. diameter. These pillars are set 25·4 cm. apart and normal to the flat surface of a heavy steel base-plate. The cross-pieces are of steel plate, 1·5 cm. thick, and they have various widths between 10 and 15 cm.; holes are drilled near

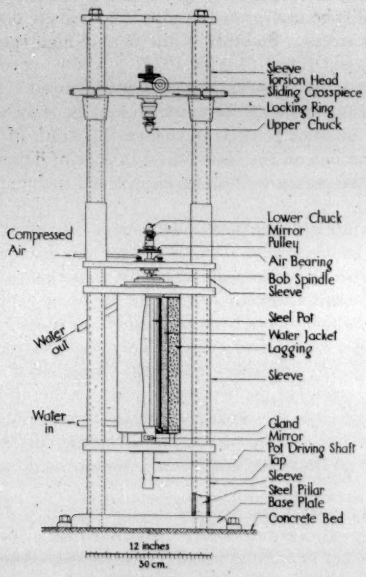

Figure 1. The coaxial-cylinder assembly and supporting framework. Elevation.

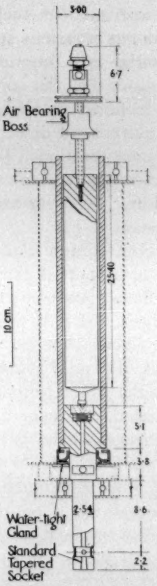

Figure 2. The coaxial-cylinder assembly. Detail.

their ends so that they slide upon the pillars, being held apart and in position by steel sleeves of the correct lengths. The top end of each pillar is threaded so that the whole framework comprising pillars, cross-pieces and sleeves can be locked together rigidly by tightening two hexagonal nuts (Figure 1). This method of construction makes it possible to dismantle and re-assemble the apparatus when necessary.

The pot is essentially a (vertical) tube closed at the bottom end by a plug, a downward extension of which forms the driving shaft (Figure 2). The longitudinal axes of this shaft and the bore of the pot body are coincident. The pot is mounted in two ball bearings, one at the top and one on the driving shaft. These bearings,

which are held in cross-pieces, are coaxial with the bore of the pot body; the pot rotates freely in them, and the setting is such that its longitudinal axis is as nearly vertical as possible.

The body of the pot was made from a solid billet of stainless steel, and the whole of the inside surface was finally honed to a mirror finish. The liquid-tight vessel, 29·90 cm. in depth, obtained by pressing a stainless steel plug into one end of this tube has the form of a right cylinder. Its internal diameter is given in the Table; other dimensions can be deduced from Figure 2, which is drawn to scale.

Dimensions of the Cylinders and Annuli.

Cylinder			Annulus	
Type	Designation	Functional diameter * (cm.)	Length (cm.)	Width (cm.)
Outer	Pot	4·3424	—	—
Inner	Bob I	4·2423	25·40	0·0500
Inner	Bob II	4·1402	25·40	0·1011
Inner	Bob III	3·9383	25·40	0·2021

* The dimensions to which the instrument was made were specified in inches, and the variation of diameter along the length of a cylinder is less than 0·0001 inch.

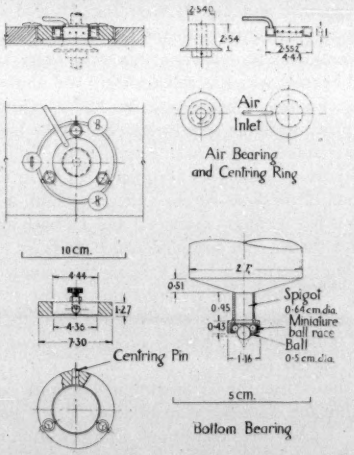

Figure 3. Details of bearings supporting inner cylinder.

A bob has the form shown in Figure 2. Basically it is a solid right cylinder of Duralumin, honed smooth, but the bottom end has been shaped to a cone of large apical angle (approximately 145°) terminating in a cylindrical spigot. There is a symmetrically tapered hole in the centre of the flat end of the bob. The longitudinal axes of this hole, of the cylindrical body of the bob, and of the spigot, are coincident. Three bobs have so far been made to this pattern: they

differ in diameter (see Table) but have the same length measured from the top surface to the end of the cylindrical body (25·40 cm.), or to the end of the spigot (26·80 cm.).

It has been arranged that when a bob is mounted inside the pot the vertical axes of the two coincide; this is accomplished by means of special bearings which locate the top and bottom ends of the bob. Details of these bearings are shown in Figure 3.

A miniature thrust ball bearing serves to locate the bottom end of the bob centrally with respect to the bore of the pot. This bearing is held in a steel sleeve which fits the spigot of the bob; it bears on a 5 mm. diameter steel ball located in a conical depression at the centre of the floor of the pot. A removable screw plug forms the central part of the pot floor (Figure 2): replacement of this plug is the only alteration of the pot that need be occasioned by a change in the form of the bottom bearing. (Similarly, different devices could readily be attached to the spigot of the bob.)

In order to locate the top end of the bob, a hollow steel spindle with a symmetrically tapered end (Figure 2) is inserted into the tapered hole provided; this spindle is locked in place by means of a threaded rod which passes through it and is screwed into the body of the bob (cf. Edsall *et al.* 1944). The longitudinal axis of the spindle then coincides with that of the bob. The bob is lowered into the pot through a heavy brass ring of rectangular section, held in a cross-piece; the free end of the spindle projects upwards through this ring when the bob rests on the bottom bearing (Figures 1 and 2). It is arranged* that the inside cylindrical surface of the brass ring is coaxial with the bore of the pot. It now remains to locate the spindle centrally with respect to the brass ring: this is done by means of an air-lubricated bearing which is self-centring and almost ideally frictionless.

The air bearing (Figure 3) has two parts, one a cylindrical boss, made of Duralumin, which slides on to the spindle attached to the bob (Figure 2), and the other, an annular air chamber having twelve radial holes, each of 0·08 cm. diameter, drilled symmetrically around the inner periphery. The air chamber fits the brass ring, and the position of the boss on the vertical spindle is adjusted so that the chamber surrounds it like a collar (Figures 3 and 1), with an annular gap 0·0064 cm. in width between them. Air supplied under pressure to the chamber issues from the holes and impinges on the boss, keeping the spindle in a central position relative to the ring. The escaping air mingles with the atmosphere above and below the gap; the down draught is prevented from entering the pot by a deflector skirt at the bottom of the boss. There is symmetry about the vertical axis and no resultant torque on the boss.

Experience has shown that the air bearing will operate satisfactorily when the excess pressure within the chamber is maintained at 0·5 atmosphere by a small rotary compressor. Under these conditions air lubrication is maintained even if a resultant force of 50 gm. wt. is applied normally to the spindle at a point above the

* The brass ring is held in the cross-piece by means of adjustable locking-screws (Figures 1 and 3). A brass disc, 1·2 cm. in thickness, which fits the annular space between the spindle and the ring, is placed on the free end of the spindle and pushed down until it rests inside the ring. The position of the ring in the cross-piece is then correctly fixed by testing that the vertical axis of the spindle remains coincident with that of the bore of the pot while the locking screws are tightened. Deviations of the spindle from the central position are detected by means of two specially shaped brass plugs which fit the annular space between it and the wall of the pot. The position of the ring is adjusted until the tightness of fit of the two plugs is the same (as judged by manipulating them with the finger-tips). There is reason for thinking that by this method the centre of the brass ring can be located within 0·0003 cm. of the vertical axis of the bore of the pot. The setting of the ring is checked at intervals.

boss. The excellent lubrication provided by the air film increases the relative importance of even the slightest imperfection in the miniature ball bearing which supports the weight of the bob, but effects due to this cause can be considerably reduced by lessening the load on the ball bearing (see § 3).

Liquid is introduced into the annular gap between the bob and the pot by forcing it upwards through an axial hole in the pot driving shaft (Figure 2). This hole bifurcates at the top so as to discharge liquid on either side of the steel ball in the centre of the pot floor, and it can be closed by a tap near the bottom end of the shaft. In the end of the shaft, below the tap, there is a tapered socket which receives a standard glass cone attached to a pneumatically operated filling apparatus. The level of the liquid in the annular gap can be deduced from observations of its level in a vertical sight-tube attached to the filling apparatus. These arrangements make it possible to fill the annular gap with liquid to any desired level without entrapping air bubbles and without altering the relative positions of the bob and the pot.

The temperature of the coaxial cylinder assembly is controlled by surrounding the pot with a lagged water-jacket (Figure 1). Water kept at constant temperature ($\pm 0{\cdot}03°$ at 25° c.) in a storage tank is pumped continuously through this jacket at approximately 2·5 litres/min. Leakage of water where the pot driving shaft passes through the floor of the jacket is prevented by a Neoprene gland. The temperature of the ambient air is maintained at $20 \pm 1°$ c. During an experiment, the top of the pot can be enclosed by a removable cover (not shown in Figure 1) which serves to improve temperature control within the annulus and to reduce evaporation of the contained liquid. The cover is designed so that it does not interfere with the movement of the pot or of the bob spindle.

(ii) *The Driving Mechanism*

The pot is moved about its vertical axis by connecting its driving shaft (Figure 1) with a mechanism actuated by a 0·5 horse-power electric motor (240 v. 50 c/s. induction type). Two kinds of motion are possible: the pot can be rotated steadily at any speed between 0·3 and 3000 rev/min. ; alternatively, a simple harmonic angular motion of the pot can be maintained at any frequency between 0·25 and 25 c/s. The amplitude of oscillation can be varied in steps: at present, five amplitudes, in the ratios 1 : 2 : 4 : 8 : 16, are available, the smallest corresponding to an amplitude of the pot equal to 0·005 radian.

The driving mechanism has been designed so that the electric motor runs continuously at its maximum speed (1,420 rev/min.). Essentially, it causes a vertical shaft (the ' primary shaft '), carrying a flywheel, to rotate steadily at any speed between 15 and 3,000 rev/min. This is accomplished by interposing an H-type gear, a clutch, one of three trains of spur gears, and a pair of bevel gears (in that order) between the motor and the primary shaft. The three speed ranges provided by the trains of spur gears overlap, and so, by employing the H-type gear, the speed of rotation of the primary shaft is made continuously variable between the limits specified. When speeds less than 15 rev/min. are required, an auxiliary 50 : 1 reduction gear-box is temporarily engaged: this is connected to the primary shaft by means of a Vee-belt and serves to drive another vertical shaft (the ' secondary shaft ') at any desired speed between 0·3 and 60 rev/min.

The pot is made to rotate continuously by fixing a pulley on the pot driving shaft and connecting it, by means of a Vee-belt, with a pulley on either the primary or secondary shaft.

The pot is given a uniform angular oscillatory motion in the following way. The pulley on the top end of the primary shaft has five threaded holes in its upper horizontal surface at different calculated distances from its centre. Above this pulley (and just clear of it) is mounted a rectangular Duralumin plate, or carriage, having two pairs of self-lubricating bushes fixed to its corners. The bushes slide on two parallel steel rods, 25 cm. in length and 12 cm. apart, which are horizontal and are supported at their ends in a frame. The direction of movement of the carriage along the rods is perpendicular to the line joining the primary shaft and the pot driving shaft. A slot, fitted with adjustable hardened steel edges, has been cut in the carriage at right angles to the direction of movement. A stout steel pin is inserted through the slot and screwed into one of the holes in the pulley beneath; this pin carries two ball races, one above the other, which run on opposite sides of the slot. When this connection between the slot and the pulley has been made, rotation of the primary shaft causes the carriage to move along its supporting rods with simple harmonic motion. The amplitude of this motion is constant and depends upon the eccentricity of the connecting-pin relative to the axis of the primary shaft, but the frequency, which corresponds with the speed of the primary shaft, can be varied between 0·25 and 25 c/s.*

The moving carriage is made to drive the pot by having on it a centrally mounted vertical pin which engages in a slot in the free end of a horizontal Duralumin beam fixed to the pot driving shaft. Since the effective length of the beam (50·8 cm., equal to the distance between the axes of the primary shaft and the pot driving shaft) is large compared with the linear throw of the carriage, the angular oscillatory motion given to the pot is almost exactly simple harmonic. The pot moves with the same frequency as the carriage and its angular displacement in a half-cycle is readily calculable.

(iii) *The Measuring Devices*

In both the kinds of experiment that we make at present with the elastoviscometer it is only necessary to know the speed with which the pot is moving when its motion is steady or uniformly oscillatory. It has therefore been possible to measure both speeds and frequencies by a relatively simple stroboscopic method. For this purpose repeating patterns of special design have been marked on the pulley which fits on the pot driving shaft, and on the rim of the flywheel mounted on the primary shaft. The speed of rotation of either wheel is then estimated by means of a commercial ' strobolamp '. The frequency of the oscillatory motion is deduced from the speed of the flywheel. The strobolamp is calibrated before each experiment by means of a standard vibrating reed.

At present it is arranged that one of two other observations can be made, depending on the type of motion executed by the pot. When this is made to oscillate, angular displacement of the bob is constrained by means of a torsion wire, and the amplitude of the uniform oscillatory motion assumed by the bob under these conditions is then observed as a function of the frequency. When the pot rotates steadily, the torque on the bob is measured. These determinations are made directly by means of simple devices, which will now be described.

A removable boss (Figures 1 and 2), on which are mounted a screw chuck, a pulley of radius 2·54 cm. and a small plane mirror, is fixed on the free end of the bob spindle above the air bearing. The chuck serves to grip the lower end of a torsion

* Higher frequencies (up to 50 c/s.) are attainable when the amplitude of oscillation is small.

wire which extends vertically between it and another similar chuck attached to an adjustable torsion head, rigidly held in a cross-piece which can be clamped to the vertical sleeves on which it slides (Figure 1). Straight torsion wires up to 30 cm. in length can be accommodated in this assembly, and wires of three different lengths and three different diameters have so far been provided. Their ends are permanently fixed in cylindrical bushes which fit in the collets of the chucks. The wires were made to our dimensional specification from a beryllium–copper alloy, and their torsional constants are, approximately, in geometrical progression between $0{\cdot}0037 \times 10^6$ and $7{\cdot}25 \times 10^6$ dyne cm/radian. The constants of the wires and the moments of inertia of the bobs were determined by a dynamical method.

If, when the pot rotates and its speed is increased, the torque on the bob becomes too large, the restoring force due to a torsion wire can be supplemented with a suitable couple applied to the pulley on the bob spindle. This is done by attaching two threads to the periphery of the pulley: these pass over auxiliary pulleys (not shown in Figure 1) which are mounted in brackets fixed on opposite sides of the cross-piece containing the air bearing. By loading the threads equally a known axial couple can be applied to the bob spindle without introducing a resultant force tending to displace its vertical axis.

Angular movements of the bob about its vertical axis are observed with the aid of an optical lever 100 cm. in length. A beam of light is reflected from the vertical mirror on the boss attached to the bob spindle, and is focused on a horizontal curved scale engraved on a flexible strip of translucent bakelite. The scale is approximately 100 cm. in length and is set so that one division corresponds to an angular movement of the bob equal to 0·000635 radian. When necessary, angular movements of the pot can also be observed by reflecting a beam of light from a plane mirror fixed to the side of the pot driving shaft (Figure 1).

§ 3. EXPERIMENTAL METHODS

It has been found that the bob will respond to very small couples when its setting on the bottom bearing is finely adjusted: this is done by raising the bob through a small distance, thus reducing the load on the miniature ball bearing, so that friction, and the effects due to minute irregularities, are virtually eliminated. The bob is lifted by retracting the chuck attached to the torsion head, and its vertical displacement is observed by means of a simple clock gauge actuated by the nose of the chuck on the bob spindle. The vertical displacement is varied according to the type of experiment: it amounts to 0·0025 cm. when the pot is to be made to oscillate, but is less than 0·00025 cm. when rotation of the pot is intended. The latter displacement is sufficient to ensure that the weight of the bob is entirely supported by the torsion wire. Experience has shown that the detrimental effect of these adjustments on the centring capacity of the bottom bearing is negligible.

When the setting of the bob has been completed the top chuck is locked to the torsion head.

In the operation of filling the annulus with liquid, sufficient time is allowed for the liquid, and the bob, to attain thermal equilibrium with the pot. The level of the meniscus in the sight-tube of the filling apparatus is then observed with the air bearing in operation, the tap in the pot driving shaft is closed, and the filling apparatus removed.

The annulus is filled to different levels according to the type of experiment which it is intended to make. It is completely filled (so that the liquid surface is

level with the top of the bob) for experiments in which the pot is oscillated; but in experiments involving continuous rotation of the pot, often at high speeds, less liquid is used. In these latter experiments, moreover, measurements of the torque on the bob, over a suitable range of pot speeds, are always made with two levels of liquid in the annulus differing by 10-20 cm. This is done so that end effects may be eliminated (see § 4).

Although no provision has yet been made for determining the temperature of the liquid in the annulus while the elastoviscometer is working, measurements made with the pot at rest have shown that at 25° C. it differs by less than 0·2° C. from the known (mean) temperature of the water passing through the jacket. Moreover, there is reason for thinking that the liquid temperature remains sensibly constant throughout an experiment in which the pot is oscillated, but when the pot rotates at constant speed it sometimes happens that heat is produced so rapidly by shearing the liquid that the torque on the bob is observed to change with time. It then becomes necessary to operate the apparatus discontinuously, stopping after each measurement has been made in order that the liquid in the annulus may cool. It is not possible, however, to accelerate the pot from rest to a steady speed, and to make the necessary observations of speed and torque, in less than 10 seconds. There is therefore a limiting rate of shear, depending on the viscosity of the liquid, above which reliable observations cannot be made.

§ 4. PERFORMANCE

(i) *Experiments involving Steady Rotation*

The observations made when the pot is rotating steadily are interpreted to give the viscosity of a liquid as a function of shear stress (or of rate of strain). Wall effects, if present, can be detected and measured.

In order to eliminate end effects, two experiments, in which the annular gap is filled to different heights (h', h'' measured on an arbitrary scale), are performed on each liquid. The couples G', G'' exerted on the stationary bob in a steady state are recorded as functions of the angular velocity Ω of the pot, and the relation between torque and angular velocity in each experiment is then defined by drawing a smooth curve through a plot of the observed values. For a Newtonian liquid the viscosity η is given by the formula

$$\eta = \frac{(r_2^2 - r_1^2)[G''(\Omega) - G'(\Omega)]}{4\pi r_1^2 r_2^2 (h'' - h')\Omega}, \qquad \ldots\ldots(1)$$

where r_1 is the radius of the bob, and r_2 is the internal radius of the pot; C.G.S. units are used in all calculations, and Ω is measured in radians/sec., so that η is obtained in poises. In this case the rate of shear γ and the shear stress τ at $r = \sqrt{(r_1 r_2)}$ are given by

$$\gamma = \frac{2r_1 r_2 \Omega}{r_2^2 - r_1^2}, \qquad \ldots\ldots(2)$$

$$\tau = \frac{G''(\Omega) - G'(\Omega)}{2\pi r\, r_2 (h'' - h')}, \qquad \ldots\ldots(3)$$

and, of course,

$$\eta = \tau/\gamma. \qquad \ldots\ldots(4)$$

When the annular gap is narrow and the liquid is non-Newtonian, the same formulae (1)–(3) give the relations between viscosity, rate of shear and shear stress parametrically, with only a second-order error. In this case τ has the same

physical significance as before, and γ is a first-order approximation to the rate of shear at $r=\sqrt{(r_1 r_2)}$ (reckoning the annulus/diameter ratio as a first-order small quantity), so long as wall effects are absent.

Wall effects are detected by plotting η against τ (or γ), as given by equations (1)–(3), for different annular gaps. Any appreciable wall effect would make the curves for different annular gaps distinct, but if wall effects are absent the curves should coincide with only a second-order error.

Liquids having viscosities between 0·02 and 20 poises approximately, can readily be studied. It is possible to make rotational experiments with more viscous liquids, but two practical difficulties are encountered. In the first place, much time is needed to adjust and determine the level of liquid in the annulus. Secondly, delays due to heating of the liquid by shearing are both frequent and protracted, even when Bob III is used and the pot rotates at relatively small speeds. The problem presented by very mobile liquids ($\eta<0{\cdot}02$) is naturally different, since the controlling factors are the sensitivity of the instrument and the stability of laminar flow in the annular gap. The conditions for stability of laminar flow between coaxial cylinders when the outer one is rotated have been investigated by Taylor (1936), and our own observations in experiments with water are broadly consistent with his. The sensitivity of the elastoviscometer in its present form is sufficiently indicated by the fact that reliable observations can be made when τ is as small as 5 dynes/cm². Because of these limitations, measurements on liquids with $\eta<0{\cdot}02$ have to be made within a relatively narrow range of fairly large pot speeds. Nevertheless, in an experiment with distilled water at 25° c., the value $\eta=0{\cdot}0087$ was obtained, and when allowance is made for the error of a single determination (see below), this estimate can be considered to be in good agreement with a standard value, $\eta=0{\cdot}00894$ (Bingham and Jackson 1917).

The accuracy of a mean value of η determined with the elastoviscometer has been assessed by making nine independent experiments with a specimen of dimethyl phthalate. The viscosity of this Newtonian liquid, measured at $25{\cdot}00\pm0{\cdot}02°$ c. by means of a standard U-tube viscometer (B.S.S. No. 2 pattern, calibrated by the National Physical Laboratory), was found to be $0{\cdot}130\pm0{\cdot}000_3$ poise; its density at the same temperature was 1·184 gm/ml. Three experiments were performed with each bob, and in each experiment measurements were made with three different levels of liquid in the annulus. The same torsion wire was used throughout, and Ω was always small enough for the torque on the bob to be measured by means of the wire alone. The temperature obtaining in all the tests was $25{\cdot}0\pm0{\cdot}2°$ c. The preparations for every independent experiment included a complete readjustment of the setting of the bob within the pot.

The mean values of η determined with Bobs I, II, and III were 0·127, 0·128 and $0{\cdot}127_5$, respectively, indicating that differences due to the replacement of one bob by another are without significance. Attaching the same weight to each of the nine experiments, we find the mean viscosity $\bar{\eta}$ to be 0·128 (standard deviation 0·002). This standard deviation is not larger than might be expected in view of the number and nature of the possible independent sources of error.

Individual errors are difficult to assess, even when they are systematic and their cause is known; but in those cases where the determination is practicable, no single error has been observed which is large enough to be a likely source of ambiguity in the kind of work that will ordinarily be done with the elastoviscometer.

(ii) *Experiments involving Oscillatory Motion*

Results obtained when the pot is oscillating uniformly are more difficult to interpret. The elastic properties exhibited by any particular liquid are measured by comparing experimental results with theoretical predictions for a series of idealized liquids characterized by different elastic constants. Agreement between theory and experiment is to be considered satisfactory only if the deductions from experiments with one bob and one torsion wire can be used to predict correctly the behaviour of the same liquid with different bobs and wires.

Oscillatory experiments are carried out with the annular gap completely filled with liquid. The amplitude of oscillation of the bob, with a torsion wire in position, is measured at frequencies in the range 0·25 to 25 c/s. The ratio ϑ of the bob and pot amplitudes is then plotted against the frequency n, several curves corresponding to different bobs and wires being obtained in the case of each liquid. A check is made that the resulting curves are (very nearly) independent of the pot amplitude when this is small; for practical convenience, most of the work is then carried out with a pot amplitude of 0·02 radian.

Predicted curves have so far been obtained by considering an elastico-viscous liquid whose behaviour in shear at small amplitudes is characterized by three constants, a coefficient of viscosity η_0 and two relaxation times λ_1, λ_2. A linear relation between the shear stress τ, the rate of shear γ, and their rates of change $\dot{\tau}$ and $\dot{\gamma}$ is assumed :

$$\tau + \lambda_1 \dot{\tau} = \eta_0(\gamma + \lambda_2 \dot{\gamma}). \qquad \ldots\ldots (5)$$

It is seen that the relaxation times have the physical significance that if the motion is stopped, the shear stress decays as $\exp(-t/\lambda_1)$, and if the stress is removed the rate of strain decays as $\exp(-t/\lambda_2)$. The relation (5) represents the behaviour of a type of material which includes as particular cases the Maxwellian elastico-viscous liquid ($\lambda_2 = 0$) and the Newtonian viscous liquid ($\lambda_1 = 0$, $\lambda_2 = 0$).

In making theoretical predictions, the amplitude of oscillation is supposed small, so that the ratio of the amplitudes of the bob and the pot is independent of the absolute value of the amplitude, and η_0 can be identified with the viscosity observed in steady rotation at very low rates of shear. The full length of the annulus is assumed filled with liquid, and end effects are ignored. The predicted (ϑ, n) curves for different bobs and torsion wires can then be obtained for a series of idealized elastico-viscous liquids. The mathematical theory involved will be outlined in another paper by one of us (J. G. O.).

The agreement between theory and experiment in the case of a Newtonian liquid (Liquid Paraffin B.P. of density 0·877 gm/ml. and viscosity 1·76 poises at 25° c.) is illustrated in Figure 4. Typical experimental points obtained at 25° c. using Bob II and a torsion wire of restoring constant $2{\cdot}79 \times 10^6$ dyne cm/radian are shown in relation to the theoretical curve. The frequency n_0 of free oscillation of the wire and bob is indicated. Inset in the figure are shown some of the individual experimental points near the peak, on an increased frequency scale, as an indication of consistency. The agreement appears to justify the neglect of end effects in the theory of small oscillations, as well as indicating the accuracy which can be expected of the apparatus in this kind of experiment.

It has been found possible to carry out oscillatory experiments with liquids having viscosities between 0·05 and 50 poises. In the tests made with liquid paraffin it was found that results obtained with the smallest pot amplitude

(0·005 radian) were unreliable, apparently for purely mechanical reasons. In practice, therefore, an agreement between observations at amplitudes 0·01 and 0·02 radian is looked for.

§ 5. BEHAVIOUR OF A SOLUTION OF A LINEAR POLYMER

As an example, we have studied a mixture of *poly* (methyl methacrylate) and pyridine at 25° c. This liquid, of density 0·98 gm/ml., contained 30·5 gm. of polymer per litre; the intrinsic viscosity $[\eta]$ of the polymer *, measured in pyridine at 25° c., was 5·50.

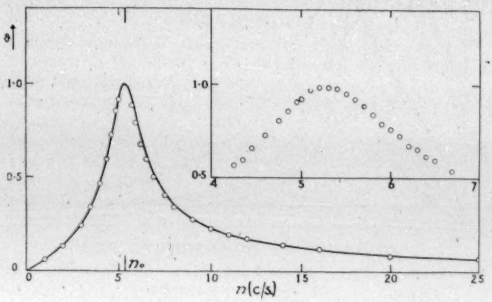

Figure 4. The relation between ϑ and n in the case of Liquid Paraffin, B.P.

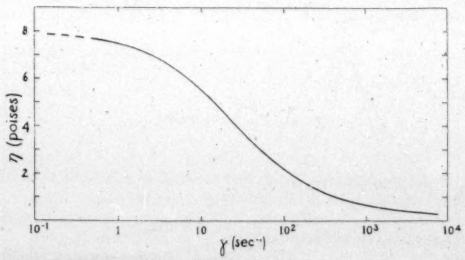

Figure 5. The relation between η and γ in the case of a mixture of *poly* (methyl methacrylate) and pyridine.

Figure 5 shows that η is not independent of γ in the range $0{\cdot}1 < \gamma < 10^4\,\text{sec}^{-1}$. Nevertheless, it is reasonable to suppose that at very small rates of shear ($\gamma < 0{\cdot}1$) the viscosity of the mixture attains a constant (limiting) value η_0, and this is estimated to be 7·9 poises.

Results obtained in oscillatory experiments are given in Figure 6. The curves refer to experiments with three bobs (I, II, III) whose moments of inertia are 2,677, 2,468 and 2,098 gm./cm², and two torsion wires (numbers 5A and 8) with restoring constants $0{\cdot}171 \times 10^6$ and $2{\cdot}79 \times 10^6$ dyne cm/radian, all carried out with a pot amplitude of 0·01 radian. In each case ϑ has a maximum value

* $[\eta] = \lim_{c \to 0} (\eta_{sp}/c)$, where the polymer concentration c is expressed in gm. per 100 ml. of solution.

greater than unity, and this occurs at a value of n greater than n_0, the appropriate frequency of free oscillation of the wire and bob. The contrast with Newtonian behaviour is very marked: all (ϑ, n) curves for Newtonian liquids, whether predicted or observed, show a maximum not exceeding unity at a frequency almost exactly equal to n_0.

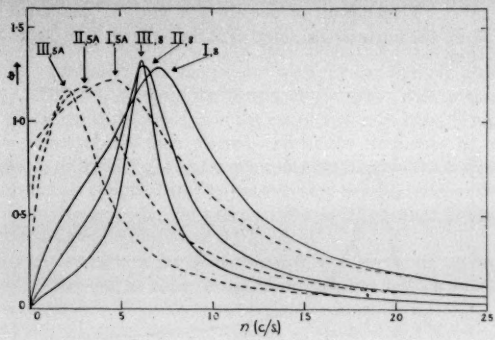

Figure 6. The observed relations between ϑ and n in the case of a mixture of *poly* (methyl methacrylate) and pyridine.

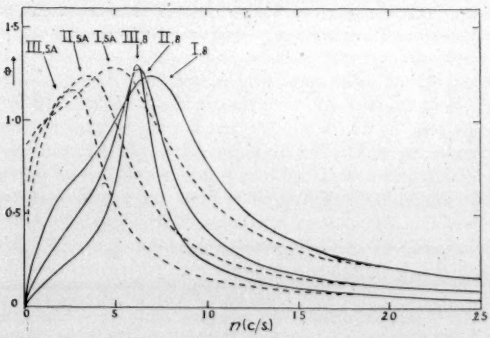

Figure 7. The predicted relations between ϑ and n in the case of an idealized elastico-viscous liquid.

The experimental curves in Figure 6 differ only slightly from those predicted for an idealized material of density 0·98 gm/ml. characterized by the constants $\eta_0 = 7{\cdot}9$ (poises), $\lambda_1 = 0{\cdot}065$ (sec.), $\lambda_2 = 0{\cdot}015$ (sec.), which are shown in Figure 7. It is therefore concluded that, to a first approximation, the mixture of *poly* (methyl methacrylate) and pyridine under consideration can be characterized by an equation of state of the form (5)—valid in simple shearing motion confined to sufficiently small rates of shear—with relaxation times 0·065 sec. and 0·015 sec.*

* The values of λ_1 and λ_2 which give the best agreement between theory and experiment in the case of a single bob and torsion wire can be estimated to within about 5%; the values quoted are those giving the best fit in the case of Bob II and Torsion Wire 8.

The Maxwellian prototype is inadequate to explain the behaviour of this polymer solution.

Results obtained in both rotational and oscillatory experiments with other polymer solutions will be described elsewhere by two of us (D.J.S. and B.A.T.).

ACKNOWLEDGMENTS

The construction of the elastoviscometer was undertaken in the Laboratory Model Shop, and much of the work was done by Mr. G. Peacock. Figures 1–3 were prepared from drawings made by Mr. R. M. Williams.

REFERENCES

BINGHAM, E. C., and JACKSON, R. F., 1917, *Bur. Stds. Bull., Wash.*, **14**, 59.
EDSALL, J. T., GORDON, C. G., MEHL, J. W., SCHEINBERG, H., and MANN, D. W., 1944, *Rev. Sci. Instrum.*, **15**, 243.
GOLDBERG, H., and SANDVIK, O., 1947, *Anal. Chem.*, **19**, 123.
OLDROYD, J. G., 1950, *Proc. Roy. Soc.* A, **200**, 523.
TAYLOR, G. I., 1922, *Phil. Trans. Roy. Soc.* A, **223**, 289; 1936, *Proc. Roy. Soc.* A, **157**, 546.
TOMS, B. A., 1949, *J. Coll. Sci.*, **4**, 511.

The Evaporation of Titanium

BY L. G. CARPENTER AND W. N. MAIR
Royal Aircraft Establishment, Farnborough, Hants.

MS. received 2nd June 1950

ABSTRACT. Data are presented on the evaporation rate of β titanium over the temperature range 1,650–1,810° K.

These are represented by

$$\log ET^{1/2} = -\frac{2{\cdot}42}{T} + 9{\cdot}79,$$

where E is in gm. cm^{-2} sec^{-1} and T is in degrees Kelvin.

The latent heat of vaporization is deduced both from the measured values of evaporation rate, together with known thermodynamic functions of the solid and gas, and also from the temperature coefficient of evaporation rate.

An estimate is made of the variation of total radiation with temperature, and of the vapour pressure at the melting point.

Experimental details are given.

§ 1. INTRODUCTION

THE vapour pressure of titanium is of interest both technologically, since the metal is attaining engineering importance, and theoretically, since, for example, its temperature coefficient gives the latent heat, and hence the binding energy of the lattice.

It was, therefore, decided, as part of the titanium research programme of the Royal Aircraft Establishment, to measure the rate of evaporation and, incidentally, the total radiation of the pure metal *in vacuo*. Some preliminary results and measurements have already been published (Carpenter and Reavell 1949, Blocher and Campbell 1949) and the present paper gives the final results of the Farnborough work with an account of the experimental technique.

§2. THEORY OF THE METHOD

The method of determining the vapour pressure p was, in essence, that of Langmuir*, in which the rate of evaporation E of a wire at known temperature T is determined *in vacuo*. It follows from kinetic theory that

$$E = \alpha p \left(\frac{M}{2\pi \boldsymbol{R} T}\right)^{1/2}, \qquad \ldots\ldots(1)$$

where M is the molecular weight of the evaporating particle, $\boldsymbol{R}$ the gas constant and α the condensation coefficient.

Using the Clausius–Clapeyron equation and assuming that the vapour is large in volume compared with the solid and behaves as a perfect gas, it can be shown that

$$\frac{d}{d(1/T)}\{\ln ET^{1/2}\} - \frac{d}{d(1/T)}\{\ln \alpha\} = -\frac{\Delta H_T}{\boldsymbol{R}}, \qquad \ldots\ldots(2)$$

where ΔH_T is the heat of sublimation at the temperature T (Guggenheim 1949, Speiser and Johnston 1950). Hence, if $\ln \alpha$ does not change significantly over the temperature range of the measurements, it is possible to deduce ΔH_T from the variation of E with T. ΔH_T can also be deduced from individual values of p provided that the difference of entropy $(\Delta S)_T$ between solid and gas is known, for

$$\Delta G_T = \Delta H_T - T\Delta S_T, \qquad \ldots\ldots(3)$$

and ΔG_T, the standard Gibbs free energy of vaporization, is given by

$$\Delta G_T = -\boldsymbol{R} T \ln (p/p_0), \qquad \ldots\ldots(4)$$

where p_0 is the pressure of the standard atmosphere. Hence equation (3) can be solved for ΔH_T.

If, during evaporation experiments, the watts supplied to the wire are measured, the relation between total radiation and temperature may be estimated. In principle, a correction should be made for the cooling of the wire due to the evaporation itself, but in practice this is negligible.

§3. APPARATUS AND EXPERIMENTAL TECHNIQUE

The experimental procedure consisted in the determination of the weight of titanium evaporated from filaments of known surface area which were heated electrically in a high vacuum for a known time, the brightness temperatures being measured optically.

The filaments were made from titanium wire, of about 0·6 mm. diameter, which had been prepared either from the chloride by the magnesium-reduction process or by thermal dissociation of the iodide.

The magnesium-reduction titanium was prepared in this establishment (Bickerdike and Sutcliffe 1949) the analysis (% by weight) being

Titanium	99·68	Silicon	0·07	Iron	0·05	Aluminium	0·02
Manganese	0·002	Chromium	0·0035	Cobalt	0·001	Nickel	trace
		Oxygen	0·2	Nitrogen	0·09		

The 'iodide' titanium, which was probably of higher purity than the 'magnesium' titanium, was prepared in the Philips' Laboratories at Eindhoven, and was kindly supplied by Dr. Fast, to whom we are much indebted.

* The Knudsen method was inapplicable as a non-reactive crucible could not be found.

The wire was dipped in 30% hydrofluoric acid for 20 seconds to clean the surface, and each new filament was heated *in vacuo* to about 1,800° K. for a few minutes in order to remove volatile impurities.

The vacuum system was made of Pyrex glass and pressures lower than 10^{-5} mm. Hg were produced by an oil-diffusion pump. Simple mechanical arrangements were used to make dismantling and reassembly easy (Figure 1), the middle of the three cone and socket joints being waxed and water-cooled. A 32 cm. length of wire was bent into a hairpin-shaped filament D the ends being spot-welded on to lugs of titanium sheet. In order to avoid sagging, the filament was mounted

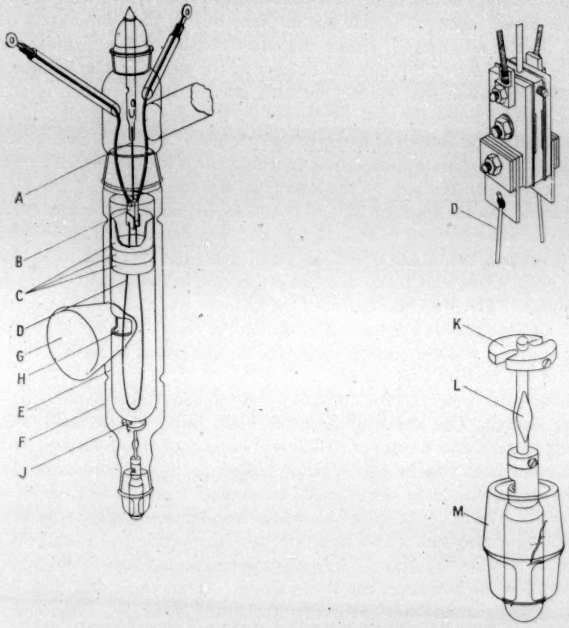

Figure 1. Evaporation apparatus.

A. Tungsten rod.
B. Terminal block.
C. Nickel screen.
D. Titanium filament.
E. Pyrex collecting sleeve.
F. Outer containing vessel.
G. Optical window.
H. Etched hole.
J. Pyrex pegs.
K. Slotted driving plate.
L. Flattened supporting rod.
M. Cone and socket seal.

vertically by clamping the titanium lugs on to a copper terminal-block B which was attached by a grub-screw to a short tungsten rod (A). This rod was sealed into the lower end of a Pyrex tube, the other end of which was integral with the cone portion of the upper of the three ground joints shown in Figure 1.

Thin platinum washers were used to separate the titanium lugs from the copper, since it was found that hot titanium reacts with copper to form a silvery alloy, whereas no reaction takes place between titanium and platinum at any rate up to

1,000° c. The terminal block was connected to a battery supply by flexible copper leads which passed out through copper-to-Pyrex vacuum seals. The power was kept constant during an evaporation run by means of a rheostat and wattmeter, the duration of the experiment varying from 8 to 115 minutes according to circumstances. The evaporated metal was collected on a cylindrical Pyrex sleeve E, made thin to aid rapid attainment of thermal equilibrium of the filament.

As the ends of the titanium filament were cooler than the rest, an artifice of the 'guard-ring' type was used to ensure that only evaporated metal appropriate to a sharply defined isothermal portion was caught on the sleeve and subsequently weighed. To this end the upper few centimetres of the sleeve were lined with a cylindrical nickel screen C which was in place during the evaporation but was removed for the weighings. Hence the effective part of the filament was that below the plane passing through the bottom of the sleeve. The validity of this artifice depends upon the 'catch' per unit area of sleeve (which is of course abnormally low opposite the cool portions of the filament) having become uniform when the level of the bottom of the screen is reached. To check this the screen C was made in three separate portions just touching and it was confirmed by weighing that the 'catch' per unit area on the lower two was the same.

To prevent the development of local hot spots, the mass of titanium evaporated during a run was restricted to about 7 mg. and was determined by weighing the collecting sleeve E, before and after a run, on a balance having a sensitivity of 0·1 mg. Suitable precautions were taken to avoid errors due to absorption of atmospheric water vapour. The evaporating area of the filament was calculated from its initial diameter and the masses evaporated in successive runs. Owing to gas pick-up, discussed in § 4, it was not possible to use the weight loss or resistance change as a measure of the amount evaporated.

A rectangular hole H ($1{\cdot}6 \times 0{\cdot}8$ cm.) was etched through the side of the collecting sleeve. The sleeve of diameter 4 cm. fitted snugly inside the outer containing vessel F and was supported on a greased cone which formed part of the lowest ground joint M, the socket being sealed on to the bottom of the outer envelope. Thus the inner sleeve could be rotated, from outside, about its own vertical axis. The inset to Figure 1 shows the detailed mechanical arrangement of this rotating vacuum seal. The flattened steel supporting rod L and the slotted driving plate K allowed sufficient movement in two dimensions to obviate fracture of the pegs J at the bottom of the Pyrex sleeve. Thus the etched hole could be brought opposite a side-arm carried by the outer envelope. The end of this side-arm was sealed by a plane window G through which the filament could be viewed by an optical pyrometer. When temperature readings were not being taken, the inner sleeve was turned so that evaporation metal did not blacken the window. Owing to the loss of evaporated metal through the hole in the collecting surface, it was necessary to add a small correction (0·8%) to the mass of titanium collected on the sleeve.

Temperatures were measured with a disappearing filament type of optical pyrometer with a red filter ($\lambda = 0{\cdot}64\,\mu$). A series of temperature readings of one particular part of the filament (the 'pyrometer observation station') were taken during each evaporation run, and the individual values were averaged to give the mean temperature of the observation station. Before and after each evaporation run, a temperature distribution experiment was performed. For this, the outer containing vessel and inner collecting sleeve were replaced by a

cylindrical envelope. The filament was heated to a temperature below that at which evaporation starts (a brightness temperature of the order of 1,100° c.) and the temperature was observed at 0·5 cm. intervals over the effective length of the filament. Filaments which, owing to wire-drawing defects, showed variations * greater than ±10° c. from the mean temperature of the 'isothermal' region were rejected. The difference between the temperature at the 'pyrometer observation station' and the mean temperature of the filament during the distribution runs was scaled up, in the ratio of the absolute temperature of the evaporation run and that of the distribution run, to obtain the difference between the mean of the observed temperatures of the 'observation station' and the required mean temperature of the filament during the evaporation run (Table 1). The pyrometer was checked against standard tungsten strip-filament lamps which had been calibrated at the National Physical Laboratory. Corrections for the absorption of the window were determined by calibrations with and without the window present. The absorption of the window was checked after each evaporation run to ensure that no blackening of the window, due to evaporated titanium, had occurred during the run. The observed brightness temperatures were converted to true temperatures by means of a linear extrapolation to 1,810° K. of the known emissivity values for titanium (Bradshaw 1950) †.

In the preliminary work (Carpenter and Reavell 1949) a constant emissivity of 0·5 was assumed, based on unpublished work of Went (Van Arkel 1939) and some preliminary results of Bradshaw. The use of Bradshaw's final results (1950), obtained on material from the same manufacturing batch as that used in the present work, has slightly altered the temperature scale and, in particular, leads to a value of the temperature coefficient of evaporation higher than that previously reported. The results of Michels and Wilford (1949) have not been used because the anomalous results they give for the resistivity and its temperature coefficient suggests that their titanium was of doubtful purity.

§4. EXPERIMENTAL RESULTS

Titanium changes from close-packed hexagonal to body-centred cubic structure at 1,155 ± 20° K. (de Boer, Burgers and Fast 1936) and the evaporation rate below about 1,500° K. is negligible. Hence, the results given below refer to the β phase.

Eleven filaments (numbered F.1 to F.11) were used in the experiments, but as the nickel 'guard screen' technique was not introduced until F.7 was reached, only the results of the last four filaments are recorded here. F.9 was unusable as it deformed and accidentally touched the sleeve E during its first run. All runs on F.7, F.8, F.10 and F.11 are included in Table 1 and are considered to be of approximately equal weight. The evaporation rate of F.10, prepared from 'iodide' titanium, was not significantly different from that of 'magnesium' titanium (Figure 2). Actually the results from the earlier filaments (in which the 'cold end' effect was allowed for by computation) are in good agreement with the later runs but have nevertheless been discarded as being of inferior reliability.

* This limit of ±10° c. was fixed after consideration of the error introduced by using the arithmetical mean temperature instead of the effective evaporation temperature, the evaporation rate not being linear with T.

† We are indebted to our colleague Mr. F. J. Bradshaw who kindly made his results available to us prior to publication.

To get rid of impurities more volatile than titanium, a filament on first heating was raised to a temperature as high as it was subsequently intended to use and about one milligram evaporated off. It was then taken down, reweighed, and replaced for use in the first recorded evaporation run.

In Table 1 the brightness temperature recorded is corrected for absorption of optical window and for errors in pyrometer scale. The true temperature given in column 5 is deduced from the brightness temperature using known values of emissivity (Bradshaw 1950). Columns 6 and 7 give the actual masses (corrected for evaporated material lost through the etched hole) and times, and column 8 the corresponding rate of evaporation.

Table 1. Experimental Results

(1)	(2)	(3)	(4)	(5)	(6)	(7)	(8)
F7.A2	1695.$_5$	104.$_5$	+8	1808	8·5	458	4·832
F8.A2	1633.$_5$	95.$_5$	0	1729	3·7	690	1·071
F8.A3	1571	88	−1	1658	4·6	3240	0·370
F8.A4	1572	88	0	1660	10·2	6900	0·390
F10.A2	1617	93.$_5$	−5	1706	4·0	1063	1·052
F10.A3	1696.$_5$	104.$_5$	−5	1796	8·3	466	5·111
F11.A2	1711.$_5$	106.$_5$	−14	1804	10·3	452	6·001

(1) Run number; (2) brightness temperature (° K.); (3) emissivity correction (° K.); (4) distribution correction; (5) true temperature (° K.); (6) m (mg.); (7) t (sec.); (8) $E \times 10^6$ (gm. cm^{-2} sec^{-1}).

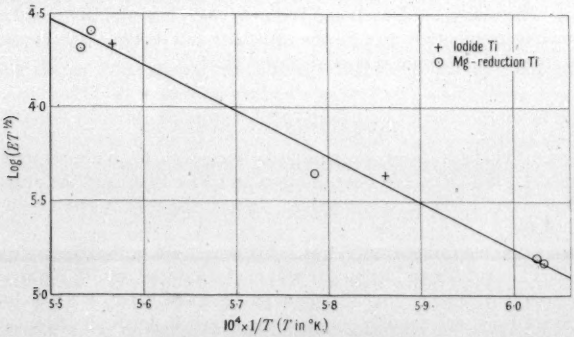

Figure 2. Evaporation rate of titanium.

It was found that the mass evaporated and caught on the sleeve usually exceeded the mass lost by the filament by about 10%. The additional matter was no doubt obtained from the gas phase, as the result of the 'gettering' property of titanium (Carpenter and Reavell 1948), and, as the filament was much hotter than the deposit on the collecting sleeve, the former is the more probable absorbent. This view was supported by the fact that at the end of its life a filament was considerably more brittle than when new, a fact consistent with gas pick-up (Fast 1938). Moreover, on several occasions the temperature

coefficient of resistance at room temperature was measured on a filament when new and after use, and found to have decreased from about 40 to about 30×10^{-4}. Also the resistance itself increased by more than was consistent with the amount evaporated. Both these observations point to the entry of gas into the lattice.

The probable error in E is estimated to be between 3 and 4%, assuming the effective area of the filament to be its geometrical area. The major part of this error arises from the uncertainty in the evaporated mass. The probable error in T is estimated to be about 5°, and arises from a combination of calibration and reading errors.

The Battelle results (Blocher and Campbell 1949) and the Farnborough results give plots of $\log p$ against $1/T$ which are approximately parallel, the Battelle line lying about 12% above the Farnborough one. This could be accounted for by a systematic difference of about 7° in the temperature scales, or by a difference in the ratio of true to apparent surface area.

In Figure 2 the values of $\log ET^{1/2}$ are plotted against $1/T$ and a straight line has been drawn through the points using the method of least squares. The equation of the line so obtained is

$$\log ET^{1/2} = -\frac{2{\cdot}42}{T} \times 10^4 + 9{\cdot}79 \qquad \ldots\ldots(5)$$

and the correlation coefficient is $-0{\cdot}992$.

The slope of this line leads to a value of $\Delta H_{1735} = 110{\cdot}9$ kcal/mole and the application of Student's t-test shows that the probability of the true value of the slope lying within ± 5 kcal. of this is one half.

The main purpose of the present work was the determination of the vapour pressure, but it seems worth while to put on record the data obtained incidentally on the variation of total radiation with temperature. The filament voltage and current were noted, the filament areas calculated, and the corresponding temperatures and values of $\log IV/A$ plotted against $\log T$. The result was a straight line. The intercept on the $\log IV/A$ axis gives the value of C in the equation

$$\text{watts/cm}^2 = CT^n \qquad \ldots\ldots(6)$$

and the slope the value of n.

In calculating A a crude attempt (based on temperature distribution) was made to allow for the presence of the cold ends of the filament, as it was not thought worth while to attach special potential leads and thus define a definite length of filament at a uniform temperature. The resulting uncertainty in C in equation (6) probably lies between 5 and 10%, but the value of n is considered to be reliable. The final result is

$$\text{watts/cm}^2 = 1{\cdot}83 \times 10^{-13} T^{4{\cdot}30} \qquad \ldots\ldots(7)$$

and is based on a plot of 31 points.

§ 5. DISCUSSION OF RESULTS

(i) *The Value of* ΔH_{298}

Equations (3) and (4) show that ΔH_T can be deduced from individual values of the vapour pressure provided that the difference of entropy of solid and gas is known.

Prof. L. Brewer has computed values of H_T and of the function $-(G_T - H_{298})/T$ for the solid and the gas from specific heat data compiled by Dr. K. K. Kelley

of the United States Bureau of Mines, Berkeley, California, and his results* are given in Table 2.

Using linear interpolation we have obtained the appropriate value of $-(\Delta G_T - \Delta H_{298})/T$ for each of our experimental temperatures. Hence we construct Table 3, computing ΔG_T using Table 1, equation (1), assuming $\alpha = 1$ and monatomic vapour, and equation (4), and thus obtaining ΔH_{298}.

The assumption that $\alpha = 1$ is not inconsistent with the data; the point is discussed later.

Assuming that there is no significant error in the values of the function $-(G_T - \Delta H_{298})/T$ derived from Table 2, the effects on ΔH_{298} of given errors in

Table 2. Thermodynamic Functions for Titanium

	298° K.	1000° K.	2000° K.
$[-(G-H_{298})/T]_{gas}$ (cal. deg^{-1} mole^{-1})	43·07	45·84	48·72
$[-(G-H_{298})/T]_{solid}$ (cal. deg^{-1} mole^{-1})	7·24	10·52	14·70
$[-(\Delta G-\Delta H_{298})/T]_{evap}$ (cal. deg^{-1} mole^{-1})	35·83	35·33	34·02
$[H - H_{298}]_{gas}$ (kcal.mole^{-1})	0	3·70	8·90

Table 3. Values of ΔH_{298} calculated from Individual Experimental Points

(1)	(2)	(3)	(4)	(5)	(6)
F8.A3	1658	$\bar{5}$·1781	55·44	34·47	112·59
F8.A4	1660	$\bar{5}$·2015	55·31	34·47	112·52
F10.A2	1706	$\bar{5}$·6381	53·43	34·41	112·12
F8.A2	1729	$\bar{5}$·6487	54·07	34·37	113·50
F10.A3	1796	$\bar{4}$·3357	50·54	34·29	112·13
F11.A2	1804	$\bar{4}$·4063	50·17	34·28	112·00
F7.A2	1808	$\bar{4}$·3127	51·06	34·27	113·02

$\overline{\Delta H_{298}} = 112{\cdot}55_6$

S.D. $= \pm 0{\cdot}55$

(1) Run number; (2) temperature (° K.); (3) log $(ET^{1/2})$ (C.G.S.); (4) ΔG (kcal/mole); (5) $-(\Delta G-\Delta H_{298})/T$ (cal/mole); (6) ΔH_{298} (kcal/mole).

our experimentally determined values of E and T can be calculated. If we take (see § 4) the probable error of E as 3·5%, and that of T as 5° K. the probable error of ΔH_{298} should not exceed 0·4 kcal. This is consistent with the standard deviation of 0·55 kcal. given in Table 3.

Using Brewer's results for the heat content of the gas as a function of temperature together with those of Kelley for the solid (Kelley 1949) one obtains

$$\Delta H_{298} - \Delta H_{1735} = 3{\cdot}85 \text{ kcal.} \qquad \ldots\ldots (8)$$

Hence, adding this to the value of ΔH_{1735} obtained from equation (5) (viz. 110·8 kcal.) we obtain $\Delta H_{298} = 114{\cdot}7$ kcal. as opposed to 112·6 kcal. which is the mean value obtained in Table 3.

* We are much obliged to Professor Brewer for kindly making the figures available to us prior to publication.

This discrepancy of 2 kcal. between the value ΔH_{298}, deduced by the method of Table 3, and that obtained from the slope of the line in Figure 2 is well within the ± 5 kcal. estimated as the probable error from Student's *t*-test. The slope method is clearly of inferior accuracy when only a small number of points are available.

(ii) *The Condensation Coefficient*

The present experiments do not provide a sensitive test for the value of α. As, however, not much is known about this quantity for metals at high temperature it is worth while to draw what conclusions are possible.

The information available can be used in three ways. We can examine Figure 2 for evidence of variation of α with temperature; we can examine Table 3 for evidence of the actual value of α, assuming it does not vary with T, and we can enquire what assumed constant value of α would be consistent with the difference between $(\Delta H_{298})_{\text{temp. coeff.}}$ and $(\Delta H_{298})_{\text{entropy}}$.

In the first place, equation (2) can be integrated and the total change of $\ln\alpha$ obtained over the experimental range T_1 to T_2, provided that ΔH_T is known as a function of T. Now, from thermodynamics, $(d/dT)(\Delta H_T)=\Delta C_p$, where ΔC_p is the difference of molar heat of solid and vapour, which we will assume independent of T. Then

$$\int_{T_1}^{T_2} d(\ln\alpha)=\int_{T_1}^{T_2} d(\ln ET^{1/2})+\frac{\Delta H_{T_1}}{\boldsymbol{R}}\left(\frac{1}{T_2}-\frac{1}{T_1}\right)+\frac{\Delta C_p}{\boldsymbol{R}}\left(\ln\frac{T_1}{T_2}-\frac{T_1}{T_2}+1\right). \quad \ldots\ldots(9)$$

We will insert experimental values between $T_1=1{,}660$ and $T_2=1{,}800°$ K. The first term with an estimate of its maximum error can be obtained from Figure 2 and is $2{\cdot}65\pm 0{\cdot}23$; the second term is $-2{\cdot}57$ and its maximum error (corresponding to a maximum uncertainty of about 2·5 kcal. in ΔH_{1660}) is $\pm 0{\cdot}06$. The third term is found to be negligible, so that the truth of the assumption that ΔC_p is temperature independent is unimportant. Now physically, $\int_{1660}^{1800} d(\ln\alpha)$ is almost certainly negative, and the most negative value it can reasonably have is $(2{\cdot}65-0{\cdot}23-2{\cdot}57-0{\cdot}06)=-0{\cdot}21$. Hence the possible decrease of α from 1,660° to 1,800° K. cannot exceed about 20%.

Secondly, if α is constant but less than unity, it is in principle possible to discover the fact by examining the variation of $(\Delta H_{298})_{\text{entropy}}$ as deduced from evaporation observations over a range of temperatures. It follows from equations (1), (3) and (4) that the true value of $(\Delta H_{298})_{\text{entropy}}$ exceeds by $\boldsymbol{R}T\ln\alpha$ the value deduced on the assumption that $\alpha=1$ from evaporation observations at temperature T. The effect is small. For example, if $\alpha=\frac{1}{2}$, the difference in the values of $(\Delta H_{298})_{\text{entropy}}$ calculated from evaporation observations at 1,660° and 1,800° K. respectively, is 0·28 kcal/mole.

Hence very accurate determinations of evaporation rates and entropy data would be necessary before a systematic trend of $(\Delta H_{298})_{\text{entropy}}$ with temperature could be attributed to a departure of α from unity. Examination of the last column of Table 3 shows that our accuracy was not sufficient to reveal the existence of such a trend.

Thirdly, as mentioned in the preceding section, the value of $(\Delta H_{298})_{\text{temp. coeff.}}$ derived from the slope of the line in Figure 2 is about 2% higher than that of $(\Delta H_{298})_{\text{entropy}}$, which is calculated from the entropy data combined with individual

values of the evaporation rate, assuming $\alpha = 1$. However $(\Delta H_{298})_{\text{temp. coeff.}}$ has a probable error of 5% compared with less than ½% for $(\Delta H_{298})_{\text{entropy}}$. Taking $\alpha = \frac{1}{2}$ and 1/10, the calculated values of $(\Delta H_{298})_{\text{entropy}}$ decrease by 2 and 8% respectively. Thus, assuming $\alpha = 1/10$ would make a discrepancy between $(\Delta H_{298})_{\text{temp. coeff.}}$ and $(\Delta H_{298})_{\text{entropy}}$ of nearly twice the probable error of the former.

Summarizing, the experimental data are consistent with α being as low as ½ but not as low as 1/10, while a temperature variation over the temperature range of more than 20% is not likely.

(iii) *The Vapour Pressure*

Using equation (1) to convert equation (5) to atmospheres on the assumption that $\alpha = 1$, we obtain

$$\log p_{\text{atm}} = -\frac{2{\cdot}42}{T} \times 10^4 + 7{\cdot}30. \qquad \ldots\ldots (5\,a)$$

Linear extrapolation gives a value of $1{\cdot}2 \times 10^{-2}$ mm. Hg for the vapour pressure at the melting point, $2{,}000 \pm 10°$ K. (Van Arkel 1939).

(iv) *The Radiation Characteristics*

The total radiation results do not call for much discussion except to note that for metals the value of n usually exceeds the black body value of 4 (see for example Blanc 1921) and the equation (7) implies a total emissivity for titanium at 1,735° K. of about 32% of that of a black body.

ACKNOWLEDGMENTS

The authors wish to acknowledge the help of their colleagues at the Royal Aircraft Establishment and the unfailing interest and support of the Director; in particular, they wish to thank Mr. F. R. Reavell *, who was a co-worker during the early part of this research.

Acknowledgment is also made to the Chief Scientist, Ministry of Supply, and to the Controller of H.M. Stationery Office for permission to publish this paper.

REFERENCES

Bickerdike, R. L., and Sutcliffe, D. A., 1949, *Metallurgia*, **39**, 303.
Blanc, A., 1921, *Rayonnement Collection Armand Colin*, No. 1, 82.
Blocher, J. M., and Campbell, I. E., 1949, *J. Amer. Chem. Soc.*, **71**, 4040.
de Boer, J. H., Burgers, W. G., and Fast, J. D., 1936, *Proc. K. Ned. Akad. Wet.*, **39**, 515.
Bradshaw, F. J., 1950, *Proc. Phys. Soc.* B, **63**, 573.
Carpenter, L. G., and Reavell, F. R., 1948, *Metallurgia*, **39**, 63; 1949, *Nature, Lond.*, **163**, 527.
Fast, J. D., 1938, *Metallwirtschaft*, **17**, 641.
Guggenheim, E. A., 1949, *Thermodynamics* (Amsterdam : North Holland Publishing Co.), p. 123.
Kelley, K. K., 1949, *U.S. Bur. Mines, Bull.* 476.
Michels, W. C., and Wilford, S. E., 1949, *J. Appl. Phys.*, **20**, 1223.
Speiser, R., and Johnston, H. L., 1950, *Trans. Amer. Soc. Metals*, **44**, 283.
Van Arkel, A. E., 1939, *Reine Metalle* (Berlin : Julius Springer), p. 187.

* Now Research Physicist with Messrs. Lever Bros. and Unilever Ltd.

An Electrostatic Focusing System and its Application to a Fine Focus X-Ray Tube*

By W. EHRENBERG and W. E. SPEAR
Birkbeck College, London

MS. received 26th May 1950

ABSTRACT. The description is given of an electrostatic focusing system by which electrons emitted from the tip of a hairpin filament are reunited at a distance of 2 to 3 cm. No intermediate potentials are required. An X-ray method is used for the experimental investigation of its properties. The electron spot is a reduced image of the tip of the filament and has a diameter of about 40 μ. On the basis of this system, a fine focus X-ray tube is designed, with a peak specific target loading of about 11 kw/mm^2. Some performance data are given.

§ 1. INTRODUCTION

The development of X-ray analysis and its application to problems demanding increased intensity and resolution led early to the construction of tubes with rotating anodes (e.g. Müller 1929, Astbury and Preston 1934, Müller and Clay 1939). It has been found possible in this way to increase the specific load W (the energy per unit area per second) applied to the anode by a factor 5 to 10 as compared with tubes employing a stationary anode and a focal spot of the same dimensions.

There is, however, another approach to the problem of increasing the specific load in the focus; an investigation of the heat dissipation in the stationary, water-cooled anode of an X-ray tube shows that as the radius R of the focal spot, assumed to be circular, is reduced to dimensions much smaller than the thickness of the anode, then $W \propto 1/R$ for a given target material (Goldsztaub 1947, Oosterkamp 1948). Thus a focus of $R = 15\,\mu$ may safely be loaded 30 to 40 times as high as one of normal dimensions, with a corresponding increase in X-ray intensity. Other advantages of a fine X-ray source in connection with crystallography have been pointed out by Bernal (1945). The production of fine, highly loaded electron foci is a problem of electron optics; in view of the considerable advantage of such foci in X-ray tubes, it is surprising to find that comparatively few attempts have been made to apply electron optical ideas to this problem.

Demountable fine focus tubes employing magnetic focusing have been described by Goldsztaub (1947) and Metropolitan-Vickers Electrical Co., Ltd. (1948). The tubes follow closely in construction and design the example of the cathode-ray tube or the electron microscope. The crossover, or a first image, produced by the electron gun, is demagnified by a magnetic lens whose image plane coincides with the anticathode. The results so obtained are good, but the need for a stabilized H.T. and lens current, and therefore complicated power unit, is a serious disadvantage. In addition, the object–image distance has to be comparatively large to obtain the required demagnification, which also makes the focusing system very sensitive to stray fields.

This points to the use of electrostatic focusing systems which do not require a stabilized H.T. unit. One would like this system to have the following

* This paper forms part of a Ph.D. thesis presented by W. E. S. to the University of London.

properties: (*a*) concentration of electrons to a spot of less than 0·1 mm. diameter at the maximum permissible load, (*b*) no intermediate potentials which would complicate the H.T. unit, (*c*) simple external adjustment to optimum focus, (*d*) comparatively short filament–anode distance.

The object of this paper is to give an account of a simple electrostatic focusing system, and to describe its application to a fine focus X-ray tube.

§ 2. THE FOCUSING SYSTEM

A preliminary experimental and theoretical study of the more conventional electrostatic lens systems (Myers 1939, Zworykin *et al.* 1945) led to the conclusion that the electrostatic focusing system of an X-ray tube presents a distinctly separate electron optical problem. The system eventually developed and examined in detail is shown in Figure 1. It consists of the grid cylinder G, mounted coaxially

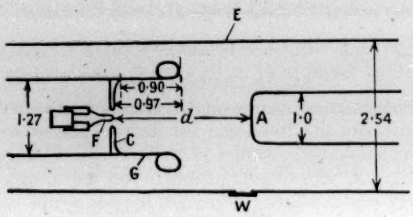

Figure 1. Section through focusing system.
Dimensions are given in cm.

with the anode rod A. G surrounds the hairpin filament F, whose tip lies on the axis of symmetry of the system. C is a cathode shield, containing a central aperture of 0·25 cm. diameter. Anode and grid cylinder are enclosed by a coaxial electrode E, which also forms the outer wall of the tube and carries the X-ray window W. The H.T. is applied between A and G; the filament is kept at a small positive potential V_F with respect to the grid cylinder. The electrode E forms an integral part of the electron optical system and the focusing properties are affected fundamentally by the potential applied to it. The system is suitable for the intended purpose if E is at or near the potential of G. The experimental data given in the following section refer to the case $V_E = V_G$. The spot size observed on the anode surface depends critically on the grid aperture–anode distance d, and the position of the tip of the filament with respect to the plane of the aperture. The bias V_F, of the order of 50 v., contributes little to the actual focusing; in addition to controlling the beam current, it largely suppresses emission from the sides of the filament. Electron concentrations of half width 30 μ are obtained on the anode surface, at $V_A = 50$ kv. and beam currents up to 500 μa.

§ 3. EXPERIMENTAL INVESTIGATION OF THE FOCUS

The intensity of the X-rays produced at any point of a metal anode is proportional to the electron intensity, so that, by means of an X-ray pinhole camera, a magnified image of the electron spot can be observed on a fluorescent screen or recorded photographically.

In fact, it was found advantageous to use a fine slit rather than a pinhole for imaging the focus. Obviously, for a faithful representation, the pinhole should be

small compared with the electron spot. It was found difficult to make suitable pinholes of diameter appreciably less than 30 μ, but good slits could be made well below 10 μ. The x-ray slit used in the experiments (Ehrenberg 1949) consists of two slightly etched silver steel rods of 4 mm. diameter, pressed together by set screws in a small brass frame and separated by a pair of spacers (7 μ nylon sheet). The use of the slit technique has the further advantage that the intensity distribution across the slit image may be measured with a normal microphotometer. It should be noted, however, that the slit image will only represent the true distribution of intensity across the centre of the spot if the distribution is of the form $A\exp(-Br^2)$, where A and B are constants. As this condition is very nearly satisfied in the present case, the intensity curves given may be taken as essentially correct.

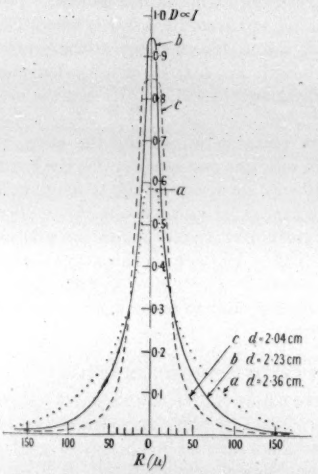

Figure 3. Intensity distribution curves of three of the slit images shown in Figure 2.

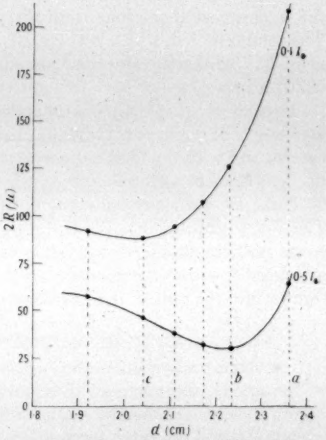

Figure 4. Variation of spot size, $2R$, with grid aperture–anode distance d for $I(R)=0{\cdot}5\ I_0$ (half width), and $I(R)=0{\cdot}1\ I_0$.

Photographic records were usually made on Kodak R20 recording film, with a magnification of 10, and a slit–spot distance of 6 cm. In order to obtain the spot dimensions without foreshortening, the slit was set in a plane normal to the surface of the anticathode. With a 35 mm. camera up to 40 exposures could be taken in succession and developed under the same conditions. The width of the slit was measured on a photograph taken with the slit placed close to the film.

Figure 2 (Plate) shows a series of slit images, recorded to investigate the effect of changing the grid aperture–anode distance d. For each value of d (given in the central column of Figure 2) two slit images are shown, one exposed for 5 minutes, the other for 25 minutes. In all exposures $V_A=50$ kv., and V_F is adjusted to give a beam current of 300 μa. The plane of the filament is horizontal. In the case of x-rays the photographic density D is directly proportional to the x-ray intensity up to about $D=1{\cdot}5$. The maximum density obtained in the 5 minute exposure is less than unity and these photographs may therefore be

regarded as faithfully representing relative x-ray intensities. The same applies to the outer regions of the 25 minute exposure, which is used to investigate the 'tail' of the intensity distribution. The densities were measured with a Hilger Spectral Photometer. Figure 3 shows intensity distribution curves for some of the slit images. Their variation with d appears to be similar to that which would be produced by a lens system, imaging a point on the axis with positive spherical aberration. Thus curve a, for the largest value of d, corresponds to a section of the beam beyond the paraxial image plane. Curve b represents a section close to the paraxial image plane; a fine central peak, of diameter less than $10\,\mu$ is formed, and the tails have become less intense. Curve c shows a section near the circle of least confusion. As expected, the peak of the intensity distribution curve is now wider, and a further widening is observed on decreasing d.

The change in spot size with d is more clearly brought out in Figure 4. The curves give spot diameters $2R$ measured at $I/I_0 = 0{\cdot}5$, and $I/I_0 = 0{\cdot}1$, where I is the intensity at R microns from the centre, and I_0 the intensity at the centre. The minimum half width is about $30\,\mu$, with fairly large 'tails' of $125\,\mu$ diameter at $0{\cdot}1\,I_0$. At the circle of least confusion, these are reduced to $85\,\mu$, but the half width is now $45\,\mu$.

Further series of slit photographs were taken to investigate the effect of asymmetry of the filament and the change in spot size and quality with the beam current and with the filament position relative to the aperture. It is found that the spot is slightly elliptic, the length of the axes differing by about 25%. The spot size is practically constant for beam currents between $100\,\mu$a and $500\,\mu$a. The position of the filament, however, is critical. The results show that the tip of the filament should always lie in the plane of the aperture, or slightly above; withdrawing it into the aperture leads to a considerable increase in the intensity thrown into the tails of the distribution curves.

§4. THE NATURE OF THE ELECTRON CONCENTRATION

In order to understand the formation and the nature of the electron concentration on the anode, the potential distribution produced by the electrodes shown in Figure 1 was determined by means of the relaxation method for the cases $V_E = V_G$ (system I), and $V_E = V_A$ (system II). The filament was idealized to a thin circular cylinder, with a flat base in the plane of the aperture. Space charge was neglected. The potential distributions form the basis for the determination of the electron trajectories through the systems. A more detailed account of this investigation will be given in a second publication; here it is sufficient to state some of the general results.

(*a*) In system I, the concentration of electrons on the anode surface is due to the formation of a demagnified image of the emitting area of the filament. This is clearly brought out by Figure 5, which shows a set of trajectories leaving the axial point, and one off-axis point of the emitting surface at 42° to the axis and with different initial velocities. The rays are denoted by a group of three numbers; the first represents the velocity of emission ($\times 10^{-7}$ cm/sec.), the second the angle of emission, and the third the initial radial height in millimetres. The most probable velocity of emission is $3{\cdot}6 \times 10^7$ cm/sec. A demagnified image is formed in a plane situated a small distance beyond the anode surface. The magnification is 0·32. Experimental values of spot size and object–image distance agree closely with the theoretical results. The experimentally determined optimum position

of the anode does not coincide with the image plane found, due to the occurrence of a small group of high velocity electrons emitted at angles outside the range of the ray tracing. These rise to comparatively large radial heights, are over-focused by the field, and thus define a plane of least confusion slightly in front of the image plane.

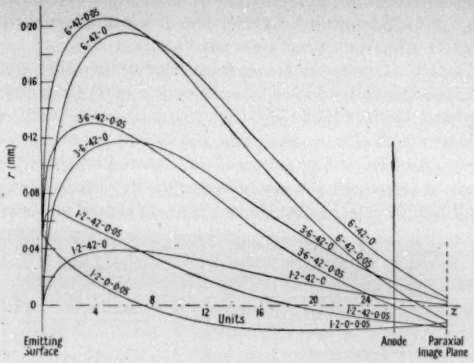

Figure 5. Electron trajectories through system I. Distances along the axis of the system (z-axis) are measured in 'units', where 1 unit ≡ 0·790 mm.; radial distances are in mm. Rays are denoted by a group of three numbers: the first represents the velocity of emission ($\times 10^{-7}$ cm/sec.), the second the angle of emission, and the third the initial radial height in mm.

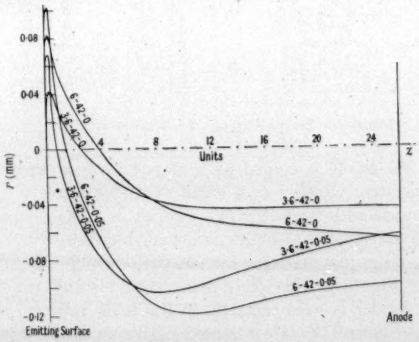

Figure 6. Trajectories through system II. Units and notation as in Figure 5.

(*b*) Figure 6 shows a similar series of rays traced through the field of system II whose focusing action resembles closely that of the more conventional type of immersion lens. It can be seen that an image is formed with considerable longitudinal aberration close to the grid aperture. The rays, having passed the image plane, are now bent back towards the axis, forming a disc on the anode surface whose diameter is strongly dependent on the velocity of emission. Obviously such a method of concentration of the electrons is unsuitable for use in a fine focus tube.

§ 5. THE DESIGN OF THE FINE FOCUS TUBE

Figure 7 (*a*) shows a complete section through the tube based on system I. The dimensions of the focusing system are given in Figure 1. The main body, supported by the exhaust tube T, carries a metal cone at its lower end which fits directly into the top of the oil diffusion pump P. To the right of T, the internal diameter of the outer tube is slightly increased to accommodate the glass cylinder G, sealed into the metal body with Apiezon wax. E is an ebonite ring, waxed on to the glass, which effectively suppresses any corona.

The cone joint C carrying the anode A is sealed to the other end of the glass cylinder. The anode is soft-soldered into the cone after the assembly of the tube has been completed, by the use of a jig which standardizes its position. It carries a disc of the target metal, of thickness $\frac{3}{4}$ mm. brazed into its end. Several anodes with different target metals can be prepared and centred for use with a particular tube. Contrary to conventional x-ray tube design, the anode is at H.T., for the metal outer wall and the external focusing adjustment should be at earth potential.

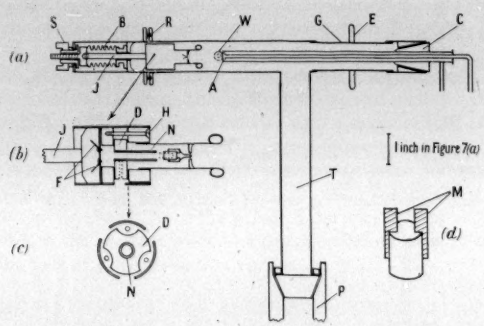

Figure 7. Section through fine focus x-ray tube.

For this reason the anode is cooled by a slow stream of carbon tetrachloride. The circulating system consists of a small centrifugal pump and a reservoir; connections are made with flexible plastic tubing.

The whole of the cathode assembly is detachable from the main body of the tube. A vacuum-tight joint between the two parts, which terminate in accurately machined flanges, is provided by slight compression of the rubber ring R. The nickel cathode cylinder is held centrally in the main tube by the brass barrel, shown in detail in Figure 7 (*b*). It is turned to give a good sliding fit in the outer tube and contains a simple mechanism which facilitates lateral and horizontal adjustment of the tip of the filament in the grid aperture. The nickel tube N carries a small ceramic filament holder shown in Figure 7 (*d*): the filament is made from 0·006 in. tungsten wire, bent into the shape of a hairpin which is spot-welded to the nickel supports M of the filament holder. The tip should be sharply bent, and the sides close to it almost parallel. The height of the filament tip above the supports M is about 3 mm. Tube N is locked by a set screw to the brass disc D, which has the shape shown in the section, Figure 7 (*c*). After inserting a new holder with filament, it is only necessary to loosen screws H and readjust disc D by gently pushing it with a screwdriver through the holes provided,

until the new filament lies centrally within the grid aperture. The grid cylinder is then adjusted axially until the tip lies in the plane of the grid aperture. The filament leads (not shown) are clipped to the nickel supports of the filament holder and pass through the tube N to the terminals F, riveted to a mica disc.

The cathode assembly is connected by rod J to the top of the bellows B. The cathode cylinder will therefore move towards the anode if the bellows are compressed by turning screw S. It is thus possible to alter the grid aperture–anode distance d whilst the tube is running, and it becomes a simple matter to refocus visually after the filament has been replaced.

Figure 8 (Plate) shows a photograph of one of the tubes which forms part of a small table unit. The supporting tube is held here by a bracket screwed to the steel frame of the table. This method of fixture allows adjustment of the tube height above the table top. The high-tension lead is led through the steel frame and table top in an ebonite cylinder, which also surrounds it above the table. A spring-loaded rod makes contact with the anode part of the tube.

Figure 9 shows the simple circuit that has been found satisfactory. T_1 is a compact H.T. transformer which incorporates metal rectifiers for half-wave rectification. It has been designed for this tube and gives a maximum current of 1 ma. at 50 kv. The bias V_F is produced by passing the beam current through the variable resistor R_3. This arrangement provides a certain amount of negative feedback which considerably stabilizes the beam current.

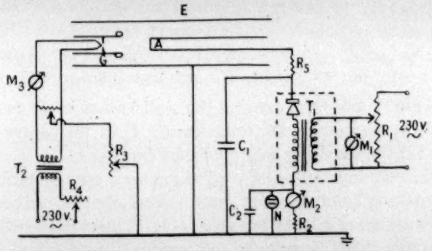

Figure 9. Diagram of electric circuit.

T_1 : H.T. transformer, 50 kv., 1 ma., incorporating metal rectifiers.
T_2 : filament transformer, 5 amp., 5 v.
C_1 : condenser, 0·05 μF., 50 kv. working.
C_2 : condenser, 0·01 μF.
R_1 : potentiometer, 1,000 Ω, 200 w.
R_2 : resistor, 100 kΩ.
R_3 : variable resistor, 300 kΩ.
R_4 : variable resistor, 2,500 Ω, 25 w.
R_5 : resistor, 300 kΩ, 25 w.
M_1 : moving-iron voltmeter, 0–250 v.
M_2 : moving-coil microammeter, 0–500 μa.
M_3 : moving-iron ammeter, 0–5 amp.
N : neon lamp, VS 70.

The tube described has now been in use, on and off, for over one year, and only very slight anode pitting has been detected. It is run at 50 kv. with a copper anode and with beam currents between 300 and 500 μa. For a half width of 40 μ, this leads to a mean specific load (load within circular area of 40 μ diameter, divided by area) of 8 kw/mm². The peak specific load (at the centre of the spot) is 11 kw/mm². Calculation shows that under these conditions the maximum temperature on the anode surface rises to approximately 450° c. For comparison it may be mentioned that typical values of the load in a commercial sealed-off tube and a rotating anode tube are 0·1 kw/mm², and 0·5–1·0 kw/mm² respectively. These two figures are probably too high, because in arriving at them no allowance is made for the tails of the distribution.

The question arises whether the combination of fine focus and rotating anode would not permit a further substantial increase in the specific load. It is possible to arrive at an estimate of the improvement by making the following assumptions: (*a*) The load W is distributed uniformly over the focal spot. (*b*) The anode is regarded as a semi-infinite, homogeneous and isotropic solid of thermal conductivity k, density ρ and specific heat s, the boundary plane of which coincides with the anode surface. The assumption is justified for fine foci, whose dimensions are much smaller than those of the anode. (*c*) The maximum temperature attained at a point P, moving with velocity v in the centre of the focal path, will be approximately the same as that produced by a stationary load W after a time $t=2R/v$, i.e. the time it takes P to traverse the focus.

In view of assumption (*b*), the solution of the time-dependent equation of heat flow will be of the form

$$dT=\frac{2W(s\rho)^{1/2}\,dA\,dt}{4(k\pi t)^{3/2}}\exp(-s\rho r^2/4kt)$$

(Oosterkamp 1948); dT denotes the contribution to the temperature at any point P arising from an instantaneous energy inflow $dE=2W\,dA\,dt$, t seconds before the time under test and r cm. from P. For an element in the centre of the uniformly loaded circular focal area $dA=2\pi r\,dr$. Assumption (*c*) makes the variable r independent of t, and the temperature T_r in the centre of the focal path of the rotating anode, is found by integrating dT from $r=0$ to $r=R$ and $t=0$ to $t=2v/R$. This leads to

$$T_r=\frac{WR}{k}\,\frac{1}{\alpha\pi^{1/2}}\{1-\exp(-\alpha^2)+\alpha\pi^{1/2}[1-\Theta(\alpha)]\},$$

where $\alpha=(Rvs\rho/8k)^{1/2}$, and $\Theta(\alpha)$ denotes the well-known error integral.

To the same approximation, the temperature T_s in the centre of a stationary anode is obtained from the above expression by putting $v=0$, so that $T_s=WR/k$. For the comparatively high value of $v=785$ cm/sec., corresponding to a disc of 5 cm. diameter making 3,000 rev/min., and a focal spot of radius 20μ, $\alpha=0{\cdot}43$, if the material constants of copper are used. T_r/T_s now becomes 1·2 for a given value of W. At the given maximum temperature, the loading of the rotating anode is therefore only 20% higher than that of a stationary anode. The technical difficulties of increasing the speed of rotation appreciably above 50 rev/sec. are considerable, particularly as it is essential that the anode should run true to within a fraction of the focal diameter.

The results show that the improvement in loading that can be obtained by rotating the anode of a fine focus tube with approximately circular spot is in no way comparable with that for focal spots of normal size, and seems hardly to warrant the additional complication and cost.

§6. THE PERFORMANCE OF THE TUBE

Figure 10 (Plate)* shows a shadowgraph of a platinum grid supporting two 10μ platinum wires at right angles. The grid was placed against the window of the tube and the shadowgraph taken at a distance giving a magnification of 20. The sharp shadow of the vertical wire is due to the effective horizontal source width of 5μ produced by foreshortening. Although the vertical half width of

* See end of issue.

the source is at least of the order of the size of the object, the shadow of the horizontal wire is still fairly well defined; its definition depends, of course, on the grid aperture–anode distance. Observation of the shadow image provides a simple method of adjusting the tube visually to optimum focus. Figure 10 also indicates the possibility of using the tube for micro-radiography.

The successful application of the tube to problems in x-ray crystallography involves essentially the design of a special set of cameras, for focal spot and camera really form one single unit (Bernal 1928). To use the highly loaded fine focus to its full advantage, both camera and specimen have to be small. A programme of camera design has only recently been started, but the results obtained are encouraging. One of the cameras used so far is of the Seemann–Bohlin type (radius 2 inches). It is clamped rigidly to the body of the tube, close to the window. For this camera no collimator or pinhole is necessary. A fully exposed photograph of the diffraction pattern of ZnO was obtained in one minute using Cu-radiation and a Ni-filter. In this diagram the α_1 and α_2 lines of the (102) reflection (i.e. Bragg angle $=23{\cdot}9°$) are resolved. Using the same camera and a General Electric Ca-6 diffraction tube, an exposure of 2 hours was required to obtain an equivalent photograph.

ACKNOWLEDGMENTS

The authors wish to thank Professor J. D. Bernal for drawing their attention to the problem and for his continued encouragement and valuable discussions, and the Nuffield Foundation for generous support of the work. One of the authors (W. E. S.) has received grants from the Ministry of Education under the Furher Education Scheme. Messrs. Hilger & Watts, Ltd., London, have taken over the further development and the manufacture of the tube described.

REFERENCES

Astbury, W. T., and Preston, R. D., 1934, *Nature, Lond.*, **133**, 460.
Bernal, J. D., 1928, *J. Sci. Instrum.*, **5**, 1; 1945, *Nature, Lond.*, **155**, 713.
Ehrenberg, W., 1949, *J. Opt. Soc. Amer.*, **39**, 741.
Goldsztaub, S., 1947, *C. R. Acad. Sci., Paris*, **224**, 458.
Metropolitan-Vickers Electrical Co., Ltd., 1948, in the *Catalogue of the 32nd Annual Exhibition of Scientific Instruments and Apparatus* (London: The Physical Society), p. 240.
Müller, A., 1929, *Proc. Roy. Soc.* A, **125**, 507.
Müller, A., and Clay, E. H., 1939, *J. Instn. Elect. Engrs.*, **84**, 261.
Myers, L. M., 1939, *Electron Optics* (London: Chapman & Hall, Ltd.), p. 465.
Oosterkamp, W. J., 1948, *Philips Res. Rep.*, **3**, 49–59, 303–317.
Zworykin, V. K., *et al.*, 1945, *Electron Optics and the Electron Microscope* (New York: Wiley & Sons, Inc.), p. 44.

Low Reflectance Coatings and the Sensitivity Curve of the Eye

By J. H. van der Merwe and H. Verleger *
National Physical Laboratory, Council for Scientific and Industrial Research, Pretoria, South Africa

Communicated by B. F. J. Schonland; MS. received 22nd May 1950

ABSTRACT. Heterochromatic light is treated and the spectral sensitivity of the human eye is taken into account. In spite of certain simplifying assumptions, conclusions of a general character may be drawn, the most important being that the optical properties required for low reflectance coatings can be obtained by treating the incident light as monochromatic.

§ 1. INTRODUCTION

The use of thin coatings for reducing the reflection of monochromatic light at glass surfaces in optical instruments has been the subject of extensive theoretical research by various workers (Vasicek 1947, Caballero 1947, Dell 1949). The reflection, considered as a function of nt (n is the refractive index and t the geometrical thickness) of each coating has its minimum at $nt=\lambda/4$, or odd multiples of $\lambda/4$, where λ is the wavelength. This minimum reflection becomes zero for the proper choice of refractive indices ; for example, for a single coating of refractive index n on a substrate of refractive index n_2, the proper choice is $n=(n_0 n_2)^{1/2}$, where n_0 is the refractive index of the outer medium, usually air (for which $n_0 \simeq 1$).

§ 2. PROBLEM

The light radiated from sources used in practice is in general heterochromatic, with the complication that, if the optical thickness is chosen to destroy reflection at a certain wavelength, there still remains a certain amount of reflection at adjacent wavelengths (Jacobs 1943). The total amount of reflection, i.e. the reflected intensity over all wavelengths, may still be a large fraction of the incident intensity. An important aim in an optical design is to make this fraction as small as possible, thereby reducing the loss in brightness of the object which is viewed.

A further complication that enters into the problem of improving the efficiency of an optical system, and one that is often neglected, is that the human eye is not equally sensitive to equal radiant energy fluxes at different wavelengths. We take this into account when defining the 'reflection R', that is the fractional loss in the useful incident radiant energy, by the equation

$$R = \frac{\text{Visible intensity of reflected light}}{\text{Visible intensity of incident light}}.$$

Mathematically, this may be written in the form

$$R = \frac{\int_{\lambda_l}^{\lambda_u} a(\lambda)b(\lambda)\rho(\lambda)d\lambda}{\int_{\lambda_l}^{\lambda_u} a(\lambda)b(\lambda)d\lambda}, \qquad \ldots\ldots(1)$$

* Now Director of the Physical Laboratory of the University of Pretoria.

where λ is the wavelength, λ_l the lower limit and λ_u the upper limit of the visibility spectrum, $a(\lambda)$ the energy distribution of the incident light, $\rho(\lambda)$ the reflecting power of the optical system, i.e. the fraction of the incident light reflected at wavelength λ, and $b(\lambda)$ the spectral sensitivity of the average eye to equal radiant energy fluxes.

The factor $\rho(\lambda)$ takes care of the effect of the coatings which are used to reduce reflection. This effect is characterized in the final functional result by the appearance of the refractive index n and optical thickness nt of each coating as variables. The present problem is that of finding this functional result and its minimum with respect to these variables.

In order to evaluate the reflection R by using equation (1) it is necessary to know the explicit forms of the functions $a(\lambda)$, $b(\lambda)$ and $\rho(\lambda)$.

The curve of $b(\lambda)$, known as the relative luminosity curve, is shown in Figure 1

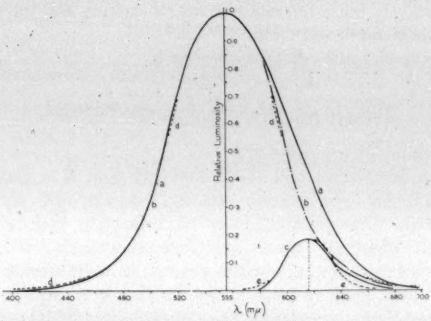

Figure 1. Relative luminosity curve $b(\lambda)$. Curves *a*, *b* and *c* are respectively the graphs of $b(\lambda)$, the symmetrical part $F(\lambda)$ of $b(\lambda)$ and $f(\lambda)=b(\lambda)-F(\lambda)$. Curves *d* and *e* are the graphs of the analytical representations of $F(\lambda)$ and $f(\lambda)$ respectively.

and has been drawn by using the tables given by Hardy and Perrin (1932). The analytic expression

$$b(\lambda)=\left\{1+\frac{1}{3}\left(\frac{\lambda-\lambda_0}{\beta_0}\right)^2+\frac{2}{3}\left(\frac{\lambda-\lambda_0}{\beta_0}\right)^4\right\}^{-1}+B_1\left\{1+\left(\frac{\lambda-\lambda_1}{\beta_1}\right)^4\right\}^{-1}, \quad \ldots\ldots(2)$$

where $\lambda_0=555\ \mathrm{m}\mu$, $\beta_0=45$, $\lambda_1=616\ \mathrm{m}\mu$, $\beta_1=20$ and $B_1=0{\cdot}185$, is seen from Figure 1 to give a curve which is a good substitute for the experimental curve.

The reflecting power $\rho(\lambda)$ has been evaluated by various workers (Vasicek 1947, Caballero 1947) for single, double and multiple coatings. For simplicity we treat two cases of *normal* incidence. These are as follows :

Case (*a*). *A single coating.*

In this case (Vasicek 1947, Caballero 1947)

$$\rho(\lambda)=\frac{A+Be^{i\delta}}{1+ABe^{i\delta}}\times\frac{A+Be^{-i\delta}}{1+ABe^{-i\delta}}, \quad \ldots\ldots(3)$$

where $$A=\frac{n-n_0}{n+n_0}, \quad B=\frac{n_2-n}{n_2+n}, \quad \delta=\frac{4\pi nt}{\lambda}\left(=\frac{\alpha}{\lambda}, \text{say}\right)$$

and n_0, n, n_2 and t have been defined above. Further, it has been assumed that $n_0<n<n_2$.

Case (b). Approximate treatment for a number of coatings.

When there is more than one coating, the expressions analogous to (3) are less simple and the corresponding calculations of R extremely complicated. An approximate calculation can be carried out by neglecting all light beams which are reflected more than twice. Let there be k successive coatings. If the incident beam is monochromatic the reflected wave is given in amplitude and phase by

$$l = l_0 + (1-l_0^2)l_1 e^{-i\delta_1} + (1-l_0^2)(1-l_1^2)l_2 e^{-i\delta_2} + \ldots .$$

$$= y_0 + y_1 e^{-i\delta_1} + \ldots . \; y_r e^{-i\delta_r} + \ldots .$$

where $l_r = (n_{r+1}-n_r)/(n_{r+1}+n_r)$; $n_{r+1} > n_r$ for $r = 0, 1, \ldots, k$

and $\delta_r = 4\pi(n_1 t_1 + n_2 t_2 + \ldots . + n_r t_r)/\lambda \quad (= \alpha_r/\lambda, \text{ say})$.

The subscript r ($= 1, 2, \ldots . k$) refers to the rth coating and the subscripts 0 and $k+1$ to the outer medium and substrate respectively.

Putting $\alpha_s - \alpha_r = \alpha_{sr}$, the reflected intensity is

$$\rho(\lambda) = l\,l^* = \sum_{r=0}^{k} y_r^2 + 2 \sum_{s>r\geq 0}^{s=k} y_r y_s \cos(\alpha_{sr}/\lambda), \qquad \ldots\ldots (4)$$

where l^* is the complex conjugate of l.

The energy distribution $a(\lambda)$ of the incident light is in general completely different for different light sources. In (1), however, $a(\lambda)$ occurs only in the product $a(\lambda)b(\lambda)$. This product plays an important rôle and, like $b(\lambda)$, is (practically) everywhere zero except in the region $\lambda_l < \lambda < \lambda_u$, where it is positive. In certain practical cases the curve of this product strongly resembles that of $b(\lambda)$ in departing very little from symmetry and in having a *single* maximum which is in general at a different wavelength (λ_m say) from that of $b(\lambda)$. Useful information on the reflection that arises when the product has this typical form may be obtained by treating $a(\lambda)$ as a constant, in which case $\lambda_m = \lambda_0$.

The reflection then becomes

$$R = \frac{\int_{-\infty}^{\infty} b(\lambda)\rho(\lambda)\,d\lambda}{\int_{-\infty}^{\infty} b(\lambda)\,d\lambda}, \qquad \ldots\ldots (5)$$

where λ_l and λ_u are replaced by $-\infty$ and ∞ respectively. This is permissible because (practically) $b(\lambda) = 0$ for $\lambda < \lambda_l$ and for $\lambda > \lambda_u$.

§ 3. EVALUATION OF THE REFLECTION

Case (a). It is convenient to begin with the case of the approximate equation (4). By substituting (2) and (4) into (5) we find

$$R_k = \sum_{r=0}^{k} y_r^2 + 2I_{00}^{-1} \sum_{s>r\geq 0}^{s=k} y_r y_s I_{rs}, \qquad \ldots\ldots (6)$$

where $$I_{rs} = \int_{-\infty}^{\infty} \frac{\cos(\alpha_{sr}/\lambda)\,d\lambda}{1 + \frac{1}{3}\left(\frac{\lambda-\lambda_0}{\beta_0}\right)^2 + \frac{2}{3}\left(\frac{\lambda-\lambda_0}{\beta_0}\right)^4} + B_1 \int_{-\infty}^{\infty} \frac{\cos(\alpha_{sr}/\lambda)\,d\lambda}{1 + \left(\frac{\lambda-\lambda_1}{\beta_1}\right)^4}.$$

These integrals have been evaluated by means of the theory of residues. We find

$$I_{rs} = P\{\exp(-a_1\alpha_{sr})\sin(\tfrac{1}{2}\phi - b_1\alpha_{sr}) + \exp(-a_2\alpha_{sr})\sin(\tfrac{1}{2}\phi + b_2\alpha_{sr})\}$$
$$+ Q\left\{\exp(-a_3\alpha_{sr})\sin\left(\frac{\pi}{4} - b_3\alpha_{sr}\right) + \exp(-a_4\alpha_{sr})\sin\left(\frac{\pi}{4} + b_4\alpha_{sr}\right)\right\}, \quad \ldots\ldots(7)$$

where

$$P = 3\pi\beta_0/4\rho^{3/2}\sin\phi, \quad Q = \tfrac{1}{2}\pi\beta_1 B_1, \quad \rho = 1{\cdot}5^{1/2}, \quad \tan\phi = 23^{1/2},$$
$$a_p = \sin\psi_p/\sigma_p\beta_r, \quad b_p = \cos\psi_p/\sigma_p\beta_r; \quad (p = 1, 2;\ \nu = 0),\ (p = 3, 4,\ \nu = 1),$$
$$\sigma_1^2 = (x_0\beta_0^{-1} + \rho^{1/2}\sin\tfrac{1}{2}\phi)^2 + \rho\cos^2\tfrac{1}{2}\phi, \quad \tan\psi_1 = \rho^{1/2}\cos\tfrac{1}{2}\phi/(x_0\beta_0^{-1} + \rho^{1/2}\sin\tfrac{1}{2}\phi),$$
$$\sigma_2^2 = (x_0\beta_0^{-1} - \rho^{1/2}\sin\tfrac{1}{2}\phi)^2 + \rho\cos^2\tfrac{1}{2}\phi, \quad \tan\psi_2 = \rho^{1/2}\cos\tfrac{1}{2}\phi/(x_0\beta_0^{-1} - \rho^{1/2}\sin\tfrac{1}{2}\phi),$$
$$\sigma_3^2 = x_1^2\beta_1^{-2} + 2^{1/2}x_1\beta_1^{-1} + 1, \quad \tan\psi_3 = (2^{1/2}x_1\beta_1^{-1} + 1)^{-1},$$
$$\sigma_4^2 = x_1^2\beta_1^{-2} - 2^{1/2}x_1\beta_1^{-1} + 1, \quad \tan\psi_4 = (2^{1/2}x_1\beta_1^{-1} - 1)^{-1},$$

and $$I_{00} = [I_{rs}]_{s=r=0} = 2^{-1/2}\pi\{6^{1/2}\beta_0(24^{1/2}+1)^{-1/2} + \beta_1 B_1\}.$$

Case (*b*). Equation (3) can be written in the form

$$\rho(\lambda) = 1 - H + 2H\sum_{\nu=0}^{\infty}(-1)^\nu (AB)^\nu \cos\nu\delta, \quad \ldots\ldots(8)$$

where $$H = (A^2 + B^2 - 1 - A^2B^2)/(1 - A^2B^2).$$

On substituting (2) and (8) in (5) we find

$$R = 1 - H + 2HI_0^{-1}\sum_{\nu=0}^{\infty}(-1)^\nu (AB)^\nu I_\nu,$$

where I_ν is of the same form as I_{sr} except that α_{sr} must be replaced by $\nu\alpha$ (see (6)) and $I_{00} = I_0$. On substituting from (7) and summing the series one finds

$$R = 1 - H + 2HPI_0^{-1}\left\{\frac{\sin\tfrac{1}{2}\phi + ABe^{-c_1 nt}\sin(\tfrac{1}{2}\phi + d_1 nt)}{1 + A^2B^2e^{-2c_1 nt} + 2ABe^{-c_1 nt}\cos d_1 nt}\right.$$
$$\left. + \frac{\sin\tfrac{1}{2}\phi + ABe^{-c_2 nt}\sin(\tfrac{1}{2}\phi - d_2 nt)}{1 + A^2B^2e^{-2c_2 nt} + 2ABe^{-c_2 nt}\cos d_2 nt}\right\}$$
$$+ 2HQI_0^{-1}\left\{\frac{\sin\tfrac{1}{4}\pi + ABe^{-c_3 nt}\sin(\tfrac{1}{4}\pi + d_3 n_3 t)}{1 + A^2B^2e^{-2c_3 nt} + 2ABe^{-c_3 nt}\cos d_3 nt}\right.$$
$$\left. + \frac{\sin\tfrac{1}{4}\pi + ABe^{-c_4 nt}\sin(\tfrac{1}{4}\pi - d_4 nt)}{1 + A^2B^2e^{-2c_4 nt} + 2ABe^{-c_4 nt}\cos d_4 nt}\right\} \quad \ldots\ldots(9)$$

where $$c_r = 4\pi a_r \quad \text{and} \quad d_r = 4\pi b_r;\ r = 1, 2, 3 \text{ and } 4.$$

When nt is taken as a single independent variable, n still remains a second independent variable of R. That this is the case follows from the fact that H, A and B are, as seen from (8) and (3), functions of n.

The coordinates on the graph of $R(nt)$, curve *a* of Figure 2, have been calculated for an air ($n_0 = 1$) outer medium, a glass ($n_2 = 1{\cdot}6$) substrate and a coating with a refractive index of $n = (n_0 n_2)^{1/2} = 1{\cdot}2649$.

In order to obtain some idea of the magnitude of the error involved in the derivation of the approximate formula (6) a few points on the graph of $R(nt)$ were obtained by using (6). These points are indicated in Figure 2 by circles.

The broken curve b in Figure 2 is the curve of $R(nt)$ when $b(\lambda)$, which in equation (2) is of the form $b(\lambda) = F(\lambda) + f(\lambda)$, is taken to be $b(\lambda) = F(\lambda) - f(\lambda)$. This curve is useful for the purpose of investigating the influence of the asymmetrical form of $b(\lambda)$ on the location of the minimum of $R(nt)$.

The graph of $R(n)$, when nt is fixed at 138·1 mμ ($\lambda_0/4$), is shown in Figure 3.

§4. REMARKS AND CONCLUSIONS

It is seen, under the conditions set out below equation (4), that the minimum reflection occurs for practically the same values of n and nt, namely $n = (n_0 n_2)^{1/2} = 1{\cdot}265$ and $\lambda_0/4 = 138$ mμ respectively, as in the case of monochromatic light of wave-

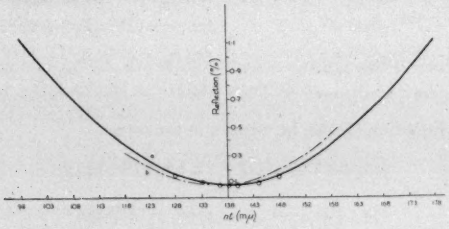

Figure 2. Graph of the reflection R plotted against nt for an air ($n_0 = 1$) outer medium, a glass ($n_2 = 1{\cdot}6$) substrate and a coating of refractive index $n = (n_0 n_2)^{1/2} = 1{\cdot}2649$. Curves a and b are obtained from equation (9) and correspond respectively to $b(\lambda) = F(\lambda) + f(\lambda)$ and $b(\lambda) = F(\lambda) - f(\lambda)$ (see Figure 1). The circles represent points obtained from the approximate equation (6).

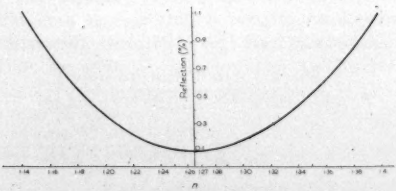

Figure 3. Graph of the reflection R plotted against n for $nt = 138{\cdot}1$ mμ ($\lambda_0/4$), $n_0 = 1$ and $n_2 = 1{\cdot}6$.

length λ_0, and this is true in spite of a slight asymmetry in the curve of $a(\lambda)b(\lambda)$. Also, when the actual value of nt in a practical case is different from $\lambda_0/4$ by as much as 40 mμ and n is different from $(n_0 n_2)^{1/2}$ by 11%, the reflection will still be small, less than about 3%. The minimum reflection, namely 0·1%, is negligible.

Under the above mentioned conditions the rule of considering the incident light as a monochromatic beam of wavelength λ_0 is therefore satisfactory when a choice must be made of the proper values of n and nt for a single low reflectance coating. Also, these results are not inconsistent with the idea that the same rule may be applied to obtain good estimates in the case of multiple coatings. It must be pointed out that, though the actual calculations were made for glass, the rule applies equally to other optical materials.

It may also be mentioned that the approximate formula may be used to attain high accuracy in the case of single coatings. It is probably less accurate for multiple coatings.

Once the coating material is chosen and the thickness appropriate to the given light source determined, the problem of forming the film still remains. An important part of this problem is that of measuring the film thickness. The most simple way of doing this is by making observations on the interference colours and using the relationship between the optical thickness and interference colour. A mathematical examination of this relationship has now been made by Kubota (1950), who gives a plot of his results on the I.C.I. Diagram.

ACKNOWLEDGMENT

This paper is published with the permission of the South African Council for Scientific and Industrial Research.

REFERENCES

CABALLERO, D. L., 1947, *J. Opt. Soc. Amer.*, **37**, 176.
DELL, H. A., 1949, *Proc. Phys. Soc.* B, **62**, 81.
HARDY, A. C., and PERRIN, F. H., 1932, *The Principles of Optics* (New York: McGraw-Hill), p. 18.
JACOBS, D. H., 1943, *Fundamentals of Optical Engineering* (New York: McGraw-Hill), p. 121.
KUBOTA, H., 1950, *J. Opt. Soc. Amer.*, **40**, 146.
VASICEK, A., 1947, *J. Opt. Soc. Amer.*, **37**, 145, 623.

LETTERS TO THE EDITOR

The Interpretation of Dielectric Measurements using the Cole–Cole Plot

Stark (1950) has considered the equivalence of frequency and temperature in dielectric measurements with particular reference to the Cole–Cole plot (Cole and Cole 1941); we here consider the use of this representation in the interpretation of dielectric measurements and compare the plots using frequency or temperature as the parameter. A plot of the imaginary part of the dielectric constant ϵ'' against the real part ϵ' for a given temperature, with frequency as the parameter, almost always results in a curve which is the arc of a circle. In the rare case when the dispersion can be represented by a single relaxation time the arc is a semi-circle.

This diagram is useful in several ways. Suppose for example that only a part of the dispersion is covered by the frequency range available, as is often the case, then by drawing

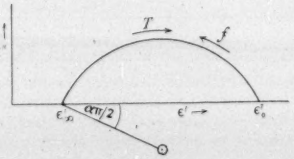

the best fitting arc of the Cole–Cole plot one is able to deduce, with an accuracy depending on the proportion of the total arc determined, both the zero-frequency dielectric constant ϵ'_0 and the limiting high-frequency value ϵ'_∞, assuming that only one absorption occurs in the total frequency range. In addition the angle is a measure of the distribution of relaxation times (Kauzmann 1942). This representation enables one to see at a glance the extent of the distribution of relaxation times and its variation with temperature, whereas the usual method requires calculation and curve fitting. Further, when one has two or more domains of dispersion which may not be widely separated in frequency, as for instance in the case of solid hydrogen bromide and deuterium bromide below the transition at −184° c. (Powles

1950 a, b), a slight extension of the analysis using the Cole–Cole plot enables one to determine the values of ϵ'_0 and ϵ'_∞ and of the distribution of relaxation times of each dispersion as if it existed separately. The details of this analysis will be published elsewhere (Powles 1950 c).

In the representation at fixed frequency with temperature as the parameter much more care is required in interpretation: in fact useful information can be deduced only in particular cases. If the temperature range, which should, in theory, cover all temperatures, includes a phase transition of any kind, for instance liquid → gas, this type of plot is quite inappropriate; a plot with frequency as the parameter on the other hand is valid at any temperature. Evidently one may obtain an arc only if the frequency of measurement is such that the dispersion region passes through this frequency for a range of temperature sufficiently far removed from any phase transition, and not necessarily even in this case. The end points of the arcs have no meaning if only because of the variation of the dielectric constant due to thermal expansion or contraction. The effect mentioned above is quite easy to see analytically. The expression for the Cole–Cole arc is

$$\frac{\epsilon^*-\epsilon'_\infty}{\epsilon'_0-\epsilon'_\infty}=\frac{1}{1+(j\omega\tau_0)^{1-\alpha}},$$

where $\epsilon^*=\epsilon'+j\epsilon''$. It is not, however, possible in general to eliminate the temperature as a parameter even with the aid of a relation such as $\log\tau_0=ST_0+C$ as proposed by Stark, since ϵ'_0 and ϵ'_∞ are also functions of temperature.

The angle $\alpha\pi/2$, which is a measure of the spread of relaxation times in the constant temperature diagram, evidently only represents in the constant frequency diagram some sort of average of the spread of relaxation times over the whole temperature range used to determine the arc. In fact in nearly all cases the spread of relaxation times is a function of temperature. If in a particular case we find an arc of a circle the angle $\alpha\pi/2$ might be considered as the qualitative spread of relaxation times. Care is necessary, however, as a particular variation of ϵ'_0, ϵ'_∞ and the spread of relaxation times might combine to produce an arc in the Cole–Cole plot and thus lead to misinterpretation.

There is at present no theoretical reason why so many substances have a distribution of relaxation times corresponding to an arc in the Cole–Cole plot (there are in fact many exceptions (Kauzmann 1942)); we therefore stress the purely practical utility of this representation.

Department of Theoretical Physics,
The University, Liverpool, 7.
29th September 1950.

J. G. Powles

Cole, K. S., and Cole, R. H., 1941, *J. Chem. Phys.*, **9**, 341.
Kauzmann, W., 1942, *Rev. Mod. Phys.*, **14**, 12.
Powles, J. G., 1950 a, *Nature, Lond.*, **165**, 686; 1950 b, *C. R. Acad. Sci., Paris*, **230**, 836; 1950 c, *J. Chim. Phys.*, in the press.
Stark, K. H., 1950, *Nature, Lond.*, **166**, 436.

Characteristics of Selenium Photocells

While the forward characteristics of rectifier cells are not yet clearly understood, it has been shown (Landsberg 1949) how their reverse characteristics can be analysed accurately. The application of this method (previously outlined for a Mott barrier) to a Schottky barrier leads, with the previous notation, to reverse characteristics of the form *

$$\frac{j}{j_0}=y^{3/2}\exp y, \quad \text{where } y=\left(\frac{V_D-U}{V_0}\right)^{1/4},$$

$$j_0=\left(\frac{2}{\pi}\right)^{1/2}nv\epsilon W^2\exp\left(-\frac{V_D}{W}\right) \quad \text{and} \quad V_0=\frac{\epsilon^3W^4}{8\pi ne^3}.$$

ϵ is the dielectric constant of the semiconductor. The purpose of this note is to point out that the characteristics recently given by Preston (1950) are in excellent agreement with the theoretical relation, as shown by the accompanying Figure. In this case zinc oxide films were deposited on the selenium by sputtering for varying times t, while a gold electrode was deposited on the oxide film by sputtering for 7 seconds. The numerical constants

* The detailed theory and the interpretation of the results will be published elsewhere.

which can be derived from the curves assuming room temperature, $V_D = \frac{1}{2}$ volt, and $\epsilon = 6{\cdot}3$ (Tammann and Böhme 1931), are given in the Table. They reproduce the main features

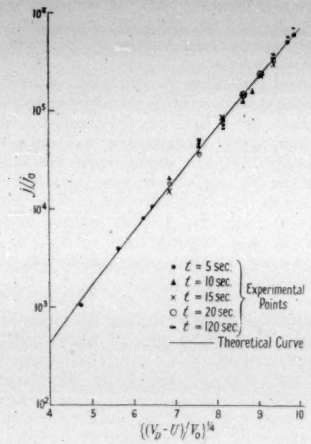

obtained by analysing the curves given by Williams and Thompson (1941) for selenium rectifiers *, except that they show in addition that *the mobility of the current carriers decreases*

(sec.)	5	10	15	20	120
n ($cm^{-3} \times 10^{18}$)	0·65	1·46	1·46	1·46	1·46
Av ($\times 10^{-3}$)	40	1·19	0·59	0·26	0·099

t = time of sputtering, n = volume density of impurity centres, A = area of contact (11·3 cm^2 †), v = mobility of current carriers in cm^2/volt sec.

as the thickness of the zinc oxide film increases. The present and previous notes show the advantage to be gained by plotting reverse characteristics in a form suitable for comparison with the curve $z = x^{3/2}e^{x}$.

Department of Natural Philosophy,
University of Aberdeen.
7th September 1950.

P. T. Landsberg.

Landsberg, P. T., 1949, *Nature, Lond.*, **164**, 967.
Preston, J. S., 1950, *Proc. Roy. Soc.* A, **202**, 449 (Figure 6).
Tammann, G., and Böhme, W., 1931, *Z. anorg. Chem.*, **197**, 1.
Williams, A. L., and Thompson, L. E., 1941, *J. Instn. Elect. Engrs.*, Pt. 1, **88**, 353 (Figure 5).

* The detailed theory and the interpretation of the results will be published elsewhere.
† Private communication from Dr. Preston.

The Measurement of Ultrasonic Vibration Potentials (Debye Effect) with Pulse Techniques‡

Debye (1933) proposed a method involving ultrasonic waves for the determination of the relative masses of electrolytic ions in solution. If an electrolytic solution is irradiated with ultrasonic waves, periodic differences in potential should appear within the solution primarily as a result of the dynamical reaction of the ions to the material wave. The existence of this effect, however, was not established experimentally for fifteen years

‡ This research has been partially supported by the U.S. Office of Naval Research under Contract No. N7 onr 47002, Project No. NR 051 162.

following its prediction because of the small magnitude of the alternating potentials (10^{-6} volts for unit velocity amplitude) and the problem of preventing electromagnetic coupling between the ultrasonic generator and the detection apparatus. In 1948 the authors (Yeager *et al.* 1949) detected the effect with standing wave techniques but were limited to semi-quantitative measurements because of the problem of determining the acoustical parameters in a complex field.

Hunter (1950) has indicated his interest in investigating the Debye effect with pulse techniques. Apparatus for the measurement of the Debye effect and related phenomena with pulse-modulated ultrasonic waves has been developed during the past two years in the Ultrasonic Research Laboratory at Western Reserve University (Yeager *et al.* 1949, Ultrasonics Research Laboratory 1949) and measurements are in progress at the present time. The use of pulse techniques affords two advantages in this application: (i) acoustically produced effects can be differentiated from electromagnetic coupling because of the finite time required for the propagation of a material wave, and (ii) measurements can be made under virtually free-field conditions (Yeager *et al.* 1949) because the alternating potentials resulting from the directly incident waves can be differentiated from those produced by reflections.

Preliminary measurements have been made with pulse-modulated ultrasonic waves at 200 kc/s. with a pulse width of 400 microseconds and a repetition frequency of 400 per second in a large tank which permits delay times of approximately 1,000 microseconds. The alternating potentials are amplified with a conventional tuned amplifier and viewed with a cathode-ray oscilloscope. The magnitude of the effect has been measured by the substitution method with signals of known amplitude. The acoustical velocity amplitudes have been determined with a barium titanate hydrophone (Ultrasonic Research Laboratory 1949, Bugosh *et al.* 1949) which has been calibrated at the Naval Underwater Sound Reference Laboratory at Orlando, Florida (U.S.A.).

The effect has been found to be approximately 5 microvolts for unit velocity amplitude in 0·005 normal potassium chloride. The amplitude of the effect has also been shown to be essentially independent of the concentration of the electrolyte for dilute solutions and dependent on the nature of the electrolyte. These characteristics are in general agreement with those found previously with standing wave techniques.

The use of pulse-modulated ultrasonic waves has also been extended to a similar effect in colloidal systems (Rutgers 1938, 1946, Vidts 1945, Hermans 1938 a, b, Causse 1950, Rutgers and Vidts 1950). Measurements with colloidal suspensions of silica with low ionic conductivities are in progress and appear to be of the same order of magnitude as obtained by Rutgers and Vidts with arsenic trisulphide sols (Rutgers and Vidts 1950).

Details concerning the experimental methods as well as the results will be published in the near future.

Ultrasonic Research Laboratory,
Department of Chemistry,
Western Reserve University,
Cleveland 6, Ohio, U.S.A.
1st October 1950.

E. YEAGER.
J. BUGOSH.
F. HOVORKA.

BUGOSH, J., YEAGER, E., and HOVORKA, F., 1949, *Phys. Rev.*, **76**, 1890.
CAUSSE, J., 1950, *C. R. Acad. Sci., Paris*, **230**, 826.
DEBYE, P., 1933, *J. Chem. Phys.*, **1**, 13.
HERMANS, J., 1938 a, *Phil. Mag.*, **25**, 427; 1938 b, *Ibid.*, **26**, 674.
HUNTER, A. N., 1950, *Proc. Phys. Soc.* B, **63**, 58.
RUTGERS, A., 1938, *Physica*, **5**, 46; 1946, *Nature, Lond.*, **157**, 74.
RUTGERS, A., and VIDTS, J., 1950, *Nature, Lond.*, **165**, 109.
ULTRASONIC RESEARCH LABORATORY, WESTERN RESERVE UNIVERSITY, 1949, *Technical Report*, No. 2.
VIDTS, J., 1945, *Konikl. Vlaamsche Acad. voor Wetenschappen*, **7**, 5.
YEAGER, E., BUGOSH, J., HOVORKA, F., and MCCARTHY, J., 1949, *J. Chem. Phys.*, **17**, 411.
YEAGER, E., CHESSIN, H., BUGOSH, J., and HOVORKA, F., 1949, *Phys. Rev.*, **76**, 1890.

A Note on Resonance Damping, at Injection, in Betatrons and Synchrotrons

It has not yet been satisfactorily explained how an electron can be injected into betatrons and synchrotrons providing maximum particle energies of the order of 50 MeV., without colliding with the injector structure on subsequent revolutions. Experimental work (Westendorp and Elder 1949) has shown, however, that the presence of large circulating currents are essential for efficient injection, and a semi-quantitative theory has been developed by Kerst (1948) based on this fact and on the assumption that while the circulating current in such machines increases, it induces a corresponding change in the orbit linking flux, resulting in deceleration of the electrons, and a consequent shrinkage of the radius of their instantaneous orbits. Apart from the fact that the application of these ideas to explain internal injection appears unconvincing, the extra energy provided by the circulating currents stored in the magnetic field is reversible; it is likely, therefore, that an appreciable fraction of the energy initially lost by the electron will be subsequently regained within a very few revolutions, as the heavy injection currents dissipate themselves. The present note proposes a mechanism which may assist in the successful operation of a large number of betatrons and synchrotrons.

Consider electron motion in an azimuthally inhomogeneous axial magnetic field, $H_z(r, \phi)$. The azimuthal error field will be assumed to be a circular function of ϕ with a period $1/l$ times that of orbital motion of the electron. The ' free ' vertical and radial oscillations are then given, with some approximation, by

$$\frac{d^2\zeta}{d\chi^2} + [a - 2q\cos 2\chi]\zeta = 0, \qquad \ldots\ldots (1)$$

where a change in the independent variable has been made. The parameters a and q are related to the axial magnetic field index n, to the magnitude and phase of the ' error ' fields, and to the integer l.

Equation (1) is the usual form for the generalized Mathieu equation, its solution being stable (periodic or non-periodic, and bounded) or, in the general case, unstable ($\zeta \to \infty, \chi \to \infty$) depending on the relative magnitude of the parameters a and q. In particular if $a = 1, 2^2, 3^2, 4^2, \ldots$, solutions of (1) are always stable provided $q = 0$, i.e. if the axial magnetic field is azimuthally homogeneous. For $0 < n < 1$, the most important cases of general instability arise for $a = 1$, $l = 1$, or $(1-n)^{1/2}$. For oscillations wholly in the median plane, i.e. radial oscillations, the condition $a = l = 1$ gives $n = \frac{3}{4}$, while for ' free ' vertical oscillations the same conditions give $n = \frac{1}{4}$. The case $a = 1$, $l = (1-n)^{1/2}$ occurs only in the case of vertical oscillations, giving $n = \frac{1}{5}$.

For $a \simeq 1$, the general solution of (1) can be written

$$\zeta = Ae^{\mu\chi}\sin(\chi - \sigma) + Be^{-\mu\chi}\sin(\chi + \sigma) \qquad \ldots\ldots (2)$$

where A and B are arbitrary constants much less than 1, and terms of the order of q^2 are neglected. The constants μ and σ are related to each other and to a and q by the equations

$$\left.\begin{aligned} \mu &= \tfrac{1}{2}[q^2 - (a-1)^2]^{1/2} \neq 0 \\ 2\sigma &= \cos^{-1}[(1-a)/q] = \sin^{-1}[-2\mu/q] \end{aligned}\right\} \qquad \ldots\ldots (3)$$

It is obvious therefore that ζ is stable and bounded only if μ is imaginary, i.e. $q^2 < (a-1)^2$; the boundary between the unstable regions is thus given by the equation

$$q^2 = (a-1)^2 \quad \text{or} \quad \pm q = a - 1. \qquad \ldots\ldots (4)$$

If $\zeta = \zeta'$, $d\zeta/d\chi = \eta$, $\chi = \gamma/2$, when $\phi = 0$, we have, writing $A = \tau B$, and putting $a = 1$,

$$[2\eta/\zeta]_{\substack{\tau \to 0 \\ 0 < \mu \leqslant 1}} \simeq \cot(\tfrac{1}{2}\gamma - \tfrac{1}{4}\pi) \qquad \ldots\ldots (5a)$$

$$[2\eta/\zeta]_{\substack{\tau \to \infty \\ 0 < \mu \leqslant 1}} \simeq \cot(\tfrac{1}{2}\gamma + \tfrac{1}{4}\pi) \qquad \ldots\ldots (5b)$$

Equation (5 *a*) gives the initial conditions resulting in $A = 0$, $B \neq 0$, while equation (5 *b*) gives initial conditions resulting in $A \neq 0$, $B = 0$, the former specifying initial conditions giving exponental damping of ζ, and the latter initial conditions giving exponential divergence of ζ. The constant γ represents the phase of the inhomogeneity relative to the azimuthal

situation ($\phi=0$) of the injector, and μ is directly proportional ($a=1$) to the magnitude of the inhomogeneity. In fact, from (3), $\mu=q/2$, giving $\sigma=-\pi/4$.

For the particular case of vertical oscillations $\zeta=z$, so that $\zeta'=z'$ represents the height of the injector above the median plane and η is the angle of injection measured relative to the plane parallel to the median plane and containing the injector. Thus when $a=1$, $n=\frac{1}{4}$, we have the case of resonance between the 'free' vertical oscillations and the fundamental of the electronic orbital motion in the accelerator. It follows from (5 *a*) that the most favourable conditions for resonance damping occur when $\tau=0$, $\gamma=-\pi/2$, from which

$$n(\phi)=\tfrac{1}{4}-\alpha\sin\phi. \qquad \ldots\ldots(6)$$

Thus, if the field index varies azimuthally as (6), damping of the 'free' vertical oscillations follow. If $0<\tau\ll 1$, however, the oscillation amplitude will reach a minimum and subsequently diverge so that, for effective damping, α in (6) must be a large quantity, consistent with $q\ll 1$, but must fall to zero after a period very short in comparison with the period of the acceleration cycle. These are precisely the conditions found necessary by Jones *et al.* (1950) for successful injection into a non-ferromagnetic synchrotron.

For similar resonance damping of free radial oscillations, it can be shown that the azimuthal variation of n must be of the form

$$n(\phi)=\tfrac{3}{4}+\alpha\sin\phi, \qquad \ldots\ldots(7)$$

when ζ is proportional to the displacement of an electron from its instantaneous circle, and η is the angle subtended by its trajectory at injection.

Assume that the large currents circulating at injection provide such a coupling coefficient α. It is almost certain that a large number of electrons do not complete even one revolution. The charge and current density will thus be very large in front of the injector, and will fall to a minimum behind the injector after completing one revolution. The charge and current density will, therefore, have a large first harmonic component. The charge density produces an electrostatic (space charge) field which has the same effect as an increase in the field index n. The magnitude of this effect on n is of the order of $(c/v)^2$ times that of the opposite effect on n produced by the field generated by the current elements, where v is the electron velocity at injection and $c/v\sim 2$. Thus α in (7) will be positive; the damping condition (5 *a*) is therefore satisfied, and the circulating space charge at injection (lasting for a period short relative to the period of acceleration cycle) should initiate resonance damping of the 'free' radial oscillations.

Thus, for example, if $\alpha=0{\cdot}05$ we have $\mu=0{\cdot}05$ and $q=0{\cdot}01$, so that the damping per revolution is given by:

$$\left|\frac{\Delta r}{(r_{\text{inj}}-r_{\text{i}})}\right|\simeq 0{\cdot}05\pi\simeq 0{\cdot}15 \qquad \ldots\ldots(8)$$

where r_{inj} and r_{i} are the radii of the circle on which the injector is situated, and of the instantaneous circle respectively. For $|r_{\text{inj}}-r_{\text{i}}|\simeq 2$ cm., $\Delta r\simeq 3$ mm.

Qualitative arguments, based on this theory, can be given to show that injection efficiency tends to increase with the energy of the injected electrons when the coupling constant is large. A further important point is that such damping is *not* reversible.

As a consequence of these considerations, and the fact that a large number of betatrons and synchrotrons have values for the field index in the neighbourhood of $\frac{3}{4}$, over a large part of doughnut space, it is suggested that the mechanism of resonance damping of the 'free' radial oscillations, brought into operation through the creation of favourable inhomogeneities by the large currents circulating at injection, plays an important part in the successful internal *and* external injection of electrons. Details of this theory will shortly be published elsewhere.

Research Department,
Metropolitan-Vickers Electrical Co., Ltd.,
Manchester.
9th October 1950.

S. E. Barden.

Jones, W. B., *et al.*, 1950, *Phys. Rev.*, **78**, 60.
Kerst, D. W., 1948, *Phys. Rev.*, **74**, 503.
Westendorp, W. F., and Elder, F. R., 1949, *Phys. Rev.*, **76**, 445.

REVIEWS OF BOOKS

La théorie des images optiques; Colloques internationaux. Pp. 322. 1st Edition. (Paris: Service des Publications du Centre National de la Recherche Scientifique, 1949.) 2,000 fr.

This collection of papers represents a series of contributions by various authors to the proceedings of the International Reunion held in the Institut d'Optique, Paris, in October 1946. It owes much to careful editing by Professor P. Fleury, Dr. A. Maréchal, and Mme C. Anglade. The subjects cover practically the whole field of Technical Optics, and the book is interesting as giving a survey of the state of optical science at the end of the second world war, not a few war-time researches being brought together (though the majority of the topics form the subjects of fuller papers published elsewhere).

When the armistice of November 1918 brought the *first* world war to an end, it was found that pressure of circumstances had compelled a fresh interest in Technical Optics, especially in England, France and America. But German workers had established a long lead in this field and had already begun to make progress along a good many lines which have since been followed up elsewhere. The works of Gleichen, Czapski, Eppenstein, von Rohr and others were studied in translation and otherwise, and renewed attention was also given to non-German writers such as Dennis Taylor. On the whole, however, the practice of lens design was dominated by traditional and empirical methods helped out by much ray-tracing. In spite of the pioneer work of Rayleigh, Strehl, and others, little was known quantitatively of the physical characteristics of aberration effects; and the tolerances for aberration residuals in calculation were based entirely on geometrical aberrational intercepts. Few designers were producing adequate formulae without recourse to trial lenses in which separations and lens forms were modified in numerous practical trials. The actual use in instruments of aspheric surfaces (apart from hand-figured systems) was almost unknown, although fairly numerous attempts had been made to produce machines for their production, and A. Koenig with M. von Rohr had given formulae for the calculation of primary aberrations in systems containing them. Physiological optics had already become a fairly well-developed study but the conditions and limitations under which really valid and useful results could be obtained were only too often misunderstood, and the implication of the phenomena of vision and photography in regard to the design of optical instruments had received little attention.

It is very interesting then, for those of us who know something of the optical field as long ago as 1918 to look through the volume under review. It opens with a series of papers on the classification and calculation of aberrations. Mr. T. Smith summarizes the investigations of many intervening years in a paper on Hamilton's characteristic function and shows that in principle the problem of forming the function for a system of coaxial surfaces can be solved. He expresses the opinion that modern calculating machines are capable of dealing effectively with the numerical aspect of the work, though we have yet to see a paper on the coding of an electronic machine for exploiting the remarkable properties of the Hamilton Function.

It was much to be desired that Smith's earlier work on this field (1921–27) should have been adapted for practical calculations, and the explicit formulae of J. Korringa and W. G. Stephan reported by A. S. van Heel now make this more readily possible; they have been adapted for calculations of fifth order aberrations, and include differential formulae for the effects of variations of axial separations of surfaces and refractive indices of the media. The paper gives some interesting curves showing the comparison between aberrations calculated by third order formulae, by third and fifth order combined, and the total aberration. It will be inferred that ray-tracing will still remain a *sine qua non* for the design of systems of large aperture and field! But the work does indeed represent a stage in the development of optical calculations. The contemporary work, published in the *Proceedings of the Physical Society*, of H. Buchdahl will be remembered. Abstracts of work on similar lines by M. Herzberger and by P. P. Platzeck appear in the book; and H. H. Hopkins has an interesting paper suggesting the calculation of the aberration coefficients of rays associated with a trigonometrically traced principal ray; this has been more recently followed up by W. Weinstein. Space does not permit any comment on other papers in this section.

Turning now to the physical characteristics of optical images, the study indispensable for the better knowledge of tolerances in design, we have papers on geometrical aberration patterns by M. Herzberger, A. C. S. van Heel and E. Durand; and (in a later section) on aberration diffraction effects by F. Zernike with B. R. A. Nijboer, also by H. H. Hopkins and others. The integrator designed by A. Maréchal receives only a short notice.

A valuable section deals with the possibilities of aspheric surfaces. J. W. Perry discusses *inter alia* some war-time attempts at the correction of photographic lenses for off-axis aberrations by figuring of two or more surfaces; B. O'Brian and R. E. Hopkins describe new attempts at the 'dropping' technique; and H. Rinia with P. M. van Alphen describe their technique for the production of Schmidt plates etc. by the drying of moulded gelatine films. F. Dourneau describes a machine for deep parabolic surfaces which is the revival of a method known to Newton. One has the impression here of increasing possibilities. Chapters on researches in the theory of diffraction and in phase contrast include some material which is not yet well enough known in England, e.g. the calculation and manufacture of amplitude filters which suppress the lateral fringes in spectral lines. This topic is discussed by P. Jacquinot, P. Boughon, and Brigette Dossier; also by G. Lansraux. The application of phase contrast to observe the irregularities of a polished glass surface is described by B. Lyot. This will be of much interest to those who have taken an interest in the design of the coronagraph. F. Zernike's discussion of the phase-contrast microscope is, of course, now well known from papers available in English.

The volume concludes with a group of papers on "The Intervention of the Receptor". The researches of A. Arnulf and his collaborators on the capacity of the eye to resolve gratings of different fineness and contrast are now well known, and he contributes here a short paper discussing the general plan of the work. V. Ronchi summarizes and foreshadows a series of investigations also dealing with the effect of the receptor on resolving power. The final paper of the whole collection (contributed by J. L. Tearle) describes the work of the Kodak Research Laboratory, Harrow, on photographic resolving power.

It has not been possible in the course of a short review even to mention many other interesting articles. The flavour of the whole collection is (as the title conveys) theoretical, and there are comparatively few descriptions of actual apparatus. It is interesting to speculate how far the intense intellectual effort reflected in this work will affect the main developments or changes which may be apparent in these coming years. It is unfortunately true in optics that much which has been written during the last thirty years has had (so far) no effect whatever in technical practice, but delayed action in such a difficult field is not unexpected. Some of the more popular modern topics, e.g. the 'meniscus plate' systems, anti-reflection films, interference filters, reflecting microscopes and other things, find no echo here; nevertheless in many fields this book will serve, as records of few other symposia can, to give some impression at least of the general optical outlook at the close of the second world war. Its forty-seven papers and summaries (though of varying merit and value) accompanied by many useful references, will stimulate thought and serve to suggest future avenues of progress.

L. C. MARTIN.

Introduction to Physical Optics, by J. K. ROBERTSON. Pp. x+512. 3rd Edition. (New York: D. van Nostrand Co., Inc., 1948.) 22*s*.

This is the eighth printing of the third edition of an already established textbook on elementary physical optics. It therefore needs little comment from a reviewer, and in particular the contents of the book will not need listing here. Because there is so little that needs saying about the book in general, the following comments on particular points should not be regarded as unnecessarily carking.

On p. 12 occurs the sentence "The modern position, then, is that light has a dual nature". This is epistem logically unsound, and rather confusing to the student. Light has both wave and corpuscular attributes, but light has a single *nature*. Moreover the 'modern position' harmonizes the two attributes in one theory.

On p. 92 it is suggested that the spherical aberration of a single lens is a minimum when the deviation is the same at the two surfaces. This is an old error, and the author may perhaps be excused. It should, nevertheless, be recorded that the rule is not true, except in the trivial case of an equiconvex lens having unit magnification.

On p. 274 the author characterizes Fresnel diffraction by saying that (*a*) ' the intensity at any point is the resultant of disturbances coming directly to that point from all parts of the exposed wavefront ', while in Fraunhofer diffraction (*b*) ' a lens is placed beyond the aperture or obstacle, and the diffraction pattern is examined in the plane where a sharp image of the source would be formed in the absence of the aperture or obstacle '.

What distinction is made in (*a*) is difficult to see, while (*b*) really describes the conditions of observation.

The real distinction is as follows : At a point near the focus of a wave, the secondary disturbances arrive with only small phase differences. Hence the whole of the exposed part of the wave is effective, and it is necessary to integrate over the whole wavefront. This is Fraunhofer diffraction, which, in the case of a plane wavefront, gives ' diffraction at infinity '.

At a point near to a geometrical shadow, but remote from a region of focus, the phases of the secondary disturbances arriving at the point vary rapidly with the positions of the points on the primary wavefront at which they originate, except for those points on the wave near to the diffracting edge. Hence it is only the part of the wave in the neighbourhood of the edge which contributes effectively to the disturbance at a point near to the geometrical shadow. The diffraction fringes then tend to follow the outlines of the diffracting edges. This is Fresnel diffraction.

Speaking of Faraday and the conception of tubes of forces, the author suggests that it was ' impossible for him, as for most Anglo-Saxon minds, to think of an electrified body repelling or attracting another at some distance from it, with nothing taking place in the intervening space '. It came as a surprise to at least one reader to know that such a thing as the ' Anglo-Saxon mind ' existed. The sentence smacks of woolly racial theory—harmless in this case, it is true.

It is to be hoped that these few blemishes can be removed in a next edition of the book, which, for the most part, makes an excellent introduction to an interesting subject.

H. H. H.

Die Brechzahlen einiger Halogenidkristalle, by H. HARTING. Pp. 25. 1st Edition. (Berlin : Sitzungsberichte der deutschen Akademie der Wissenschaften, 1948.) 2.50 DM.

Using an interpolation formula due to Ketteler, the refractive indices of a series of halides have been calculated. The formula contains five constants, which were determined independently for the two ranges 1083·03–390·64 and 404·66–239·98 mμ, using widely spaced lines. Tables give the calculated refractive indices for the range 1120–238 mμ, with intervals of 10 mμ for 1120–400 mμ and 2 mμ for 400–238 mμ. For each crystal, a large number of indices was measured and the results compared with the calculated values. The error rarely exceeds 5×10^{-5}. The crystals included are NaF, LiF, CaF_2, NaCl, KCl, KBr, KI.

These tables and measurements should prove invaluable to a great number of workers in many fields.

H. H. H.

Introduction to Electron Optics, by V. E. COSSLETT. Pp. xvi + 293. 2nd Edition. (Oxford : Clarendon Press, 1950.) 27*s*. 6*d*.

This book needs no recommendation. In the four years which have passed since the first edition it has gained well-deserved popularity with students and teachers alike. The second edition is not essentially altered. It is noted with regret that Figure 22 has not been corrected, and that the plates illustrating electron microscopes and electron micrographs have been retained, though they do not illustrate any longer the most modern models or achievements. Nor is it surprising, in view of the rapid development in this field, that the sections on particle accelerators are considerably out of date. It is hoped that this will be remedied in the third edition, which may require also some re-balancing of the theoretical parts, with more emphasis on Hamiltonian methods, which are now represented only in an excellent Appendix, also on wave optics, and on the optics of non-centred systems, which have become increasingly important since it has been realized that workshop accuracy is a major limitation of electron optical systems. But though there is room for

improvement, this is of little importance to the student, who will find in Cosslett's book an excellent account of what he ought to know first, before venturing into the more advanced fields of the subject. The research worker on the other hand will find in the newly added Notes a short, but almost complete and up-to-date collection of the most important recent advances in electron optics.

D. GABOR.

Theory of Hearing, by E. G. WEVER. Pp. 484. (New York: Wiley & Sons; London: Chapman & Hall, 1949.) $6.00.

The appearance of this volume will be welcomed not only by physicists but also by physiologists, anatomists and psychologists. It is most appropriately dedicated 'to my associates in the study of the ear'. Dr. Wever has been engaged in auditory research throughout his career, and is a well-known leader in this field. Twenty years ago, when his work commenced, an interesting situation had arisen—two rival theories of hearing, the 'place' and 'frequency' theories, held the field on the physical side at a time when the new electro-physical techniques which provided basic evidence on sensory nerve action were being developed. Under these circumstances Dr. Wever and Dr. C. W. Bray carried out their classical experiments on auditory nerve impulses, leading to the discovery of the electrical potentials of the ear—work which laid the foundations of much further research in many laboratories.

As one might expect, therefore, Dr. Wever's book deals principally with his own researches and theories in considerable detail, but nevertheless it does not neglect to refer to the work of many other investigators on the complex problem of hearing. The volume is divided into three parts containing, in all, 18 chapters. The first part deals with the historical side of the subject, the 'classical' theories, and is mainly concerned with the Helmholtz resonance theory, the 'place' theories and the 'frequency' (or 'telephone') theories. These theories, some plausible and some rather fantastic, are explained in four very interesting chapters. The second part of the book includes four chapters on (1) modern developments of the classical theories, (2) auditory nerve responses, (3) frequency representation in the auditory nerve and (4) the 'volley' principle. In part three the 'volley' principle is developed and further evidence on cochlear localization is discussed. In this part also the various auditory characteristics and their bearing on the theories of hearing are considered, viz. sensitivity, loudness and fatigue, pitch discrimination, auditory abnormalities (deafness, etc.), transient phenomena, and binaural effects.

The chapters on auditory nerve responses are particularly interesting in showing that the alternating fluid pressures in the ear, which themselves faithfully represent the sound waves, are communicated to the hair cells, and the cochlear potentials (which are traced to the hair cells) are representative of the form of the stimulus—the sound wave. The cochlear potentials are observed over a wide range of magnitudes from the smallest experimentally demonstrable, a tenth of a microvolt, to as much as a millivolt—a range of 10,000-fold—the potential being proportional to sound pressure. The description of the remarkable experiments involved in such investigations makes extremely interesting reading. As a mere physicist the reviewer 'takes off his hat' to the anatomical physiologist who can carry out successfully such delicate operations, as, for example, the demonstration (by display on a cathode-ray tube) that the electro-physiological response of the ear lies in the hair cells of the cochlea.

The book is full of interest and leaves one with the feeling that the physicist is lagging behind the anatomist. There is clearly plenty of scope for further research—particularly of the 'combined operations' variety in which the physicist must work closely with the physiologist and anatomist. For the benefit of physicists studying the book it would be an advantage if, in a future edition, the principal dimensions and other physical characteristics of the important parts of the ear could be tabulated or collected together in an appendix. Such information is at present scattered throughout the pages of the book and is not easily available for reference.

The book is well written and inspiring. It displays the great complexity of the subject and clearly shows that there is still much to be learnt. The volume can be recommended unreservedly to all those interested in the subject of hearing in man and animals.

A. B. WOOD.

Counting Tubes, by S. C. CURRAN and J. D. CRAGGS. Pp. xi+238. (London: Butterworth's Scientific Publications Ltd., 1949.) 35*s*.

Books on ion counters are few and far between. There is still an urgent need for a comprehensive and up-to-date treatment of the subject. The present book deals almost exclusively with the gas-filled type of counter, with the exception of one chapter which gives a brief discussion of some other types such as scintillation and crystal counters. The early part of the book summarizes the relevant background information on electrical discharges and of the ionization produced by fast particles, and then goes on to analyse the behaviour of counting tubes in the different voltage regimes. There follow three chapters which deal with the efficiency of counters, their construction, and some of the auxiliary circuits to be used with them. The remainder of the book comprises the chapter on special types of counter already mentioned and some chapters dealing with representative applications of counter tubes in different fields of research.

The authors have included a great deal of useful information on the different phenomena which occur in counter tubes and there is a good selection of references to the original literature. The book was, however, found to be a difficult one to read. This was due in part to insufficient care in the definition of terms and symbols in a number of places and, in part, to an over-condensed treatment of the material. In fact—rightly or wrongly—the impression was gained that the book had been written rather hurriedly. Nor, unfortunately, is the text free from error. In the section dealing with the resolving power of counters, the argument leading to equation (40) on page 95 is definitely fallacious and it is not correct for the authors to state, as they do on the following page, that it is difficult to decide whether this or equation (42) is the more nearly correct. Certainly confusion has existed on this point in the past, but it has now been clarified and the matter is adequately dealt with in the literature.

The authors state in their preface that they hope that "this book will appeal both to graduates about to commence experimental work and to undergraduate students who find it necessary to use Geiger counters as instruments. In other fields such as medicine and chemistry an increasing number of workers are finding it necessary to use counters in their researches and we hope that this book will be of assistance to them, if only as a source book". It is felt that the potential value of the book has been diminished by trying to cast the net too wide. Those whose interest is primarily in the use of the counter as a tool are liable to find their understanding of the broad principles of its behaviour obscured by a fog of detail concerning little-understood processes in the discharge, while to those for whom these details are of importance, the chapters dealing with sundry applications of counter tubes are likely to be redundant. It is to be hoped that the authors will find it possible to remedy these defects in a second edition.

J. L. M.

The Strength of Plastics and Glass, by R. N. HAWARD. Pp. viii+245. 1st Edition. (London: Cleaver-Hume Press, Ltd., 1949.) 30*s*.

Although the science of glasses and plastics is a comparatively new subject, a considerable amount of theoretical and experimental work on the strength properties of these materials has been reported in the literature over the past thirty years. The need for collecting together the results of this work into one volume has been felt for some time by specialists in these subjects. For this reason alone, the appearance of this monograph by Dr. Haward is to be welcomed. However, there is much of fundamental interest in the book which will appeal to a wider scientific public and particularly to the rheologist outside the field of applied science, for Dr. Haward has whenever possible directed attention to the contrasting behaviour of plastics and glass under stress. Glass may be regarded as an ideal isotropic solid whose deformation is almost entirely Hookean, while relationships based on the classical theory of elasticity are not generally applicable to plastics.

A major difficulty arises in comparing the results of work on strength properties from different sources, because the measured basic quantities frequently differ in dimensions; for this reason it is sometimes possible to draw misleading conclusions because there appears to be a correlation between two such quantities simply because some other relevant factor is not changing sufficiently to affect the correlation. These difficulties are explained clearly in the

introductory chapter. The next five chapters deal in turn with the static strength of plastic materials, the static strength of glass, the deformation of these materials under stress, hardness and related properties and the impact strength of glass and plastics. The final chapter which concerns the properties of some composite materials, such as those in which plastics and glass are combined in the form of laminates, is of particular interest to the technologist.

These chapters take the form of a presentation of the results of the most important published work and, where necessary, reasons are advanced for the apparent contradictions between the results obtained by different workers. Where theoretical explanations are in doubt, the author confines himself to theories accompanied by the results of experiment.

The subject-matter of each chapter covers a wide field but much of the detailed description of the behaviour of individual plastic materials will be of interest to the technologist rather than to the pure scientist. So far as the glass technologist is concerned, the inclusion of a survey of the behaviour of glass under thermal stresses would have enhanced the value of the book.

The bibliography at the end of each chapter comprises nearly 400 references, mostly to work published within the past ten years. Particular mention should be made of the considerable assistance which the reader derives from the clear presentation of the line diagrams. The author, printer and publisher are to be congratulated on the production of an easily readable work.

R. E. BASTICK.

Recent Advances in Radio Receivers, by L. A. MOXON. Pp. ix + 183. 1st Edition. (Cambridge: University Press, 1949.) 18*s*.

The advances which have been made in radio receiver design during the last decade have arisen mainly from wartime requirements and the postwar expansion of the television service. The present book in the series *Modern Radio Technique* is primarily concerned with design for low noise factor and good pulse response, which are among the most important characteristics of a radar or television receiver.

Chapter 1 is a brief introduction explaining the scope of the book. Chapters 2 to 5 are concerned with the definition, calculation and measurements of noise factor and strike a satisfactory balance between the rigour required in the formulation of the fundamental concepts and the many practical considerations which determine the performance of actual amplifiers. The influence of feedback, partition noise and transit-time loading are discussed and emphasis is directed to the necessity of compromise between the conflicting requirements of a wide bandwidth and a low noise factor. R.F. amplifiers, especially triodes, for frequencies up to 600 Mc/s. and mixers for higher frequencies form the basis of the input circuit considerations.

Chapter 6 is concerned with the design of intermediate-frequency amplifiers and, in particular, the use of coupled, staggered and cascaded circuits to provide a desired bandwidth with sufficient uniformity of gain and time delay to give an acceptable pulse response. The chapter concludes with a brief discussion of overloading, unwanted feedback and the choice of intermediate frequency; much useful advice is given in a small space.

The last three chapters comprise a miscellany of recent features in the design of radio receivers, the selection of which was, inevitably, determined by the author's own interests. The Appendix which concludes the book outlines the analysis of the frequency response of multi-stage I.F. amplifiers.

The errors in the text are relatively few and unimportant, and the diagrams, with one or two exceptions, are clear and useful.

The book can be recommended as a primer on receiver design. For more detailed information on some problems the reader would turn naturally to Volume 18 of the Radiation Laboratory series on *Vacuum Tube Amplifiers* but in the field of British books, Mr. Moxon's contribution has no rival at present.

R. E. BURGESS.

Le Vide et ses Applications, par L. DUNOYER. Pp. 114. 1st Edition. (Paris: Presses Universitaires de France, 1950.) 90 fr.

Most physicists will have heard of Dunoyer because of his book *Vacuum Practice*, published in 1926: it was a pioneer work on the subject. His recent little book is a contribution to the series "Que sais-je?" which includes over four hundred titles. A small, paper-covered volume with only twenty-six diagrams, it is not to be expected that it would cover the subject adequately, or give those practical details of apparatus and materials so useful to the vacuum technician. Nevertheless, it is written so well, and so delightfully, and the material included is selected with such great experience, that it can be read with profit by all interested in vacuum physics provided they have a reasonable knowledge of French. Especially noteworthy are the clarity and conciseness of the earlier parts on kinetic theory, adsorbed gas layers, and the flow of gases through orifices and tubes. Vacuum pumps, gauges, speed measurements, vacuum stoving, getters, and some industrial applications are all discussed in simple terms, with an occasional flash of humour, yet in a manner which convinces the reader that this is the work of a scientist with a wealth of experience from which to draw. The text is singularly free from error: the reviewer discovered only one small mistake. Some criticism might be levelled at the sections on electron-tube manufacture, the production of optical mirrors, vacuum metallurgy, and the preparation of penicillin and of dehydrated orange juice. Here the lack of illustration and detail is such that a rather vague impression must be left in the minds of those not already familiar with these topics. Again, it is a pity that nothing is said about leak-hunting.

It is a book particularly suitable for the physics student, or for the layman with some mathematical knowledge and an intelligent interest in science. At the same time, even the physicist with years of experience in vacuum practice will frequently come across ideas and descriptions which throw new light on many of his problems. J. YARWOOD.

THE INSTITUTION OF ELECTRICAL ENGINEERS

Proof and Reprint Service

The following details of the Proof and Reprint Service of The Institution of Electrical Engineers, London, have been received, with a request that they should be brought to the attention of our members. Formerly the proofs of a paper allocated for reading before the Institution of Electrical Engineers were made available to members only 10 days before the meeting; thus, if accepted at a time when the current programme of meetings was complete, authors' manuscripts might sometimes lie dormant for several months. Since October 1948 "early proofs" of all papers have been printed without avoidable delay.

As soon as the early proofs of a paper are available, an announcement to that effect, together with a synopsis, appears in the monthly *Journal* of the Institution. Application for such proofs can then be made, and those who avail themselves of this service are given the opportunity of applying for a reprint, from the *Proceedings* of the Institution, of the paper in its final form, together with a report of the discussion. The object of the reprint service is to ensure that the permanent record available to its users shall not consist of an early proof which, however carefully prepared, may contain minor errors and will certainly not include the discussion.

The inclusive charge for an early proof and its associated reprint is 2*s*. 6*d*. (post free). This charge is made whether or not the reprint is required, but a reprint alone can be supplied at the price of 1*s*. 6*d*. (post free) if ordered shortly after the paper has been read in London.

Requests for proofs should be sent, accompanied by a remittance, to The Secretary, The Institution of Electrical Engineers, Savoy Place, London W.C.2, England.

CONTENTS FOR SECTION A

PAGE

Prof. L. JÁNOSSY and Mr. H. MESSEL. Cascade Theory including Ionization Loss . 1

Mr. K. H. BARKER and Dr. C. C. BUTLER. The Nuclear Interaction Length of the Particles in Penetrating Cosmic-Ray Showers 4

Mr. L. RIDDIFORD. The Importance of Gas Scattering in Particle Accelerators . 10

Dr. P. E. CAVANAGH, Mr. J. F. TURNER, Mr. D. V. BOOKER and Mr. H. J. DUNSTER. An Investigation of the Secondary Electron Spectrum of ^{198}Au 13

Mr. J. W. BREMNER. A Method for Determining Uranium and Thorium in Rocks by the Nuclear Photographic Plate 25

Dr. P. TORKINGTON. The Planar Vibrations of Ethylene and Tetra-deutero-ethylene : A Critical Analysis of the Potential Function 32

Mr. SURAJ N. GUPTA. On the Elimination of Divergencies from Classical Electrodynamics 50

Dr. J. C. WARD. On the Renormalization of Quantum Electrodynamics . . . 54

Dr. A. PAPAPETROU. Equations of Motion in General Relativity 57

Prof. P. B. MOON. Resonant Nuclear Scattering of Gamma-Rays : Theory and Preliminary Experiments 76

Dr. J. V. JELLEY. Detection of μ-Mesons and other Fast Charged Particles in Cosmic Radiation, by the Cerenkov Effect in Distilled Water 82

Letters to the Editor :

Dr. J. D. JOLLEY and Dr. F. C. CHAMPION. The Angular Distribution of Protons Emitted in some F(α, p)Ne Resonance Reactions. 88

Mr. K. R. WILKINSON and Mr. J. WILKS. The Thermal Conductivity of Solid Helium 89

Miss J. M. M^{C}ALISTER and Mr. D. W. KEAM. Factors Involved in the Accuracy and Reproducibility of Depth Measurements on Nuclear Research Emulsions 91

Mr. F. K. GOWARD and Mr. J. J. WILKINS. Measurement of Gamma-Ray Momenta and the Thresholds of the Photo-disintegrations $^{12}C \rightarrow 3\,^4He$ and $^{16}O \rightarrow 4\,^4He$ 93

Mr. F. K. GOWARD and Mr. J. J. WILKINS. The Photo-disintegration of Oxygen into Two ^8Be Nuclei 94

Mr. F. K. GOWARD, Mr. E. J. JONES, Mr. H. H. H. WATSON and Mr. D. J. LEES. Determination of Fission and Neutron Yields, and the Average Neutron Energy in the Photo-disintegration of Uranium 95

Mr. P. GOODMAN, Mr. K. P. NICHOLSON and Dr. H. D. RATHGEBER. The Ionization of Cosmic-Ray Particles 96

Mr. W. H. DOVELL and Dr. R. F. BARROW. A New Ultra-Violet Band-System of SiF 98

Dr. G. STEPHENSON. Calculation of the Oscillator Strengths for certain Band-Systems of N_2 and C_2 99

Reviews of Books 101

The Institution of Electrical Engineers. Proof and Reprint Service 102

Contents for Section B 102

Abstracts for Section B 103

ABSTRACTS FOR SECTION A

Cascade Theory including Ionization Loss, by L. JÁNOSSY and H. MESSEL.

ABSTRACT. The Bhabha–Chakrabarty solution of the cascade equations with ionization loss is discussed, and a simplified method of numerical evaluation suggested.

The Nuclear Interaction Length of the Particles in Penetrating Cosmic-Ray Showers, by K. H. BARKER and C. C. BUTLER.

ABSTRACT. The work of Rochester and Butler, published in 1948, and that of Butler, Rosser and Barker, published in 1950, has been continued. In particular, the interaction properties and the spectrum of the penetrating particles are considered. The interaction length of the shower particles with momenta greater than 10^9 ev/c. is found to be 18 cm. lead ($\pm 20\%$).

The Importance of Gas Scattering in Particle Accelerators, by L. RIDDIFORD.

ABSTRACT. In electron and proton synchrotrons there exists a minimum useful vertical aperture of the vacuum chamber, and for apertures less than this the beam intensity falls to zero. It is considered, on the basis of a comparison of theory and experiment, that this phenomenon is in the main due to free oscillations which arise from gas scattering. The final beam size in proton synchrotrons may be substantial for this reason also, but for cyclotrons the large spread which is known to exist must be attributed to some other phenomenon.

An Investigation of the Secondary Electron Spectrum of ^{198}Au, by P. E. CAVANAGH, J. F. TURNER, D. V. BOOKER and H. J. DUNSTER.

ABSTRACT. The secondary electron spectrum of ^{198}Au has been studied using very strong sources, up to 0·3 curie, in a magnetic lens spectrometer. In addition to the well-known γ-ray at 0·411 MEV., evidence of two much less intense higher energy γ-rays at 0·67 MEV. and 1·09 MEV. has been found, both from the Compton and photoelectric spectra. The intensities of these two γ-rays with respect to the one at 0·411 MEV. have been measured. Two photoelectric peaks at low energy, in about the region expected for Kα and Kβ x-radiation from elements in the neighbourhood of gold, have been examined with radiators of different atomic number. The radiation responsible for these peaks has been subjected to critical absorption measurements in the spectrometer. Its behaviour is compatible with the Kα and Kβ x-radiation of gold, and no evidence of platinum x-radiation, such as would suggest K-capture, has been found.

A Method for Determining Uranium and Thorium in Rocks by the Nuclear Photographic Plate, by J. W. BREMNER.

ABSTRACT. A nuclear photographic emulsion which has been in contact with material containing traces of uranium and thorium shows on processing α-ray stars arising from atoms which have undergone several successive disintegrations during the exposure. The relative frequency of the various multiple stars, which depends on the uranium/thorium ratio, is here evaluated on simple assumptions to show the possibility of determining these elements by star counting.

The Planar Vibrations of Ethylene and Tetra-deutero-ethylene : A Critical Analysis of the Potential Function, by P. TORKINGTON.

ABSTRACT. A careful analysis of the planar modes of vibration of ethylene and ethylene-d_4 is carried out in order (*a*) to determine finally the value of the C=C stretching force constant in these key molecules, (*b*) to find what interactions, particularly those between the two ends of the molecules, are real, and (*c*) to determine the vibrational forms and the potential energy distributions in the normal modes, and how they are affected by altering the potential function. Solutions are obtained both with and without correction for anharmonicity, and estimates are made of the effects of other corrections which may be necessary. The limits found for the C=C stretching constant are $9{\cdot}336$, $9{\cdot}388 \times 10^5$ dyne/cm., with a most probable value of 9·343, the carbon atoms being uncorrected for anharmonicity. The zero-order constant is unlikely to be greater than 9·57. There is detectable real interaction between the two ends of the molecule, for both stretching and bending coordinates. Interactions are discussed.

On the Elimination of Divergencies from Classical Electrodynamics, by SURAJ N. GUPTA.

ABSTRACT. It is shown that the divergencies in classical electrodynamics may be removed by subtracting the self-energies of isolated electrons by means of a modification of the usual expression for the force density in an electromagnetic field. The results obtained are equivalent to those of Dirac and Wentzel.

On the Renormalization of Quantum Electrodynamics, by J. C. WARD.

ABSTRACT. The subtraction procedure of Dyson is modified in order to eliminate a certain difficulty in the renormalization programme, namely the so-called ' b ' divergencies. The conclusions of Dyson concerning the finiteness of the renormalized S matrix are confirmed.

Equations of Motion in General Relativity, by A. PAPAPETROU.

ABSTRACT. This paper contains a new derivation of the equations of motion of bodies moving slowly in their (weak) gravitational field, up to terms of the order $(v/c)^2$. In contrast to the method developed previously by Einstein and co-workers, in which only the field outside the bodies has been considered, in the present paper a new method is used in which the field outside as well as inside the bodies, and the internal structure of the bodies, is taken into consideration. The equations of motion derived by this new method are identical with those obtained by Einstein and co-workers, but the new method is essentially simpler and the necessary calculations much less lengthy.

Resonant Nuclear Scattering of Gamma-Rays : Theory and Preliminary Experiments, by P. B. MOON.

ABSTRACT. Since the lower excited states of nuclei have very small widths ($\ll 1$ ev.), resonant scattering of gamma-rays requires precise matching of the energy available from the gamma-ray with the energy necessary to excite the scattering nucleus.

Resonant scattering should be observable if (1) the emitting and scattering nuclei are of identical type, (2) the gamma-transition goes to the ground state and (3) the source and scatterer are given such a relative velocity that Doppler effect restores the energy lost by the gamma-ray to nuclear recoils. Thermal velocities of the emitting and scattering nuclei broaden and correspondingly weaken the resonant scattering peak, and the cross section at the optimum speed of $32E/A$ cm/sec. is $3{\cdot}6\times10^{-3}(I\Gamma/E^3)(A/T)^{1/2}$ cm^2, where E and Γ are the energy and intrinsic width of the excited state in electron volts, I the isotopic abundance of the resonantly scattering isotope, A its atomic weight and T the absolute temperature.

Preliminary experiments have been made with the 0·411 MeV. radiation from the nucleus ^{198}Hg, the source being carried by a high-speed rotor up to a speed of about 7×10^4 cm/sec. and the scatterer being liquid mercury (10% ^{198}Hg). A small but apparently significant increase of scattering was found, corresponding to a width Γ of the order of 10^{-5} ev.

No such increase was observed with ^{181}Ta gamma-rays scattered from tantalum carbide.

The negative result for ^{181}Ta and the positive result for ^{198}Hg are consistent with the latest information about the life-times of the excited states concerned, viz. $1{\cdot}1\times10^{-8}$ sec. for ^{181}Ta and less than 2×10^{-10} sec. for ^{198}Hg.

Detection of μ-Mesons and other Fast Charged Particles in Cosmic Radiation, by the Čerenkov Effect in Distilled Water, by J. V. JELLEY.

ABSTRACT. The Čerenkov effect has been established for the passage of cosmic-ray μ-mesons through distilled water. The light pulses were observed using a photomultiplier and fast amplifier; the experiments were carried out using the detector alone, and in a coincidence-telescope arrangement. The ratio of the light emitted in the downward and upward directions was measured as a function of discriminator bias. In addition measurements were carried out at various depths of water and with various orientations of the detector with respect to the vertical. Estimates of the absolute efficiency were made and other characteristics of the detector are discussed.

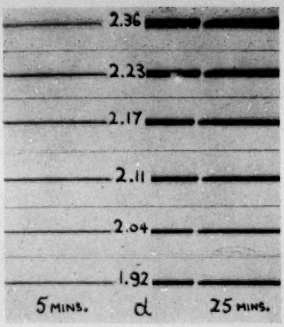

Figure 2. Slit images showing the variation of spot size and quality with grid aperture–anode distance d. Exposure times: 5 min. and 25 min. Slit width 7 μ, magnification 10 times.

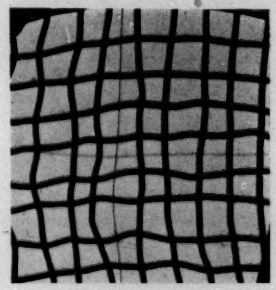

Figure 10. Shadowgraph of two 10 μ platinum wires at right angles, supported by a platinum grid. Direct magnification about 20 times.

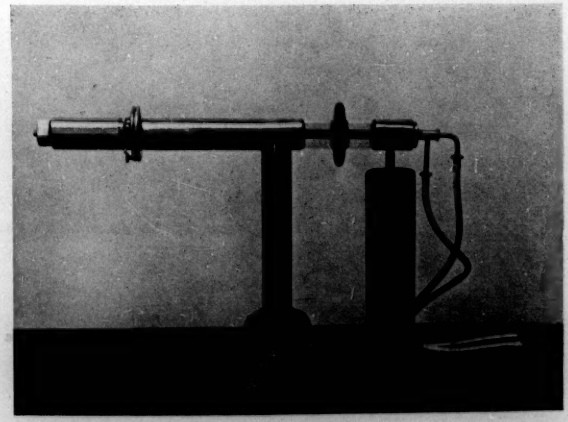

Figure 8. Photograph of tube.